

Universidade de Lisboa  
Faculdade de Ciências  
Departamento de Física



**Modeling key uncertainties in technology development:  
The case of Twente Photoacoustic Mammoscope  
(PAM)**

Gil Eduardo Rocha Braz

Dissertação

Mestrado Integrado em Engenharia Biomédica e Biofísica  
Perfil em Sinais e Imagens médicas

**2013**

Universidade de Lisboa  
Faculdade de Ciências  
Departamento de Física



**Modeling key uncertainties in technology development:  
The case of Twente Photoacoustic Mammoscope  
(PAM)**

Gil Eduardo Rocha Braz

Dissertação orientada pelos Professores Doutores Maarten J. IJzerman e Nuno Matela  
Mestrado Integrado em Engenharia Biomédica e Biofísica

Perfil em Sinais e Imagens médicas

**2013**



*“What does “affordable” mean when you are talking about human life? Take a moment to imagine what the society we live in could do with an infinite amount of money. We could build a huge public transportation system that eliminates car accidents, pollution, and noise. We could use only solar power and switch to 100 per- cent recycling, eliminating the major remaining causes of pollution; this would greatly reduce environmental carcinogens and oxidizing agents that cause cancer, heart disease, and premature aging. In addition, it would delay global warming, which threatens to put much of civilization under water, leading to countless deaths in the process. We could completely mechanize industry, eliminating occupational accidents. Finally, we could create a highly advanced health system that provides full MRI body scans and comprehensive laboratory screening tests for everyone in the population to ensure that cancers and other disorders are detected at the earliest possible stage. As it is, there are very few nations that can even provide safe drinking water to all their citizens. The challenge, then, is to figure out how best to spend the money we have so that the quantity and quality of life can be maximized.” (Muennig 2008)*



# Acknowledgements

This thesis is the product of the support and help from many people, to whom I truly would like to thank.

Firstly, I would like to thank Professor Marjan Hummels for all the support and guidance given in our weekly meetings. I also would like to thank Ellen Ten Tije for the suggestions in an area that she knows so well and to the PAM designers for giving me the possibility to assist some clinical trials at the Hospital of Oldenzaal. The help of my external supervisor, Professor Maarten Ijzerman, was also important for the experience in HTA that he brings. The help of my internal supervisor, Professor Nuno Matela, was also essential.

I would like to thank to Jacinta Boot, my landlord, that made me feel like family during my stay in her house, and to all my house mates (from all over the world) I had the opportunity to meet for the cultural diversity and fun moments we could share. To André Girão and Andreia Silva, also students at U. Twente during our experience abroad that allowed me to speak a bit of Portuguese once in a while.

Finally, I would like to thank to my girlfriend Neuza for all the support and a huge package of Dutch moments in a thousand of different places we had the opportunity to visit, and of course to my family for the support and peace of mind they can give me.

# Resumo

O efeito fotoacústico foi apresentado pela primeira vez por Alexander Graham Bell em 1880. Este princípio enuncia que a absorção de ondas eletromagnéticas por um certo meio provoca uma sequência de eventos que culmina na geração de ondas sonoras. Desde a sua descoberta surgiram inúmeras aplicações fotoacústicas, entre as quais aplicações de imagiologia médica. Estes sistemas fotoacústicos utilizam os componentes óticos como sondas e os componentes acústicos como recetores do sinal gerado, produzindo imagens de carácter tomográfico, daí a designação atribuída – sistemas fotoacústicos tomográficos, do inglês *photoacoustic tomography* (PAT). A fusão dos componentes óticos e acústicos minimiza algumas desvantagens que as modalidades apresentam individualmente e apresenta algumas vantagens relativamente às imagens captadas por sistemas puramente óticos ou puramente acústicos, uma vez que permitem reduzir a elevada dispersão dos fotões nos tecidos biológicos: os sistemas óticos apresentam bom contraste, mas fraca resolução, enquanto os sistemas acústicos apresentam boa resolução e bons níveis de penetração no tecido biológico. Fruto desta combinação, os sistemas fotoacústicos permitem visualizar a angiogênese, um dos principais fenómenos biológicos associados à vascularização tumoral. Tal visualização é possível devido ao aumento da concentração da hemoglobina que apresenta excelentes níveis de contraste ótico e uma boa resolução acústica, sem o recurso a agentes de contraste, nem a radiação ionizante. Por estas razões os sistemas PAT são considerados ideias para o rastreio e diagnóstico do cancro da mama. Dentro dos equipamentos médicos PAT destacam-se aqueles que utilizam como sonda ótica a radiação próxima dos infravermelhos, do inglês *Near Infrared Light* (NIR), cujo intervalo de comprimento de onda se situa entre os 750 e os 1400 nm. A utilização do comprimento de onda neste intervalo representa a optimização do compromisso entre a resolução espacial e a profundidade de alcance no tecido biológico.

O departamento de imagiologia fotónica médica da Universidade de Twente (department of Biomedical Photonic Imaging, MIRA Institute for Biomedical Technology and Technical Medicine of University of Twente, Netherlands) desenvolveu um equipamento médico que utiliza todos os princípios físicos PAT e radiação NIR – mamografia fotoacústica, do inglês *Photoacoustic Mammoscope* (PAM). O PAM apresenta algumas vantagens próprias, uma vez que, por exemplo, ao contrário dos restantes equipamentos médicos PAT não requer uma compressão excessiva da mama entre a janela de iluminação e o detetor acústico. O PAM utiliza como fonte ótica um laser da classe Q-switched Nd:YAG que opera com comprimentos de onda de 1064 nm com pulsos de 5 ou 10 ns e a uma taxa de repetição de 10 Hz. Relativamente à composição e funcionamento do seu sistema de receção acústico o PAM apresenta um detetor plano com 590 elementos (matriz circular) disposto numa geometria de pratos paralelos, o que facilita a sua comparação direta com imagens de mamografia convencional e digital. O PAM em associação com o algoritmo de reconstrução de imagem atraso e soma, do inglês *delay and sum algorithm* apresenta um

alcance máximo em profundidade de 15 a 60 mm relativamente à superfície de iluminação, dependente do tamanho e contraste do objeto absorvente e uma resolução espacial (lateral ou axial) de 3 a 4 mm, dependente da profundidade do objeto absorvente.

Os primeiros testes piloto foram efetuados em 2007. Apesar de bem-sucedidos relativamente aos objetivos de funcionalidade, o tempo de medição foi considerado excessivo (25 min). Tendo como ponto de partida os testes piloto, iniciaram-se em Dezembro de 2010 um conjunto de testes clínicos de maior escala no Hospital de Oldenzaal (Center for Breast Care of the Medisch Spectrum Twente Hospital in Oldenzaal, Netherlands). O objetivo passa por incluir em três fases distintas 100 pacientes até 2014. Os pacientes no seu trajeto clínico normal entre os testes de radiologia convencional (raios-x e ultrassons) e a biópsia são questionados a participar no estudo. As imagens das diferentes modalidades são posteriormente comparadas entre si. A 1ª fase dos testes clínicos (Dezembro, 2010- Abril, 2011) já terminada permitiu retirar três conclusões: a performance do PAM é independente da densidade mamária; os quistos não apresentam contraste suficiente; as dimensões das lesões visualizadas no PAM são inferiores às dimensões resultantes da histopatologia. Por sua vez, a 2ª fase dos testes clínicos (Abril, 2011 - Abril, 2012) procurava testar duas configurações de scan: “fixed scan” em que o feixe de luz é mantido fixo durante todo o processo de medição; “Tandem Scan” em que o feixe de luz se move ao longo da ROI. Durante esta fase foi possível concluir que a configuração “fixed scan” era mais vantajosa permitindo, entre outras vantagens, diminuir o *signal-noise ratio* e aumentar o contraste. A 3ª fase de testes encontra-se a decorrer. As principais alterações nesta fase estão relacionadas com o número de elementos do detetor acústico ativados de cada vez, uma vez que passou de 1 para 10, resultando numa diminuição do tempo de duração de cada teste de 25 min para 10 min.

Além dos testes clínicos, 3 estudos utilizando métodos de *health technology assesment* (HTA) foram realizados. Um deles realizado por *Haakma W. 2011* - “Expert Elicitation to Populate Early Health Economic Models of Medical Diagnostic Devices in Development”. Neste estudo foram utilizados modelos matemáticos para aglomerar as opiniões de 18 radiologistas com experiência em imagiologia mamária sobre a performance do PAM ao nível da sua sensibilidade e especificidade. Os resultados obtidos estão contidos no intervalo de confiança de 95%.

Os testes clínicos efetuados conjuntamente com os estudos de HTA já realizados (que facultam estimativas de performance do PAM) não dão indicações sobre o *custo-eficácia* (do inglês *cost-effectiveness*) da utilização do PAM nos diferentes cenários no trajeto de rastreio e de diagnóstico do cancro da mama, bem como nos diferentes grupos de risco. Foi este contexto que estimulou a principal questão desta tese: Quais são os melhores potenciais cenários de utilização do PAM no trajeto de rastreio e de diagnóstico do cancro da mama do ponto de vista económico?

Para responder a esta questão foi utilizado o método económico de *análise de custo-eficácia* (do inglês *cost-effectiveness analysis*) em diferentes potenciais cenários de aplicação aglomerados em 3 grupos e em dois contextos económicos e epidemiológicos distintos (Portugal e Holanda): Grupo I, Grupo II e Grupo III. O Grupo I inclui o



rastreio (efetuada pela mamografia convencional ou digital), o diagnóstico precoce (efetuada pela mamografia convencional ou digital + exame ultrassonográfico + exame clínico) e o diagnóstico tardio (Ressonância Magnética) no trajeto clínico regular em pacientes sem níveis de risco extraordinários de desenvolver cancro da mama. O Grupo II contempla os cenários de rastreio de diferentes grupos de risco avaliados conforme a probabilidade de desenvolver a doença. O Grupo III é uma réplica do Grupo I com a diferença que não procura testar o PAM com os dados de performance estimados, mas sim com dados hipotéticos em que a performance é assumida como sendo 5% melhor do que as técnicas utilizadas geralmente (*Status- Quo*). A *análise de custo- eficácia* foi realizada através da simulação de percursos de vida durante horizontes temporais pré-determinados em que cada cenário é testado através de 100.000 micro-simulações Monte Carlo. Os diferentes dados necessários para modelar e avaliar o percurso de vida, desde os custos associados às diferentes técnicas e tratamentos às performances para diferentes modalidades envolvidas foram recolhidas da literatura utilizando critério pré-definidos. Os resultados para cada cenário em cada contexto são dados em custo/ por QALY, em que o QALY (*Quality -adjusted life year*) equivale a um ano de vida num estado de perfeita saúde. A avaliação de cada estado/passo no modelo é feita através das *utilities* que avaliam cada estado/passo no modelo, permitindo obter uma total de QALY's em cada microsimulação realizada durante um dado horizonte temporal. A ponderação da viabilidade de cada cenário em termos de *custo- eficácia* é sempre efetuada mediante a análise dos respectivos ICER's (*Incremental cost-effectiveness ratio*) relativamente ao *status quo*.

De uma forma geral, o estudo efetuado permitiu concluir que o PAM apresenta rácios de *custo- eficácia* viáveis em 2 cenários do grupo II: no grupo de indivíduos de alto risco com mamas densas com idades compreendidas entre os 40 e os 59 anos e no grupo de indivíduos de médio risco com mamas densas com idades compreendidas entre os 40 e os 49 anos. Por outro lado, os resultados obtidos com o grupo III de cenários permitiu concluir que a melhoria em 5% da performance dos equipamentos utilizados presentemente (*satus-quo*) com os custos do PAM permite obter rácios de *custo-eficácia* viáveis em todos os cenários do trajeto regular de rastreio e de diagnóstico do cancro da mama (rastreio, diagnóstico precoce e diagnóstico tardio).

# Abstract

Breast cancer is one of the most common forms of cancer and one of the main causes of cancer death among females. The breast imaging standard procedures - X-ray mammography, MRI or ultrasound - suffer from some shortcomings such as insufficient specificity or sensitivity or carcinogenic risks (X-ray mammography) and high costs (MRI). Several alternatives have been suggested, among which photoacoustic technologies with near infrared (NIR) light are included. The medical photoacoustic devices merge the advantages of *pure optic* devices and of *pure acoustic* devices minimizing the respective disadvantages. Furthermore, the photoacoustic imaging can visualize the angiogenesis due to the associated increased hemoglobin concentration, with optical contrast and acoustic resolution, without the use of ionizing radiation or contrast agents and is therefore theoretically considered an ideal method for breast imaging. Under this principle, the department of Biomedical Photonic Imaging of University of Twente has designed an innovative device – The Twente Photoacoustic Mammoscope (PAM). The PAM optical source is a Q-switched Nd:YAG laser operating at 1064 nm with 5/ 10 ns pulses and a 10 Hz repetition rate. For acoustic signal reception PAM has a flat array ultrasound detector with 590 elements in a parallel plate geometry. The measured lateral and axial resolution is 2.3 to 3.9 mm and 2.5 to 3.3. mm respectively. The assessment of PAM is in process and can be placed at the *main stream HTA* – phase I: The first of 3 phases of clinical trials has started in December 2010 and so far, 3 HTA studies were conducted to assess the viability of its clinical implementation.

However the cost-effectiveness of PAM is still unknown. The aim of this project is to implement and evaluate Markov models through Monte Carlo simulation in order to assess the cost-effectiveness of PAM in different scenarios. The tested scenarios were aggregated in 3 distinct groups: in the regular stages of the clinical pathway of breast cancer – screening, early diagnosis and late diagnosis – named *Group I*, and in the screening of multiple groups of high to moderate risk of breast cancer as suggested by the guidelines, named *Group II*. The last group of scenarios- *Group III* had the purpose of measuring the *cost-effectiveness* for a hypothetical technology that has sensitivities or specificities 5% higher than the standard of care and the same cost of PAM. The scenarios were tested simultaneously in 2 different epidemiological and economical contexts: Portugal and Netherlands. The obtained results for the different scenarios were analysed, specifically the CE ratio and the ICER ratio considering a willingness to pay threshold for each country. The *cost-effectiveness* results suggest that the clinical application of PAM is viable in high to moderate risk groups of breast cancer with dense breasts. Therefore, the future PAM design and development should continue to pursue a constant effectiveness in dense and non dense breasts because it is one of the major competitive advantages of PAM.

**Keywords:** Photoacoustics, Health Technology Assessment, PAM, Cost Effectiveness Analysis, Markov modeling

# Acronyms

AHP- Analytical Hierarchy Process  
ALND – Axillar lymph node dissection  
BCS – Breast Conserving Surgery  
CEA - Cost-effectiveness analysis  
CUA – Cost-Utility analysis  
CBA – Cost Benefit analysis  
CBE- Clinical breast examination  
CMA – Cost minimization analysis  
CT- Computed tomography  
CM - Confocal microscopy  
CE-MRI - Contrast enhanced magnetic resonance imaging  
DES- Discrete event simulation  
DS - Direct DNA sequencing  
DCIS – Ductal Carcinoma in Situ  
DHPLC- Denaturing high performance liquid chromatography  
DGGE - Denaturing gradient gel electrophoresis  
FM - Frequency-modulated tomography  
FFDM- Full-field digital mammography  
FDG–PET - Positron emission tomography using fluorodeoxyglucose as contrast  
FAMA - Fluorescent assisted mismatch analysis  
GC- Genetic counseling;  
GSCI- Genetic study of the index case  
HA- Heteroduplex Analysis  
HTA – Heal technology assessment  
HRQOL – Health- Related Quality of Life  
ICPC -Incremental cost per additional cancer detected  
ICER - Ratio of the change in costs to incremental benefits of a therapeutic intervention or treatment.  
IDC – Infiltrating Ductal Carcinoma  
ILC – Infiltrating Lobular Carcinoma  
LCNB- Large-core needle biopsy  
LE- Life expectancy  
LFT – Liver Function Tests  
LCIS – Lobular Carcinoma in situ  
MAU - Multiattribute utility  
MRM - Modified Radical Mastectomy  
MDP – Maximum Designed Pressure  
MST – Mean Sojourn Time  
MRI – Magnetic Resonance Imaging  
MSP – Mammography Screening Programme  
NLBB – Needle Localised Breast Biopsy

NIR – Near-infrared radiation  
 OSP – Opportunistic Screening Programme  
 OPS - Orthogonal polarization spectral imaging  
 OCT - Optical coherence tomography  
 PTO - person trade-off  
 PAT – Photoacoustic Tomography  
 PTT- Protein Truncation Test  
 PACT - Inverse-reconstruction based photoacoustic computed tomography  
 PAE - Rotation-scan based photoacoustic endoscopy  
 PAmic - Raster-scan based photoacoustic microscopy  
 QALY- Quality-adjusted life year.  
 RT- Radiation Therapy  
 RS - Rating scale  
 RDBreasts - Radiographically dense breasts  
 RNDBreasts - Radiographically non- dense breasts  
 SFM - Screen-film mammography  
 SSCP - Single-strand conformation polymorphism  
 SG- Standard Gamble  
 TAT - Thermo-acoustic Tomography  
 TTO - Time trade-off  
 TOF - Time-of-flight tomography  
 TP– True Positive  
 TN - True Negative  
 TCT- Thermoacoustic Computed Tomography  
 US - Ultrasound  
 VOI – Volume of interest

# Contents

<i>Acknowledgements</i> .....	<i>i</i>
<i>Resumo</i> .....	<i>ii</i>
<i>Abstract</i> .....	<i>v</i>
<i>Acronyms</i> .....	<i>vi</i>
<i>List of Tables</i> .....	<i>xi</i>
<i>List of Figures</i> .....	<i>xiii</i>
<b>1. Introduction</b> .....	<b>1</b>
<b>2. Literature Review</b> .....	<b>2</b>
<b>2.1. Technical Review</b> .....	<b>2</b>
2.1.1. The Photoacoustic Effect .....	2
2.1.2. Photoacoustic Imaging .....	2
2.1.2.1. Photoacoustic Signal Generation .....	4
2.1.2.1.1. Light Emission .....	5
2.1.2.1.2. Absorption .....	5
2.1.2.2. Ultrasound Propagation .....	6
2.1.2.3. Ultrasound Detection .....	7
2.1.2.4. Image Reconstruction .....	8
2.1.2.5. PAT Systems .....	8
2.1.2.5.1. PAT Systems in Breast Imaging .....	9
2.1.3. PAM .....	10
2.1.3.1. System Overview .....	10
2.1.3.2. The Ultrasound Detector .....	11
2.1.3.3. The Laser and Light Delivery System .....	13
2.1.3.4. The Patient-user Interface .....	14
2.1.3.5. Image Reconstruction .....	15
2.1.3.6. System Performance .....	16
2.1.3.6.1. Resolution .....	16
2.1.3.6.2. Maximum Imaging Depth .....	17
2.1.3.7. Clinical Studies .....	19
2.1.3.7.1. Measurements .....	20
2.1.3.7.2. Illumination and Scan Configuration .....	20
2.1.3.7.3. Data Handling .....	21
2.1.3.7.4. Results .....	21
2.1.3.7.5. Conclusions .....	25
2.1.3.8. Assessments Studies .....	27
<b>2.2. Standard of Care</b> .....	<b>29</b>
2.2.1. Screening .....	29
2.2.2. Diagnosis .....	30
2.2.3. Treatment .....	30

2.2.4.	Follow-Up.....	32
2.3.	Health Technology Assessment.....	32
2.3.1.	Methodologies.....	33
2.3.1.1.	Health Economic Modeling.....	33
2.3.1.1.1.	Economic Evaluation Methods.....	34
2.3.1.1.1.1.	Costs .....	35
2.3.1.1.1.2.	Outcomes.....	36
2.3.1.1.1.3.	Discounting Costs and Outcomes.....	38
3.	<i>Research Question.....</i>	<i>40</i>
4.	<i>Materials and Methods.....</i>	<i>41</i>
4.1.	Cost-Effectiveness Analysis .....	41
4.2.	The Markov Model design.....	42
4.3.	The Scenarios.....	43
4.4.	Cancer Progression .....	46
4.5.	TreeAgePro.....	47
4.6.	Data required for the model.....	48
4.6.1.	Prevalence and Incidence .....	48
4.6.2.	Mortality .....	49
4.6.3.	Clinical effectiveness data.....	50
4.6.3.1.	Standard of Care.....	51
4.6.3.1.1.	Screening .....	51
4.6.3.1.2.	Early Diagnosis .....	52
4.6.3.1.3.	Late Diagnosis .....	55
4.6.3.1.4.	Pathological diagnosis - Biopsy.....	55
4.6.3.1.5.	Treatment.....	56
4.6.3.1.6.	Follow up.....	56
4.6.3.1.7.	Recurrence .....	56
4.6.3.2.	PAM .....	57
4.6.3.2.1.	Screening and Late Diagnosis.....	57
4.6.3.2.2.	Early diagnosis.....	57
4.6.4.	Utilities .....	66
4.6.5.	Costs .....	67
4.6.5.1.	Screening and Diagnosis.....	67
4.6.5.2.	Pre-Operative Assessments.....	68
4.6.5.3.	Treatments.....	69
4.6.5.4.	Follow Up.....	70
4.6.5.5.	Recurrence.....	71
4.6.5.6.	PAM .....	72
4.7.	Simulations.....	72
5.	<i>Results.....</i>	<i>73</i>
5.1.	Group I.....	73
5.2.	Group II .....	77
5.3.	Group III.....	84
6.	<i>Discussion.....</i>	<i>89</i>

6.1.	Criteria.....	89
6.2.	Group I.....	89
6.3.	Group II .....	89
6.4.	Group III.....	90
6.5.	Model Assumptions and Limitations.....	91
6.6.	Possible extra scenarios .....	92
7.	<i>Conclusion</i> .....	93
	<i>Appendixes</i> .....	94
	Appendix I.....	94
	Appendix II.....	110
	Appendix III .....	112
	Appendix IV.....	115
	<i>References</i> .....	117

# List of Tables

Table 1. Relevant technical Specifications of the Photoacoustic Mammoscope. Addapted from [10, 11] .....	11
Table 2. Comparative Performance between PAT devices .....	16
Table 3. Simulated maximum imaging depth for different inhomogeneities dimensions and for different level of contrast with respect to the background [3].....	18
Table 4. Overview of clinical and technical definitions by trial phase. ....	20
Table 5. Measurement results from PAM in the phase 1 of clinical trial. In patients 10-15, the lesion size was estimated radiologically, since there was no histopathological measurement available. **These lesions were positioned partly in fatty tissue and partly in fibroglandular tissue. Therefore, the contrast for these lesions on x-ray mammography is given with respect to both types of background. *** In these measurements the defined lesion was only partly positioned within the region of interest and the maximum diameter could not be assessed. <i>Addapted from</i> [29]. ....	22
Table 6. Overview of the measurements results for the 2 scan configurations (only for the malignant lesions). *This value is significantly different ( $p<0.05$ ) from the value in the ‘tandem scan’ configuration [30]. ....	24
Table 7. Values of sensitivity and specificity resulted from expert elicitation [32].....	28
Table 8. Adopted periods and intervals of screening in the general population [2].....	29
Table 9. NICE guidelines for the moderate to high risk screening. HR- high risk; MR- moderate risk;.....	30
Table 10. Pre-Operative assessments by stage. Adapted from [38] .....	31
Table 11. Treatments stage of breast cancer. Adapted from [37, 39] [38].....	31
Table 12. Set of annual procedures by type of follow up [40]. ....	32
Table 13. Overview of the different economic evaluations methods. Adapted from [46] .....	35
Table 14. National discount rate [50]......	38
Table 15. Tested scenarios in the regular clinical pathway of breast cancer.....	44
Table 16. Tested scenarios in the high risk screening groups .....	45
Table 17. Group of additional scenarios teste .....	46
Table 18. The correspondence between roman staging system and the biological features of breast cancer. Adapted from [52] .....	46
Table 19. Initial association between the defined stage and the biological features. ....	47
Table 20. <i>Incidence</i> values among the different interval of ages. The rates are for the all interval of ages (4 years) [54] .....	49
Table 21. Annual incidences for different groups at risk. ....	49
Table 22. Stage distribution among the diagnosed cancers [57]. ....	49
Table 23. Biannual mortality values for the different types of recurrence.....	50
Table 24. State transitions determination based on clinical effectiveness data (sen. and spe.)...	51
Table 25. Sensitivity and Specificity values of standard of care screening procedures .....	52
Table 26. Sensitivity and Specificity values of early diagnosis standard of care procedures .....	54
Table 27. Sensitivity and Specificity values of late diagnosis standard of care procedures .....	55
Table 28. Biannual transition probabilities from follow up to local, regional or distant recurrence and contralateral cancer [66] . ....	56



Table 29. Biannual transition probabilities between different types of recurrence [60].	57
Table 30. PAM sensitivity and specificity values applied in the model.	57
Table 31. Sensitivity and Specificity values of PAM+ CE+US at early diagnosis	62
Table 32. Sensitivity and Specificity values of PAM+ CE + FFDM at early diagnosis	65
Table 33. Information about the utilities applied in the analysis for the different Health states/Interventions considered.	66
Table 34. Utilities used in the analysis by stage of breast cancer and by age	67
Table 35. Costs for screening and diagnosis procedures.	68
Table 36. Costs of pre-operative procedures.	69
Table 37. Overall costs of pre-operative assessments by stage.	69
Table 38. Costs of treatment procedures.	70
Table 39. Overall costs of treatment procedures by stage and cycle in Netherlands.	70
Table 40. Overall costs of treatment procedures by stage and cycle in Portugal.	70
Table 41. Costs of <i>limited follow up</i> every year.	70
Table 42. List of treatments by type of recurrence and primary stage of breast cancer. From [81] and [38].	71
Table 43. Costs of recurrence treatment in Netherlands by type and primary stage of breast cancer for cycle. The next cycle costs includes only the hormone therapy costs.	71
Table 44. Costs of recurrence treatment in Portugal by type and primary stage of breast cancer for cycle. The next cycle costs includes only the hormone therapy costs.	72
Table 45. Overall results from scenarios of Group I: Best scenario, base case and worse scenario	75
Table 46. Status of dominance of PAM versus Standards of care in all the scenarios of group I. <i>D- Dominated; SD – Strict dominated; ND – Not Dominated; NDWTP- dominated, requiring willingness to pay analysis;</i>	76
Table 47. Overall results from scenarios of Group II: Best scenario, base case and worse scenario	80
Table 48. Status of dominance of PAM versus Standards of care in all the scenarios of group II. <i>D- Dominated; SD – Strict dominated; ND – Not Dominated; NDWTP- dominated, requiring willingness to pay analysis;</i>	81
Table 49. Overall results from scenarios of Group III.	86
Table 50. Status of dominance of optimized hypothetical technology versus Standards of care in all the scenarios of group III. <i>D- Dominated; SD – Strict dominated; ND – Not Dominated; NDWTP- dominated, requiring willingness to pay analysis;</i>	87
Table 51. WTP analysis of relevant scenarios of group II: Netherlands - WTP =35900 € per QALY; Portugal - WTP =15600 € per QALY.	90
Table 52. WTP analysis of relevant scenarios of group III: Netherlands - WTP =35900 € per QALY; Portugal - WTP =15600 € per QALY.	91
Table 53. Methodological Overview of the group A.	97
Table 54. Overview of the results of group A.	99
Table 55. Discount rates and sensitivity analyses approaches in the group A	100
Table 56. Methodological Overview of the group B.	103
Table 57. Overview of the results of group B	108
Table 58. Discount rates and sensitivity analyses approaches in the group B	110
Table 59. TNM – Breast cancer classification system – TN specification. From [117].	110
Table 60. TNM – Breast cancer classification system – M specification. From [117].	110

Table 61. Breast cancer <i>Roman</i> Staging System. From [117].	111
Table 62. Mortality 4year-rates for the general population in Netherlands and in Portugal [118].	115
Table 63. 5-years Survival rate by stage and by age [58].	116
Table 64. Calculated values of the exponential parameter $h$ for the different stages and ages.	116

## List of Figures

Fig. 1. Schematization of the basic principle of the photoacoustic effect: After electromagnetic energy absorption a sound wave is generated by thermal expansion [7].	4
Fig. 2. a) Absorption spectra of oxyhemoglobin and deoxyhemoglobin; b) Absorption coefficients of water, blood and melanin [7].	6
Fig. 3. Piezo-electric crystal at different states on acoustic wave reception sequence [18].	7
Fig. 4. Depth and resolution for optical methods for imaging hidden structures tissue [12].	9
Fig. 5. Schematic of PAM [3].	11
Fig. 6. The flat ultrasound detector array showing (a) arrangement of the elements, (b) grouping of elements into sectors, with (c) each group leading to an ASIC [12].	12
Fig. 7. Signal trace of an element showing the PA signals arising from the irradiated tissue: A large signal produced at the breast surface at a depth of approximately 15 mm from the illuminated surface the signal is detected [11].	13
Fig. 8. Schematic of the instrument showing the light delivery system [26].	14
Fig. 9. a) General mechanic configuration of PAM [12]. b) A photograph of the PAM. 1: Laser, 2: scanning system compartment, 3: ultrasound detector electronics, 4: linear stage functioning as compression mechanism, 5: part of light delivery system, 6: laser safety curtain, and 7: aperture to insert breast impulse [26].	15
Fig. 10. The delay applied to each signal depends on the distance between the source of interest and the transducer. Signals are summed after the delay is applied. Weighting is not shown in this figure. Delays are generally applied in post-processing[7].	16
Fig. 11. Variation in axial and lateral resolutions for different depths of absorbers from the detector array [26].	17
Fig. 12. a) Schematic diagram of the concept of the photoacoustic mammoscope, based on a parallel plate geometry. (b) A photograph of the PAM laboratory prototype [8].	18
Fig. 13. AIP in 3-D reconstructed data of selected VOIs in the phantom: <i>Left</i> - the VOI containing the 2-mm-diam sphere of absorption contrast 4 at a depth of 15 mm. <i>Center</i> - VOI with 5-mm-diam sphere with contrast 7 and 30 mm from surface. <i>Right</i> - VOI with 2-mm-diam sphere with contrast 7 and depth 32 mm from surface [8].	19
Fig. 14. Diagnostic images of a 15mm infiltrating ductal carcinoma a) The cranio-caudal x-ray mammogram shows a 20 mm lesion with a calcification (white box) and is highly suspicious for malignancy. b) The ultrasound image shows a 17.5 mm lesion with an arrow form. c) The transverse view of the T1 weighted MRI after gadolinium injection confirms the presence of malignancy because of the enhancement of an 18 mm lesion (white box) in the medial upper quadrant of the right breast. This image is rotated to match the orientation of the cc x-ray view. d) A transversal cross-section with a slice-thickness of 0.24 mm through the photoacoustic	

volume at the expected lesion location shows a confined region with high contrast with respect to the background. With the chosen threshold for abnormality definition, the contrast of the abnormality in the 3D volume is 6.4 and the maximum diameter is 10 mm. This image is rotated to match the orientation of the cc x-ray view. e) The imaging planes of the different imaging modalities used in this study. Indicated are the imaging planes for cranio-caudal x-ray mammography, transverse MRI, transverse PAM and a representative ultrasound view. [29].	23
Fig. 15. a) Contrast Per BI-RADS density classification scale, the average contrast of the lesions on PAM (gray) and x-ray mammography (white) is given. b) Contrast Per BI-RADS density classification scale, segmented in ‘low’ (BI-RADS density 1, 2) and ‘high’ (BI-RADS density 3, 4) [29].	24
Fig. 16. The average contrast of the lesions on PAM (gray) and x-ray mammography (white) is compared between the two different image configurations. There is a significant increase in contrast for PAM when the image configuration is changed from ‘tandem scan’ to ‘fixed scan’ mode. Error bars indicate the plus and minus one standard deviation [30].	25
Fig. 17. Clinical pathway of breast cancer.	29
Fig. 18. Flowchart of stages in medical product development [42].	33
Fig. 19. Overview of Markov states transitions	43
Fig. 20. Every simulation was made through a decision node with two possible pathways, represented by markov models: the standard of care and scenario X.	43
Fig. 21. TreeAgePro interface	48
Fig. 22. Scenarios classification system in terms of dominance	76
Fig. 23. Cost- effectiveness ratio of the scenario <i>HRisk mam: dense (40-59) NL base case</i>	82
Fig. 24. Cost- effectiveness ratio of the scenario <i>HRisk mam: dense (40-59) PT base case</i>	82
Fig. 25. Cost- effectiveness ratio of the scenario <i>MRisk mam: dense (40-49) NL base case</i>	83
Fig. 26. Cost- effectiveness ratio of the scenario <i>MRisk mam: dense (40-49) PT base case</i>	83
Fig. 27. Cost- effectiveness ratio of the scenario <i>MRisk mam: dense (40-49) PT best scenario</i>	84
Fig. 28. Cost- effectiveness ratio of the scenario E. Diagnosis (+ 5 % sen, replacing US) in the Portuguese context	87
Fig. 29. Cost-effectiveness ratio of the scenario L. Diagnosis (+ 5 % spe) in the Portuguese context.	88
Fig. 30. Modeled pathway while in <i>Screening</i> (Markov state)	112
Fig. 31. Modeled pathway while in <i>Screening</i> (Markov state) for the groups with Screening made with MRI	113
Fig. 32. Modeled pathway while in <i>treatment</i> (Markov state)	113
Fig. 33. Modeled pathway while in <i>follow up</i> (Markov state)	114
Fig. 34. Modeled pathway while in <i>local recurrence</i> state (Markov state)	114
Fig. 35. Modeled pathway while in <i>regional recurrence</i> state (Markov state)	115
Fig. 36. Modeled pathway while in <i>distant recurrence</i> state (Markov state).	115

# 1. Introduction

Breast cancer is one of the most common forms of cancer and one of the main causes of cancer death among females [1]. According to the estimations of the International Agency for Research on Cancer (IARC), annually there are 331.000 new cases and 90.000 deaths due to breast cancer in Europe (2006 Data) [2]. The *status quo* procedures of imaging the breast suffer from some shortcomings: the interactions of the probe energy—whether X-rays, magnetic field, or ultrasound—with a tumor induces a contrast not sufficiently specific or sensitive compared with the normal tissue, leading to occurrences of false positives and false negative [3]. Moreover, the X-ray mammography, the golden standard imaging modality, has carcinogenic risks [4]. The other secondary technologies, Ultrasound and MRI have restricted use due to low sensitivity (US), poor specificity (MRI), and high-expense (MRI) [3].

Appropriate *screening* and *early diagnosis* improves the survival chances for the disease and that is what motivates the ongoing search for improved methods for visualizing breast cancer. Among the several alternatives new imaging technologies applying *the photoacoustic effect* and using near-infrared (NIR) light are included. The most important innovation that the designed photoacoustic technologies bring is the fusion of the advantages of *pure optic* devices and of *pure acoustic* devices minimizing the respective disadvantages: *Pure optical* techniques show good contrast but poor resolution, by other side *Pure acoustic* shows good resolution, good penetration depth but poor contrast [5]. Furthermore, one of the hallmarks of breast cancer is the increase in tumor vascularization that is associated with angiogenesis, a crucial factor for the survival of malignancies [6]. The photoacoustic imaging can visualize the angiogenesis due to the associated increased hemoglobin concentration, with optical contrast and acoustic resolution, without the use of ionizing radiation or contrast agents and is therefore theoretically considered an ideal method for breast imaging [6].

The department of Biomedical Photonic Imaging, MIRA Institute for Biomedical Technology and Technical Medicine of University of Twente has developed a new photoacoustic system dedicated to breast imaging – the Twente Photoacoustic Mammoscope (PAM). This system is currently in clinical trials and the data about its performance is still very short and uncertain. In order to understand the viability of introduction of PAM in the clinical pathway of breast cancer some assessment studies have been performed. However the best clinical scenarios of application are still unknown: Screening, high to moderate risk screening, early diagnosis, late diagnoses are among the possible scenarios. Moreover, there is no information about its *cost-effectiveness* in those scenarios.

In this context, the aim of this project is to implement one health economics evaluation methodology to evaluate the use of PAM in different clinical scenarios.

## 2. Literature Review

This chapter is divided in 3 sub-chapters- *Technical Review*, *Standard of care* and *Health Technology assessment*. The first will give an overview of the technical background involved in the design and construction of PAM. The second sub-chapter will give an overview of what is considered the standard of care in the screening and diagnosis pathway of breast cancer. Finally, the last sub-chapter will give a methodological overview about the techniques involved in health technology assessment.

### 2.1. Technical Review

In order to understand whether PAM can be useful, one must first understand the basic principles behind its functioning.

This section will start by giving an overview of the principle and applications of *the photoacoustic effect* (section 2.1.1). Next it will be given an overview of *photoacoustic imaging* (section 2.1.2) about the general process of image formation and reconstruction and the photoacoustic systems built so far. Further, in the *section 2.1.3* it will be given an introduction to PAM in terms of technical settings, results of clinical studies finished so far and conclusions about the assessment works already made.

#### 2.1.1. The Photoacoustic Effect

The photoacoustic effect was introduced for the first time in 1880 by Alexander Graham Bell. It states that absorption of electromagnetic waves by a medium generates sound waves [7]. A variety of biomedical Photoacoustic applications have been studied after that discovery. The great majority of application appeared since 1994, when Kruger and Oraevsky et al explored a new way to induce ultrasound through optical radiation. Among those applications it is included small-animal imaging (*Wang et al, 2003*), imaging of human blood vessels (*Kruger et al, 2003* and *Kolkman et al, 2003*), temperature (*Schule et al, 2004*) and photocoagulation (*Oberheide et al, 2003*) monitoring during ophthalmic laser therapy, material characterization (*Tam et al, 1995*), burn depth estimation (*Yamazaki et al, 2003*), port-wine stain depth estimation glucose monitoring (*Viator et al, 2003*), glucose monitoring (*Zhao et al, 2002* and *Bednov et al, 2003*), blood oxygenation monitoring (*Esenaliev et al, 2002* and *Savateeva et al, 2002*) and mammography (*Oraevsky et al, 2002* and *Kruger et al, 2001, Manohar et al, 2005*) [7-9].

#### 2.1.2. Photoacoustic Imaging

One of the main fields of application of photoacoustic effect is photoacoustic tomography (PAT) imaging systems. Those applications offer relevant potential

advantages compared to pure optic and pure acoustic techniques, by overcoming the high degree of scattering of optical photons in biological tissues and by distinguishing different structures according to their chemical composition.

Pure optical techniques using NIR (Near infra-red) light as probe show good optical contrast absorption and fast acquisition [5, 7]. Nonetheless those techniques have to face the hard problem of poor resolution [2D –  $0.01 \text{ mm}^2$  ( $0.1 \text{ mm} \times 0.1 \text{ mm}$ ) , 3D-  $1 \text{ cm}^3$  ( $1 \text{ cm} \times 1 \text{ cm} \times 1 \text{ cm}$ )] with consequent difficulties in the detection and precise localization of small tumors [5, 10]. This fact is due mainly to biological tissue scattering which also results in small optical penetration depth (approximately 3 mm) [5, 10]. To solve this problem some studies suggest methods to minimize multiple light scattering by using computational models to reconstruct the position of absorbing and scattering in thick structures (up to 10 cm) but with huge losses in resolution [5].

These problems of pure optical imaging are very evident for the NIR light (750 nm – 1740 nm), type of radiation most used as probe in optic imaging. However the use of NIR light is particular crucial for breast imaging, as it has been demonstrated in several studies (*Tromberg et al, 2000* , *Pogue et al, 2001* and *Mcbride et al, 2001*) that tumors have absorption and scattering contrast compared to healthy tissue for NIR light due to fundamental changes associated with tumor growth namely angiogenesis ( structural features, enhanced vascularization, and differences in blood oxygen consumption at tumor sites) [8].

In other hand, pure acoustic techniques have good penetration depth ( $\approx \text{cm}$  in diffuse optics), good resolution [ $1 \text{ }\mu\text{L}$  ( $1\text{mm} \times 1\text{mm} \times 1\text{mm}$ )] and presents scattering in biological tissues two to three orders of magnitude weaker than optical scattering [5, 11]. The difference in resolution is more evident for imaging for depths greater than 2–3 mm [12]. However, pure acoustic techniques show poor contrast: the signal consists in reflected waves due to small changes in the speed of sound [5, 13, 14] . Additionally, in pure acoustics techniques the functional information is only provided by Doppler imaging, where the velocity of fluids is imaged.

The challenge was to combine the advantages of pure optics and pure acoustic techniques and overcome the respective the disadvantages. Photoacoustic imaging techniques with NIR light as probe can do it without having the problem associated with scattering of pure optics but taking advantage of optical absorption contrast that this techniques bring - a optical contrast on the one hand, and low scattering of ultrasound in tissue on the other, are brought together in this hybrid technique [10]. Other important technical advantage is that, unlike other imaging techniques, photoacoustic tomography is speckle free [14].

Moreover, it is also important to mention the multi-scalability that PAT systems can have. Currently, it is possible to acquire images trough photoacoustic systems- from organelles through organs. This level of high scalability is only achievable by trading off imaging resolutions and penetration depths: Higher acoustic frequency contributes to higher spatial resolution, but is attenuated more by tissue, thus resulting in a shallower penetration depth, and vice versa. In addition, optical attenuation is another limiting factor for penetration depth, since photoacoustic waves can only be generated where photons can reach [14].

### 2.1.2.1. Photoacoustic Signal Generation

Photoacoustic signal generation is the result from induced photothermal heating effects as represented in Fig. 1. The absorption of light in a restricted volume leads to the excitation of the internal levels of energy of the matter. The following process of nonradiative deexcitation leads to the increase of temperature  $\Delta T$  which under specific conditions induces a pressure transient  $p_0$  due to thermal expansion, where  $p_0 = \beta * \frac{\Delta T}{k}$

(1) [7, 15]. The generated pressure pulse propagates as ultrasound.

$\beta$  - Thermal expansion coefficient ( $^{\circ}\text{F}$ )

$k$  - Isothermal compressibility ( $\text{Pa}^{-1}$ )

According to (1) is expected that a small raise in temperature of 1 mk induces a pressure rise of 800 Pa, which is higher than the regular noise level of a ultrasonic transducer [15]. Consequently it is possible to achieve high signal-to-noise ratio without thermally damaging the tissue.

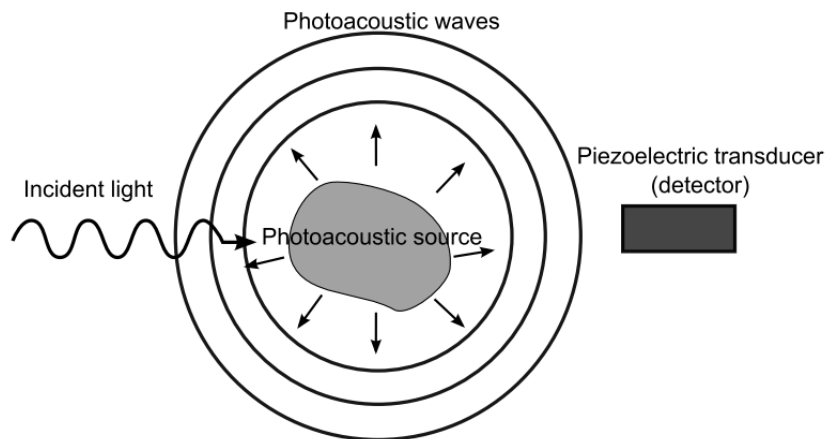


**Fig. 1.** Schematization of the basic principle of the photoacoustic effect: After electromagnetic energy absorption a sound wave is generated by thermal expansion [7].

Thermal expansion is not the only possible mechanism that might occur after absorption, but it is the most dominant mechanism at radiant power densities below the vaporization threshold. Alternative absorption processes are electrostriction, ablation, plasma formation, and cavitation, or nonabsorption processes like radiative pressure and Brillouin scattering [9].

The characteristics of the generated ultrasound pulse due to thermal expansion depends on the geometry and dimension of the absorber, its optical and acoustic properties, and properties of the exciting beam such as pulse characteristic and local fluence rate [8].

Generally, one can say that the process of photoacoustic signal generation is divided in two steps: light emission and the radiation absorption by the tissue.

### 2.1.2.1.1. Light Emission

The inductor light is emitted through laser excitation. In order to generate high frequency (short wavelength) sound waves in the tissue and thus obtain a high resolution, the length of the laser pulse  $\tau_p$  generated in this stage must be shorter than both the thermal relaxation time of  $\tau_{th}$  (so the energy deposited instantaneously, minimize heat diffusion) and the stress relaxation time  $\tau_s$  of the laser defined as follows[7, 8]:

$$\tau_s = \frac{d_c}{v}, \quad \tau_{th} = \frac{\alpha_{th}}{v}$$

The laser pulse should also be calculated according with the characteristics of the absorber (ideally considered a sphere). The laser pulse should be shorter than the thermal diffusion time  $\tau_h$  and acoustic transit time  $\tau_a$  defined as follows [8]:

$$\tau_h = \frac{r_0^2}{k_t}$$
$$\tau_a = \frac{r_0}{v}$$

$\alpha_{th}$ - Thermal diffusivity ( $m^2/s$ )

$d_c$ – Characteristic dimension of the structure of interest (m).

$r_0$  – Sphere radius (m)

$v$  – Acoustic velocity (m/s)

$k_t$  - Thermal diffusivity ( $m^2 s^{-1}$ )

### 2.1.2.1.2. Absorption

Different biological tissues properties lead to different profiles of absorption. Tissues absorption is modeled by Beer-Lamber law:

$$I = I_0 e^{-\mu D}$$

$I$  - Intensity of light after traveling  $D$  (cd)

$I_0$ - Initial intensity (cd)

$D$ - Path length (m)

$\mu$ - Absorption coefficient ( $cm^{-1}$ )

The photoacoustic signal amplitude, generated after absorption is proportional to the product of the local absorption coefficient ( $\mu$ ) and local fluence, so one can affirm that photoacoustic signal is essentially listening to the optical absorption contrast of tissue [14]. In biological tissues blood is the major absorbent, so the signal is originated mainly from regions where there is a high concentration of blood [7]. Hemoglobin linked with oxygen (oxyhemoglobin) and hemoglobin without oxygen (deoxyhemoglobin), two main components of the blood, have distinct absorption spectra (as represented in Fig. 2 a) , therefore, it is possible to control the oxygenation



ratio with an appropriate selection of wavelengths [7]. Water and melanin are also important absorbers in biological tissues but selecting NIR wavelength the signal from blood prevails because absorption by water is minimal in this region of the spectra, and absorption by blood is large as shown in Fig. 2 b)[7, 15].

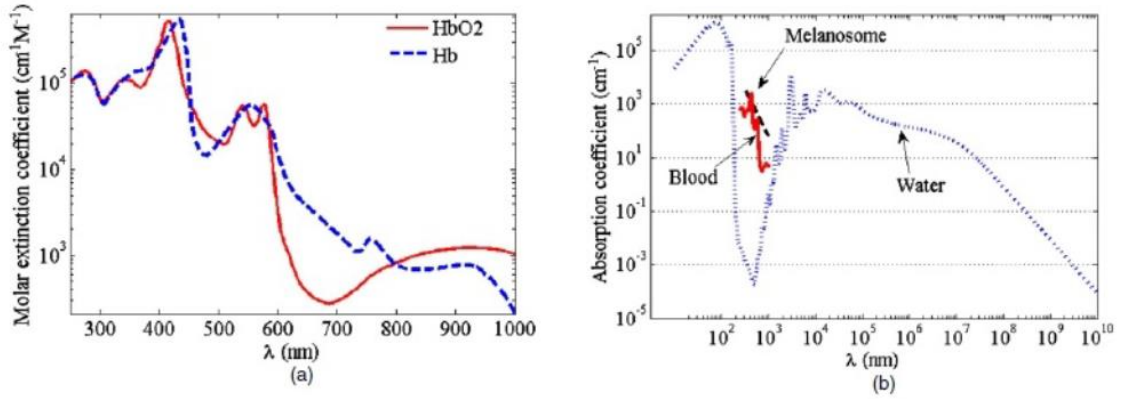


**Fig. 2.** a) Absorption spectra of oxyhemoglobin and deoxyhemoglobin; b) Absorption coefficients of water, blood and melanin [7]

#### 2.1.2.2. Ultrasound Propagation

The output signal from the source is an ultrasound wave which minimizes the problem of scattering, main disadvantages of optic waves propagation in biological tissues, but brings other major problem, the attenuation of acoustic waves [7, 16].

Attenuation in a medium can be modeled by the following formula[7]:

$$\alpha = af^b \text{ (db/cm)} \quad (2)$$

$a$  – Tissue dependent constant (db/(cm\*MHz));

$b$  – [1 – 2];

$f$  – Frequency (MHz).

Several authors consider  $b=1$ , which is close to the reality in the majority of biological tissues [13]. According to (2), higher frequencies are more affected by this type of attenuation, acting as a low-pass filter, reducing overall resolution [7]. From this fact comes the need to make a trade-off between resolution (high frequency) and penetration depth, which favors lower frequencies for being less attenuated [7]. This issue has led some authors to present multiple bandwidth systems that use different central frequencies, achieving an improved overall resolution [17].

The speed of ultrasound waves is considered to be constant at 1500 m/s in moderate to non heterogeneous tissues [7]. In these types of tissues it is acceptable to have variations of 10%, modeled by acoustic impedance, which are responsible for reflections and refractions [7]. Generally these variations are neglected unless the tissue is highly heterogeneous [7].

### 2.1.2.3. Ultrasound Detection

The acoustic reception can be done either by single transducer (fixed or moving along a certain geometry) or by an array of transducers eliminating the need for movement [18]. The produced ultrasound waves are detected at the surface of the embedding medium using either piezo- electric or optical detection sensors [8]. However, piezo-electric sensors are the most frequent used receptor in current photoacoustic techniques [10].

Piezoelectricity (electricity resulting from pressure) is a property of certain crystals in which a mechanical stress generates a voltage [7]. This electromechanical interaction between the mechanical and the electrical state in crystalline material allows piezoelectric crystal to detect pressure variation on its surface created by the impact of a sound, generating a voltage proportional to the product of the amplitude of the wave and the receiving constant of the crystal  $g$  (potential produced by a unit strain) [7, 13]. In the regular disposition electrodes are placed on both sides of a crystal. One side of the crystal is fixed to a damping so-called backing material, the other side can move freely [18]. When an acoustic wave reaches the surface, the material is compressed or expanded, inducing a voltage change on the electrodes, as illustrated in Fig. 3. This behavior is explained by the resonance exhibits by the piezoelectric crystals which occur only if the wavelength of the incident wave equals the double of the length of the crystal  $L_T$  as given in (3) [7]. The frequency of resonance is given by  $f_T$ , given by (4). [7]. Generally, these transducers are thought to have a wide band of detection around the frequency of resonance.

$$L_T = \frac{\lambda}{2} \quad (3)$$

$$f_T = \frac{c}{L_T} \quad (4)$$

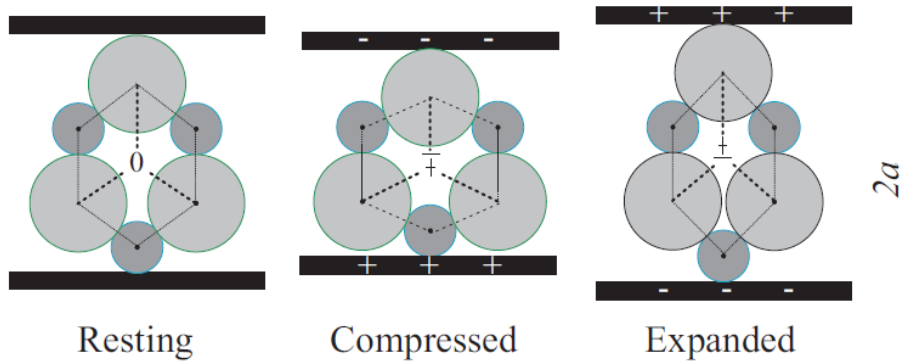


**Fig. 3.** Piezo-electric crystal at different states on acoustic wave reception sequence [18]

#### **2.1.2.4. Image Reconstruction**

Like in other imaging modalities as CT, MRI and US, the biggest challenge of PAT lies in image reconstruction associated with the inverse problem. Many approaches have been studied to solve this problem in PAT techniques. Analytic back-projection algorithm, finite-elements, Radon transform, Fourier domain analysis, diffusion equation based reconstruction and weighted delay-and-sum /synthetic aperture algorithm are some of the approaches that have been tested in PAT image reconstruction [7]. The weighted delay-and-sum algorithm is the most widely used in pure acoustics and has been shown to be suitable for PAT techniques [19].

#### **2.1.2.5. PAT Systems**

As mentioned before, the PAT systems can have multi-scalability. Due to this fact there are different levels of PAT systems. According to their imaging formation mechanisms and scale, PAT systems can be classified into four categories [14]:

- Raster-scan based photoacoustic microscopy (PAmic);
- Inverse-reconstruction based photoacoustic computed tomography (PACT);
- Rotation-scan based photoacoustic endoscopy (PAE);
- Hybrid PAT systems with other imaging modalities.

In the PAmic group techniques such as confocal microscopy (CM), orthogonal polarization spectral imaging (OPS), optical coherence tomography (OCT) are included [12].

In the PACT group one can consider 3 sub- groups: Diffuse optical imaging devices, Photoacoustics imaging with NIR and Photoacoustic imaging with green light [5, 12] . In the first group, time-of-flight (TOF) tomography and frequency-modulated (FM) tomography are some examples of techniques [12].

The devices of PAmic group, group with microscopic purposes, namely CM, OPS and OCT, require largely unscattered photons with a well-defined wavefront that allows for strong focusing giving high resolution [12]. Scattering effects such as poor focusing and loss of polarization begin to be felt after a few mm in depth in tissue, leading these devices to the region of high resolution at low imaging depths [12]. On the other hand, the diffuse techniques such as TOF tomography and FM tomography make use largely of photons that have undergone multiple scattering which penetrate deep into tissue leading to deep imaging but with low resolution [12].

Finally, Photoacoustic imaging with NIR and visible light as green fills the gap between the microscopies and diffuse imaging possessing high resolutions of the order of 50  $\mu$ m to a few mm at imaging depths of 10–40 mm as show in Fig. 4 [12].

These intermediate resolutions shown by these techniques are due to the lower scattering of ultrasound in tissue and the frequency characteristics of the ultrasound detectors that are used; by other side, imaging depths depend on the wavelengths of light used: shorter wavelengths such as green light penetrate to lower depths while the longer red and near-infrared wavelengths have high penetrations in soft tissue [12].

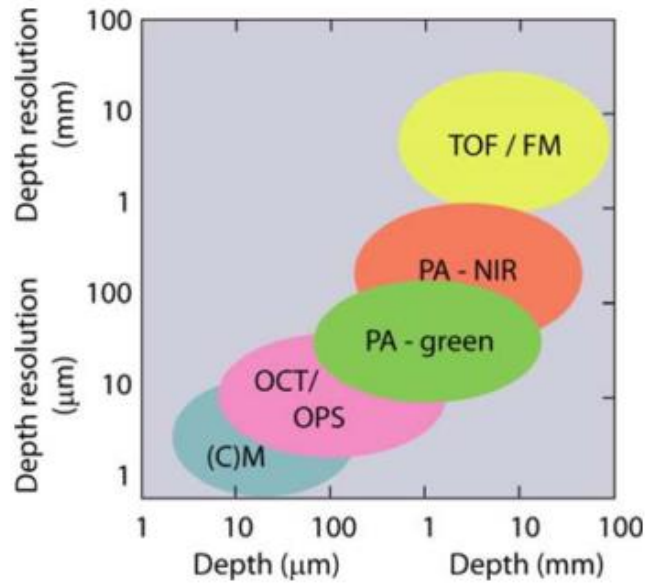


Fig. 4. Depth and resolution for optical methods for imaging hidden structures tissue [12]

#### 2.1.2.5.1. PAT Systems in Breast Imaging

In the last 15 years some PAT prototypes dedicated to breast imaging have been reported. In 2000 *Kruger et al* presented the Thermoacoustic Computed Tomography (TCT) scanner for the first time [20]. The TCT uses for excitation radiation at a frequency of 434 MHz [20]. The TCT acoustic receiver consists of three planar arrays with 128 elements, with a wide-bandwidth of 1 MHz, each arranged in a way that when rotated the pendant breast provide a whole coverage of the breast (angular view of 360° [20, 21]. The functional feature controlled is the concentration of ionic water in three dimensions (3D), which is expected to be enhanced at a tumor due to angiogenesis [20]. The latest version of TCT system has a spatial resolution of 1-2 mm and a penetration depth of 40-45 mm [21].

Later, in 2003, *Oraesvsky et al* introduced the Laser Optoacoustic Imaging Systems (LOIS) [22]. In its first version this system used as excitation probe light pulse at 1064 nm from an Nd:YAG laser, in 2009 the system has readjusted to use Q-switched Alexandrite laser of 757 nm. The designed acoustic system was an arc shaped with a ultrawide-bandwidth (10 MHz) of 32 elements in the prototype and 64 elements in the latest version (2009), providing 2-D slice images and 3-D images with an angular view of 120° [23, 24]. The functional feature measured with the selected wavelengths is the concentration of oxyhemoglobin and hemoglobin is also expected to be enhanced at a

tumor due to angiogenesis. The measured spatial resolution of LOIS is 0.5 mm and the penetration depth is 20 mm [24].

Finally, more recently in 2008 *Pramanik et al* developed a hybrid prototype that combines PAT and thermo-acoustic imaging (TAT), considering a dual contrast induced or by microwave (the source is an air-filled pyramidal horn type antenna at 3 GHz) either by light (Nd:YAG at 1064 nm) [3, 25]. The different sources can be applied simultaneously or alternatively [25]. The authors states that the motivation to combine such sources are the need to decrease the acquisition time, to optimize the cost effectiveness of the procedure, and the possibility of acquiring two images in the same setup avoids moving and realigning the patient all over again [25]. The all PAT-TAT system design allows to acquire 3-D images of the breast for a full 360° perspective scanned by a 13-mm/6-mm-diam active area with non-focused transducers operating at 2.25 MHz central frequency with a resolution of 1.2 mm and 0.7mm, respectively [25]. The maximum penetration depth of the laser beam is not mentioned by the authors.

### **2.1.3. PAM**

In this section, it is presented the primary design settings and the results obtained with the photoacoustic mammoscope (PAM) developed at the University of Twente. This system is described in detail by *Manohar et al* [8, 10, 26], *Piras et al* [3, 11] and *Jose et al* [12]. It is also given an overview of the clinical studies that have been done so far, described by *Manohar, 2007* [27], *Heijblom, 2011* [28], *Heijblom et al, 2012* [29], [30]. Finally, it is also introduced the results obtained by different assessment studies described by *Hilgerink, 2009* [31]; *Haakma W. [32], 2011*; *Roelvink, J., 2012* [33].

#### **2.1.3.1. System Overview**

Unlike the other PAT devices mentioned in *section 2.1.2.5.1*, the PAM system employs mild compression of the breast between the window of illumination and a flat array ultrasound (with 590 elements) detector in a parallel plate geometry. According with the designers, this geometry has been chosen to facilitate imaging of deeply embedded tumors, which may remain undetected in the pendant breast [26]. The parallel plate geometry also brings another advantage because it makes possible to compare PAM images with X-ray images [3]. The used optical source is a Q-switched Nd:YAG laser operating at 1064 nm with 5/ 10 ns pulses and a 10 Hz repetition rate [26]. As illustrated in Fig. 5 the forward ultrasound detection is performed opposite to the light source from the perspective of the objective.

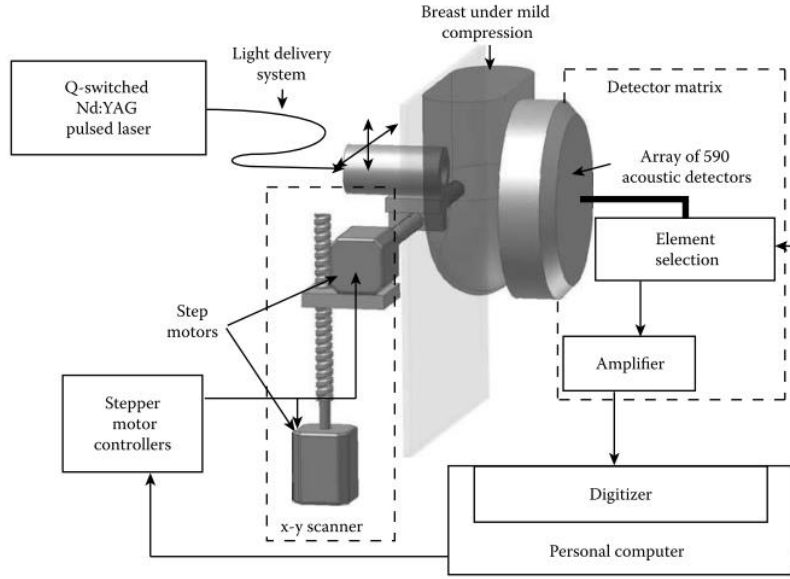


**Fig. 5.** Schematic of PAM [3]

The PAM in association with the delay-and-sum image reconstruction algorithm shows a maximum imaging depth up to 15-60 mm below the illuminated tissue surface, depending on the size and contrast of the absorbing object and a spatial resolution 3–4 mm, depending on the depth of the embedded object. The Table 1 shows the relevant technical specifications of PAM.

<b>Laser</b>	
Wavelength	1064 nm
Pulse width	5/ 10 ns
Repetition rate	10 Hz
<b>Detector</b>	
Matrix shape	Circular
Matrix size	85 mm diameter
Number of elements	590
Element Size	2x2 mm
Element Pitch	3.175 mm
Central Frequency	1 MHz
Bandwidth	130 %
<b>Reconstruction</b>	
Algorithm	Delay and sum
Lateral resolution	2.3-3.9 mm
Axial resolution	2.5-3.3 mm

**Table 1.** Relevant technical Specifications of the Photoacoustic Mammoscope. Addapted from [10, 11]

### 2.1.3.2. The Ultrasound Detector

From the characteristics of the ultrasound detector the most important definitions of the whole system are defined, such as resolution, penetration depth and acquisition time.

The used detector array is an adapted version for PAT, original designed by General Electric Lunar for bone imaging. The detector are made of a piezoelectric film,

specifically, poly vinylidene film (PVDF), 110  $\mu\text{m}$ -thick [12]. The film is covered with 590 gold electrodes defined by 2x2-mm and is supported and protected by a high-density polyethylene (HDPE) layer (18 mm-thick), which has acoustic properties similar to the tissue and forms the face of the unit [12, 26]. The 590 elements are arranged in a circular shape (diameter  $\approx 85$  mm) in a way that there are left 3.175 mm between the consecutive elements in x and y direction as illustrated in Fig. 6 a) . The central frequency of the detector is 1 MHz with a fractional frequency  $-6$  dB BW of 130% extending from 450 KHz to 1.78 MHz [3, 26].

The electrical contacts to the rear-face electrodes (covering the PVDF film) are obtained by spring-loaded conductive pins contacting the film against the PVDF film allowing to minimize the reverberation [3]. The conductive pins are mounted as a 590-element grid on a PCB (printed circuit board) , and lead on to signal processing and multiplexing electronics [12]. The elements are grouped into 10 sectors of approximately 60 elements each, as shown in Fig. 6 b) [26]. Below each group there's a connection with a buffering and amplification system - Application Specific IC (ASIC's). Each group of elements, or each ASIC has a single output, which leads to a summing amplifier. The element selection is made electronically selecting one or more of the 590 elements at a time, which increases the measurement times when a small number is defined and a large area needs to be imaged [26]. Fig. 7 shows a signal received by one single element. According the ROI dimension, each measurement requires an activation of a certain number of elements. The number of averages by element is also variable and defined by the user. According with the chosen scan configuration, normally, each element receives 90 or 30-60 averages [28, 30].

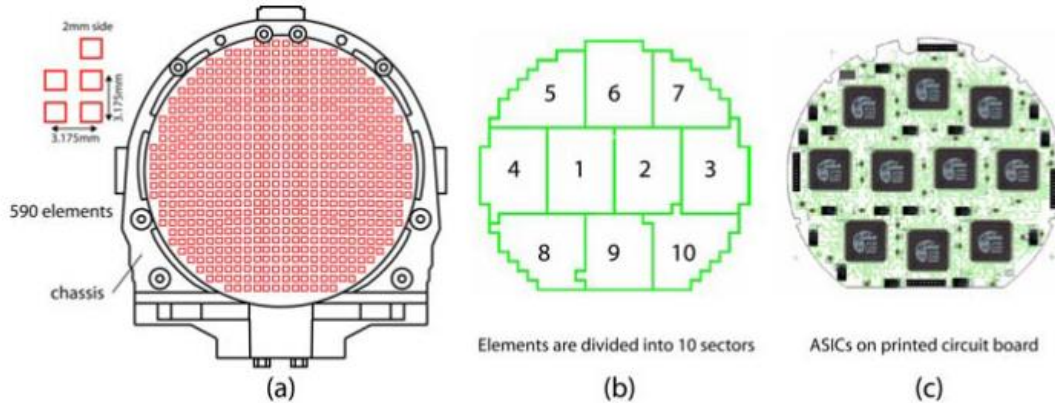


**Fig. 6.** The flat ultrasound detector array showing (a) arrangement of the elements, (b) grouping of elements into sectors, with (c) each group leading to an ASIC [12]

The element selection is made through a digital input-output card in the PC. The data line is fed to one channel of a dual-channel 100 MHz, 100 MS/s 8 bit digitizer in the PC [26]. These three components, the detector array, the digitizer, and the scanning system are controlled by a Labview™ program [26].

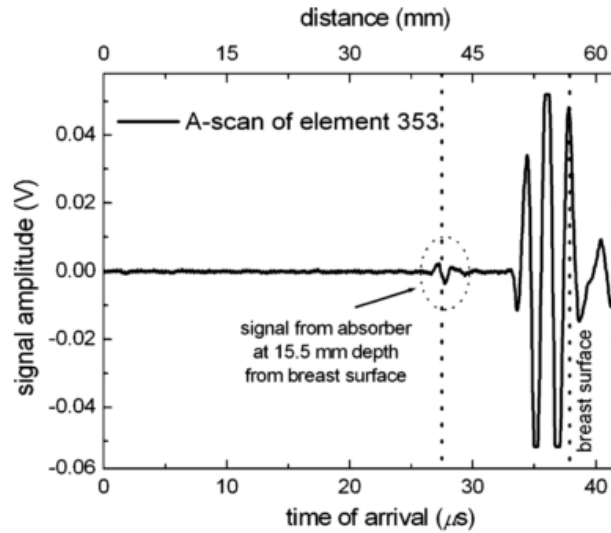


**Fig. 7.** Signal trace of an element showing the PA signals arising from the irradiated tissue: A large signal produced at the breast surface at a depth of approximately 15 mm from the illuminated surface the signal is detected [11]

### 2.1.3.3. The Laser and Light Delivery System

The imaging contrast that it's achieved depends largely on the appropriate choice of the wavelength of the tissue excitation source, the laser. As mentioned, the PAM system uses a Q-switched Nd:YAG laser (Brilliant B Quantel, Paris) capable of delivering up to 800 mJ (Deep imaging using the detector requires at least 50–60 mJ per pulse at 1064 nm with at least 100 averages) at 1064 nm in 5/ 10 ns pulses repeating at 10 Hz [3, 26].

Laser safety standards in most of the countries of EU permit a maximum permissible exposure of  $30 \text{ mJ/cm}^2$  per pulse for a pulse train of 100 pulses, for the laser class (1064-nm, 5-ns pulses, 10 Hz) in use [3]. In order to suit to these limits while meeting minimum energy requirements to acquire deep imaging, the laser beam in the regular scan configuration has 16 mm and is based on a geometry with two prisms and two movable joints [3].

Due to the fact that only one element of the acoustic detector is activated at a time in the first versions of PAM, illumination of the entire breast surface is not necessary. Thus, the laser beam is translated in steps in an x-y plane to illuminate the region of interest (ROI) while at each opposite position an element of the detector is activated [3, 26]. This method of scanning, called “tandem scan”, has been the most used but it is not the only (the other will be explained in further sections). The scanning system is enclosed within a compartment that has a glass window, which contacts the breast and compresses it against the detector array, as shown in Fig. 8 [26].



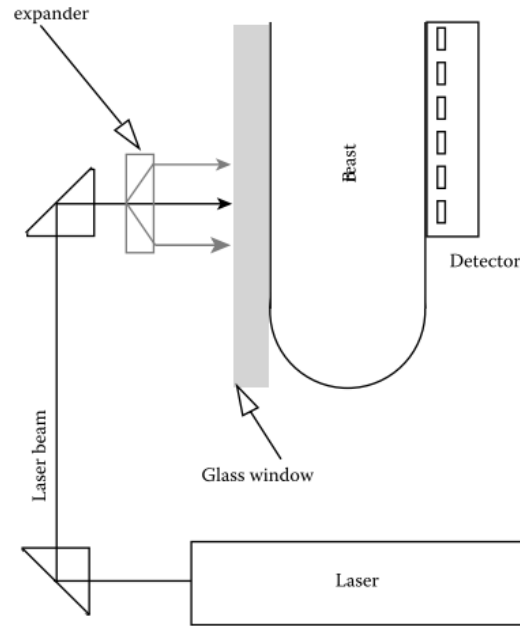


**Fig. 8.** Schematic of the instrument showing the light delivery system [26]

#### **2.1.3.4. The Patient-user Interface**

The present PAM system configuration has been already implemented in the *Medisch Spectrum Twente* Hospital located in Oldenzaal and it has been tested in clinical trials.

The system configuration, shown in Fig. 9 b) was the result of a modification of a hospital bed to accommodate the instrument. According with *Mahonar et al, 2009* the ideal patient position and procedures during the measurement are the following: the patient lies prone on the bed with her breast through the aperture and the breast is positioned between the glass plate of the scanning system compartment and the flat detector [26]. The detector is mounted on a linear stage that can be manually moved to compress the breast mildly against the glass window, the laser is mounted on the frame of the bed below as illustrated in Fig. 9 a) [26]. There is a laser safety curtain enclosing the instrument and is kept closed during measurements to protect third elements from scattered and/or reflected laser light [26]. For acoustic coupling between the breast and the detector uncolored ultrasound gel was used [29].

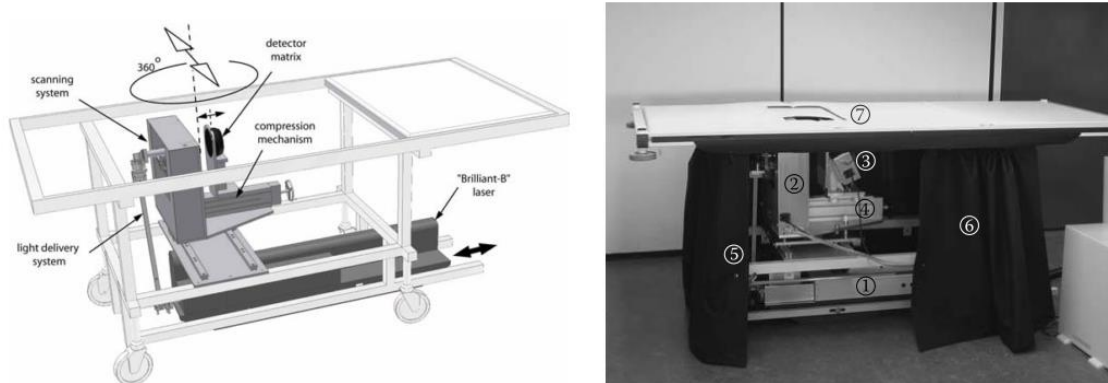


**Fig. 9.** a) General mechanic configuration of PAM [12]. b) A photograph of the PAM. 1: Laser, 2: scanning system compartment, 3: ultrasound detector electronics, 4: linear stage functioning as compression mechanism, 5: part of light delivery system, 6: laser safety curtain, and 7: aperture to insert breast impulse [26].

### 2.1.3.5. Image Reconstruction

Like the general PAT devices, the reconstruction of the images captured by PAM is made by the weighted delay-and-sum algorithm, implemented in MATLAB.

The general procedure of this algorithm is partially illustrated in Fig. 10. In this algorithm, the first step is divide the imaged volume in small elements of volume, the voxels; the positions within this window is determined by the distance between the voxel to be reconstructed and the specific detector element, assuming a constant speed of sound within the breast; the time-domain detected signal is used to determine whether a potential photoacoustic source is present in each voxel [7, 29]. The contribution of each transducer in the array is calculated for each voxel, based on the delay and the traveling time (and the weighting factor based on the directivity of the transducer) [7]. Then, each weighted signal is summed for each voxel forming the reconstructed volume [7]. As mentioned the weighting factor depends on the directivity of the transducer, that comes from the fact that the detector is not equally sensible to waves depending on their direction of propagation, mostly due to interference and refraction and depth [7, 28]. Optimizing the weight factors can lead to optimal signal to noise ratio (SNR) [7].

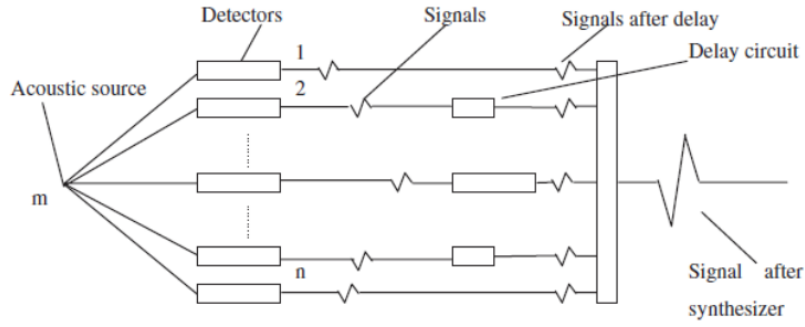


**Fig. 10.** The delay applied to each signal depends on the distance between the source of interest and the transducer. Signals are summed after the delay is applied. Weighting is not shown in this figure. Delays are generally applied in post-processing[7]

### 2.1.3.6. System Performance

The most important performance characteristics of the system are the resolution and maximum achieved imaging depth. The Table 2 shows a Comparative Performance between PAM and other PAT devices.

Device	Resolution (mm)	Correspondent penetration depth (mm)	Reference
TCT	1-2	40- 45	[21]
LOIS	0.5	20	[24]
PAT/TAT	0.7-1.2	-	[25]
PAM	2.3 – 3.9	15 – 60	[26]

**Table 2.** Comparative Performance between PAT devices

#### 2.1.3.6.1. Resolution

The most important factor that defines the resolution is the ultrasound detector characteristics, such as the number of elements used, element pitch and frequency bandwidth (BW), directional sensitivity the detector-source distance and the applied image reconstruction algorithm [3, 26].

As mentioned in the *section 2.1.3.2.* , the central frequency of the PAM detector is 1 MHz with a fractional frequency –6 dB BW of 130% extending from 450 KHz to 1.78 MHz, with the maximum detectable frequency ( $f_{max}$ ) of approximately 2.5 MHz [26].

The smallest diameter that can be resolved by an imaging system is theoretically given by (5) [26].

$$d_0 = 3 * \frac{v}{f_{max}} \quad (5)$$

For the present configuration of PAM (5) yields that the resolution is 1.8 mm.

The experimental assessment of the system's resolution was achieved by the designers examining the imaging system's impulse response, this is the point- spread function (PSF), using a 2-mm sized highly absorbing gel sphere (P2) suspended at a

depth of 30 mm from the surface and immersed in a low scattering liquid medium, a intralipid (P3) [3, 12, 26]. Images of the gel sphere were obtained from an area of 52 x 52 mm (corresponding to 15 x 15 elements), which according with the designers is representative for the clinical measurement situation [26]. From that images, a profile of the PSF along the y-axis in the XY plane, fitted to a Gaussian distribution was built estimating the full width at half maximum (FWHM) of the PSF. From this, the resolution is finally obtained by deconvolving the P2 gel sphere size of the object from the FWHM [26]. In this particular case, the lateral resolution of the system for objects located at distances of 30 mm is 2.3 mm.

In Fig. 11 it is shown the dependence of the axial and lateral resolutions on the distance between the object and detector.

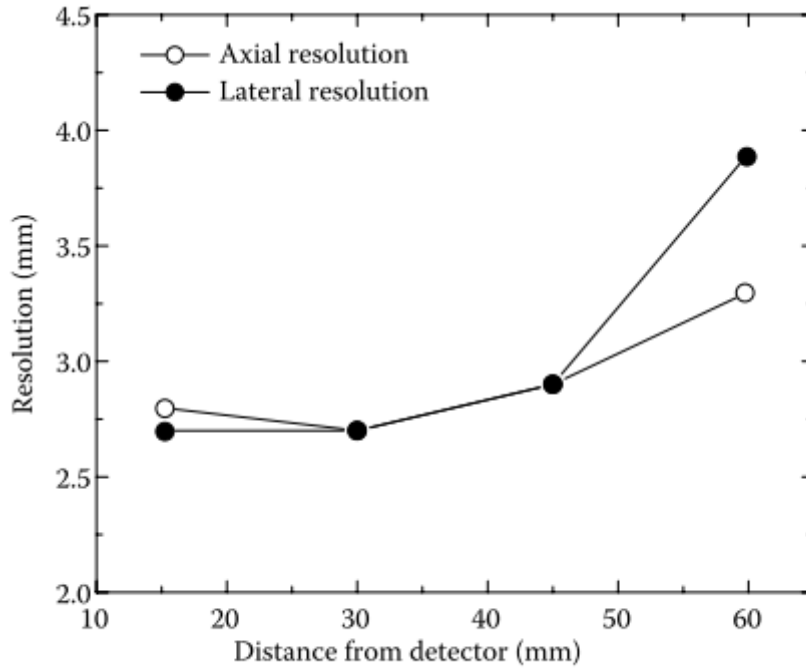


**Fig. 11.** Variation in axial and lateral resolutions for different depths of absorbers from the detector array [26]

### 2.1.3.6.2. Maximum Imaging Depth

As mentioned in the *section 2.1.2* optical attenuation is an important limiting factor for penetration depth, since photoacoustic waves are generated only where photons can reach. In this context it is crucial to know precisely the maximum imaging depth that one system can reach.

To calculate the expected maximum imaging depth, the designers used the knowledge optical energy absorbed in spherical structures of various sizes and absorption coefficients that can be easily calculated making simulations, modeling the energy fluences at various depths in tissue, mimicking materials response for radiant exposure at the surface of 20 mJ/cm<sup>2</sup>, considering similar optical property values for breast tissue from the literature [3]. With this was possible to calculate the pressures generated, and in combination with the specific MDP (Maximum designed pressure) of

the detector (the MDP can be rearranged by signal averaging or by increasing the number of detectors), it is possible to determine whether the pressure signal from a certain absorber at a certain depth is above the detection threshold [3, 26]. Using this approach, the designers calculated the maximum imaging depth for detecting different combinations of a hypothetical absorber, a sphere. It was tested 2 diameter sizes- 2-mm-sized and 5-mm-sized – for different levels of contrast 2x, 4x and 7x with respect to the background [3, 8]. The different combination results are shown in Table 3. As a consequence, it is logical that for tested combination with higher contrast and larger dimensions, the maximum imaging depth will be higher [3].

Absorbing sphere diameter (mm)	Contrast	Maximum Imaging Depth (mm)
2	2x	23
	4x	26
	7x	29
5	2x	27
	4x	30
	7x	32

**Table 3.** Simulated maximum imaging depth for different inhomogeneities dimensions and for different level of contrast with respect to the background [3]

Experimentally, this system was tested using a phantom, a poly(vinyl alcohol) (PVA) gel, that was chosen for having acoustic properties similar to the breast tissue, namely the absorption coefficient, the reduced scattering coefficient and the effective attenuation coefficient [8]. The phantom was placed with water in an imaging tank constructed with Perspex with an aperture at the bottom, through which the detector matrix is fitted as shown in Fig. 12 a) and b) [8].

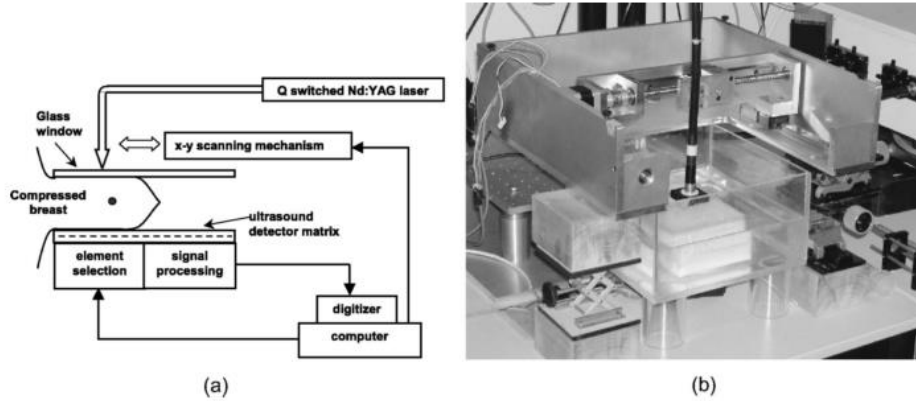


**Fig. 12.** a) Schematic diagram of the concept of the photoacoustic mammoscope, based on a parallel plate geometry. (b) A photograph of the PAM laboratory prototype [8]

The inhomogeneities, absorbing spheres of 2- , 5- and 10-mm diameter with 2x, 5x, 7x and 10x were embedded in the phantom background at various depths [3, 26]. Images were obtained by a scan area of typically 37x31 mm comprising 12x10 elements of the array averaging over 100 pulses [3, 26]. Fig. 13 shows how each pixel stores the average value encountered through the voxels in all slices along a viewing ray, the average intensity projection (AIP) [8]. This signal intensity projections appear in the 3-D reconstructed data of selected VOIs in the phantom for different levels of contrast and

imaging depth [8]. The results obtained by this method are similar to the ones from simulations, with for example, an object of 2-mm diameter with a contrast of 7x being detectable at a depth of 32 mm (In simulations was 29 mm).

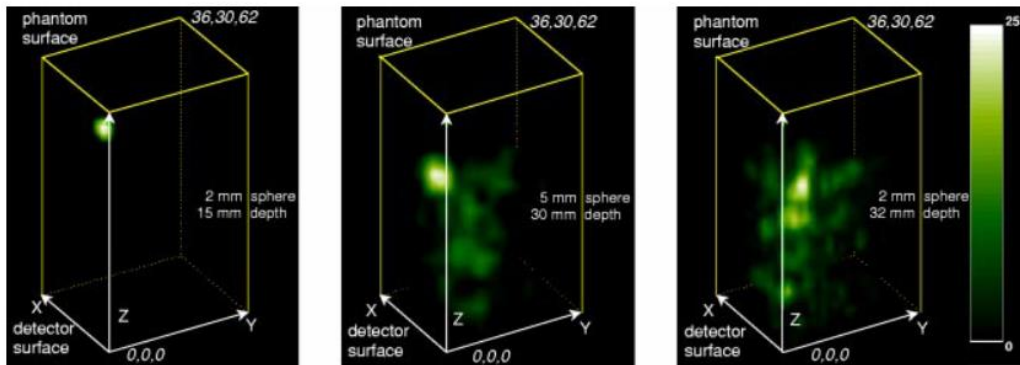


**Fig. 13.** AIP in 3-D reconstructed data of selected VOIs in the phantom: *Left*- the VOI containing the 2-mm-diam sphere of absorption contrast 4 at a depth of 15 mm. *Center*- VOI with 5-mm-diam sphere with contrast 7 and 30 mm from surface. *Right* - VOI with 2-mm-diam sphere with contrast 7 and depth 32 mm from surface [8].

### 2.1.3.7. Clinical Studies

In 2007 the first pilot study was conducted [27]. According to the designers, the most important aims at this stage were to evaluate the feasibility of the technique embodied in PAM in detecting breast tumors in symptomatic subjects, to corroborate the earlier performances on phantoms and to compare clinical, pathological, and conventional imaging findings with PA images in order to understand in retrospect the correspondence between the PA images and morphological and pathological features of tumors[26]. Finally to effect technological changes based on experiences as above, and carry forward various results to prepare the instrument for a more rigorous evaluation [26]. The results were obtained from a group of 5 technically acceptable measurements on patients with symptomatic breasts, and were globally positive: 4 of these cases revealed PA contrast associated with tumor-related vasculature [26]; and 1 was especially significant due to the fact that benign indicators dominate in conventional radiological images, while photoacoustic images reveal vascular features suggestive of malignancy, which is corroborated by histopathology [27]. The most important disadvantage detected at this point was the need to reduce the measurement times [27].

Based on the first pilot study, a large clinical study using PAM has been started in December 2010. The trials took place in the Center for Breast Care of the Medisch Spectrum Twente Hospital in Oldenzaal, Netherlands. The purpose of the study was to include up to 100 patients until January 2014 [28]. Patients within the normal diagnostic path at the Center for Breast Care, in between conventional radiology (X-Ray mammography and US exams) and the biopsy were asked for cooperation to the study [28]. According to the designers the study was divided into three phases [28]: in the first phase the purpose was to focus on a small number of patients with lesions that are highly suspicious for malignancy allowing to optimize the imaging methods for the visualization of malignancies. This phase has been completed in April 2011 and the

results including 12 patients have been reported in *Heijblom et al, 2012* [29] . In phase 2 of the study, a large number of patients with lesions that are suspicious for malignancy are measured in order to define the photoacoustic markers that are indicative for the presence of a malignancy. This phase has been completed in April 2012 and the results including 23 patients have been reported in *Heijblom et al, 2012* [30]. Finally In the last phase of the study, in process at the moment, the absence of those photoacoustic malignancy markers will be verified in subjects with either healthy breast tissue or with benign lesions.

### 2.1.3.7.1. Measurements

During the trials, the patient position to make the measurement followed the description in 2.1.3.4. The whole measurement system is illustrated in Fig. 9 b). The following table shows an overview of the whole clinical and technical specifications applied in the different phases. Some technical details will be explained in the next sections.

Period	Phase 1	Phase 2	Phase 3
	December, 2010- April, 2011	April, 2011 - April, 2012	April 2012 – January, 2014 (Expected)
N° of technical accepted measurements	12	23	65 (Expected)
Number of elements activated at a time	1	1	10
Typical ROI dimension	4x4 cm <sup>2</sup>	4x4 cm <sup>2</sup>	8x8 cm <sup>2</sup>
Scan Configuration	“Tandem Scan”	“Tandem Scan” and “Fixed Scan”	“Tandem Scan”
High Contrast Threshold	50%	50%	50%
Time of each measurement	25 min	25 min	10 min

**Table 4.** Overview of clinical and technical definitions by trial phase.

### 2.1.3.7.2. Illumination and Scan Configuration

The illumination and scan configuration are limited by a important condition, the maximum permissible exposure (MPE), normally 30 mJ/cm<sup>2</sup>, which is the maximum level of electromagnetic radiation to which a human subject may be exposed [30] From this issue comes the necessary trade-off between the increase in pulse energy that require the use of extremely powerful lasers and the effect of an increase in beam diameter [30]. Due to this fact in part of clinical trial (phase 2) it was tested two different scan configurations named: “Tandem Scan” and “Fixed Scan”.

In both configurations, the breast was illuminated with the optic system described in 2.1.3.3. pulsed at 1064 nm with a 10 ns pulse duration, instead of the 5 ns applied in the tests with phantoms an in the pilot study. The repetition rate remained equal - 10 Hz. The photoacoustic signals reception was made by the acoustic detector

described in 2.1.3.2. Each of those detector elements was activated one at a time and in order to scan a previously defined ROI of the breast [28]. The ROI definition was generally made using the information provided by the ultrasound and x-ray images [29]. In the “Tandem scan”, the breast was illuminated with a 2.5 cm<sup>2</sup> laser beam having a fluence of about 25mJ/cm<sup>2</sup>, scanning across the previously defined ROI [30]. At each position of the illuminating beam, the correspondent element was activated and the average of 90 signals was acquired [30].

In the “Fixed scan” the beam size was increased to more than 30 cm<sup>2</sup>, while the fluence was decreased to less than 10 mJ/cm<sup>2</sup> [30]. In this case the illuminating beam was kept at a fixed position during the whole measurement, while the detector elements within the ROI were activated one at a time [30]. In this case the number of averages per acquisition was reduced to 30-60 to find the optimal trade-off between scan area, scan time and lesion contrast [30].

### 2.1.3.7.3. Data Handling

The signals were reconstructed offline with a delay and sum reconstruction algorithm implemented in MATLAB, as described in 2.1.3.5.

After reconstruction, the resulting image volumes were compared to X-ray, ultrasound, and MRI (if available) images in terms of size and shape of the abnormalities. The image analysis was made in regions with high contrast considering their size and contrast with respect to the background [28]. The way that these high contrast regions are defined is important because it can change strongly the obtained results. In these trials the high contrast regions were defined by the area in which the intensity value of all pixels was more than 50 or 25% of the maximum intensity value within that specific slice respectively[28].

$$SNR = \frac{A_{lesion}}{A_{background}} \quad (6)$$

A<sub>lesion</sub> - the mean pixel value within the lesion;

A<sub>background</sub> - the mean pixel value outside the lesion;

For this, the knowledge of the contrast or the signal-to-noise ratio (SNR) of the abnormality with respect to the background was crucial.

This ratio was yield by (6) [28]. Consequently, the maximum diameter of the high and moderate contrast regions was used to compare with malignant area measured by histopathology, the golden standard method for such measurement.

In phase 1, for each patient, the fibroglandular breast density was estimated on the x-ray mammogram by a breast radiologist according to the BI-RADS breast density classification scale [29].

### 2.1.3.7.4. Results

#### Phase 1

In the first phase of the study, 17 patients were included in the study. However three patients could not be measured either because of discomfort or due to difficulties accessing the region and 2 of the remaining were technically unacceptable due to poor



acoustic contact between breast and detector in the ROI [29]. The Table 5 presents the main results from the first phase of clinical trials.

	Lesion Type	PAM lesion visibility (Positive Contrast)	PAM lesion contrast	X-ray lesion contrast	PAM – max diameter (mm)	Lesion Size (Histopathology)	BI-RADS Breast Density
1	Mixed IDC, ILC	Yes	3.2	1.6-4.7**	24	30	1
4	IDC	Yes	6.4	1-2.6 **	10	15	4
5	ILC	Yes	3.3	1.9	***	42	3
6	IDC	Yes	6.2	1.0	***	13	3
7	Mixed IDC, ILC	Yes	5.3	2.6	14	27	1
9	IDC	Yes, two lesions	1) 5.3 2) 4.7	3.5	1) 14 2) 26	31	2
10	IDC	Yes	4.5	1.2	13	>30*	4
11	Cyst	No	1.0	1.0	Not visible	28 *	4
14	IDC	Yes, scattered abnormality	4.0	3.8	Scattered	>40*	1
15	Cyst	No	1.0	1.0	Not visible	42 *	4
16	IDC	Yes	7.0	3.4	9 mm	33	2
17	IDC	Yes	4.9	1.3	***	27	1

**Table 5.** Measurement results from PAM in the phase 1 of clinical trial. In patients 10-15, the lesion size was estimated radiologically, since there was no histopathological measurement available. \*\*These lesions were positioned partly in fatty tissue and partly in fibroglandular tissue. Therefore, the contrast for these lesions on x-ray mammography is given with respect to both types of background. \*\*\* In these measurements the defined lesion was only partly positioned within the region of interest and the maximum diameter could not be assessed. *Adapted from [29].*

As example, the Fig. 14 a),b), c) d) shows images from a 15mm infiltrating ductal carcinoma obtained respectively by x-ray mammography, ultrasound, MRI and PAM. The abnormality is visible in PAM image, however the size of the ROI dimensions is quite short due to threshold for High- contrast region that was used – 50%. Figure 13 d) shows the imaging planes for MRI, x-ray and PAM. These are comparable, but the region of interest of PAM is small compared (for the reasons mentioned) to that of MRI and x-ray, which image the complete breast. The imaging plane of ultrasound is dependent on the position of the ultrasound probe [29].

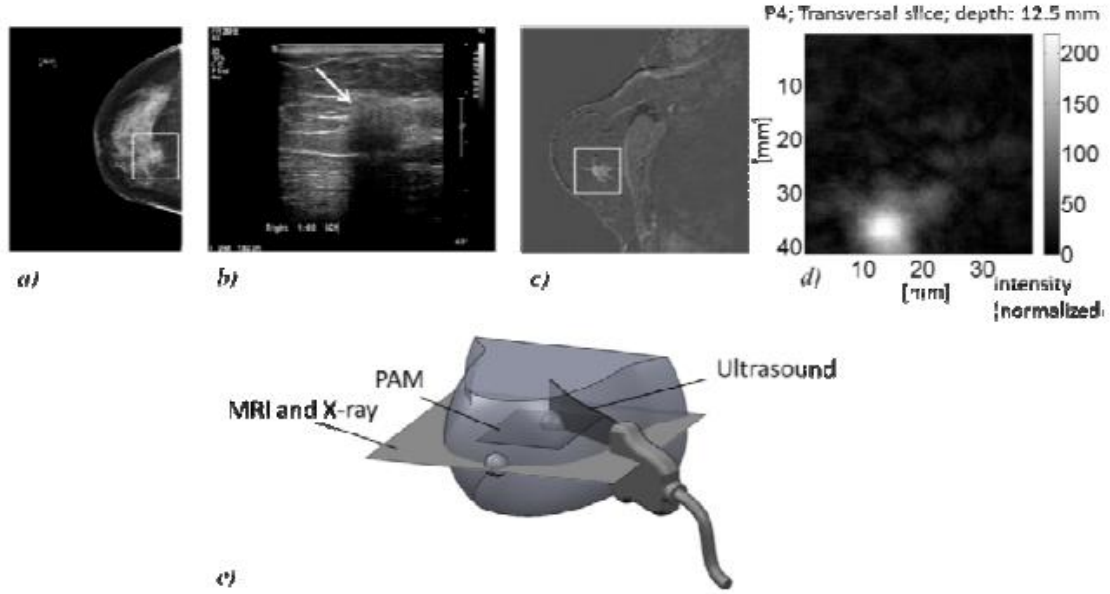


**Fig. 14.** Diagnostic images of a 15mm infiltrating ductal carcinoma a) The cranio-caudal x-ray mammogram shows a 20 mm lesion with a calcification (white box) and is highly suspicious for malignancy. b) The ultrasound image shows a 17.5 mm lesion with an arrow form. c) The transverse view of the T1 weighted MRI after gadolinium injection confirms the presence of malignancy because of the enhancement of an 18 mm lesion (white box) in the medial upper quadrant of the right breast. This image is rotated to match the orientation of the cc x-ray view. d) A transversal cross-section with a slice-thickness of 0.24 mm through the photoacoustic volume at the expected lesion location shows a confined region with high contrast with respect to the background. With the chosen threshold for abnormality definition, the contrast of the abnormality in the 3D volume is 6.4 and the maximum diameter is 10 mm. This image is rotated to match the orientation of the cc x-ray view. e) The imaging planes of the different imaging modalities used in this study. Indicated are the imaging planes for cranio-caudal x-ray mammography, transverse MRI, transverse PAM and a representative ultrasound view. [29].

In this phase of the clinical trial, the breast density was also compared with the lesion's contrast seen on both the PAM images and the x-ray mammograms with the given contrast between the low and high density groups was tested for significant difference using a Student's two-sample t-test. The results are shown in Fig. 15 a) and b) and as It can be seen the contrast on PAM is fairly constant for the different levels of breast density, while the contrast on x-ray mammography decreases with breast density. Besides, this phenomena is even pronounced when a division into two density categories is made, which is the most reproducible way of grading breast density [29]. The contrast of the lesion on x-ray is statistically different ( $p < 0.05$ ) between the high and low density breasts, while there is no statistical difference in the contrast of the lesions on PAM [29].

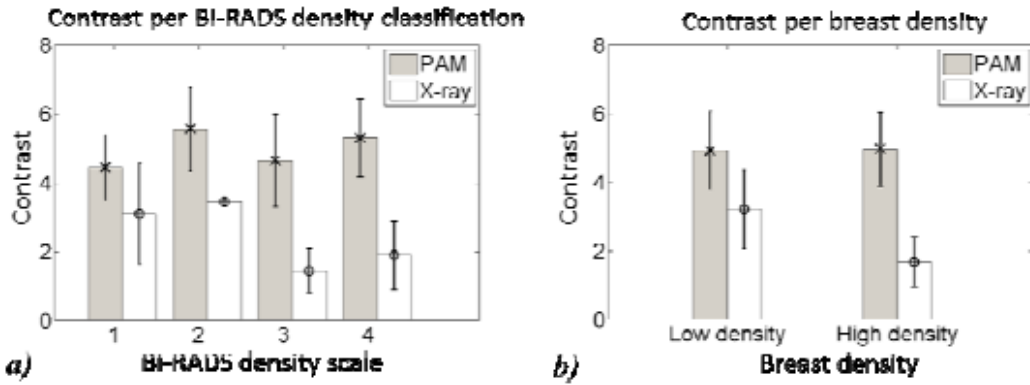


**Fig. 15.** a) Contrast Per BI-RADS density classification scale, the average contrast of the lesions on PAM (gray) and x-ray mammography (white) is given. b) Contrast Per BI-RADS density classification scale, segmented in ‘low’ (BI-RADS density 1, 2) and ‘high’ (BI-RADS density 3, 4) [29].

## Phase 2

In the second phase of the study, 23 patients were included in the study. Of those, 16 were on breasts with highly suspect breast lesions [30]. The 8 patients left 2 were measured in a test sub phase, 4 were on cysts, 1 was on a non-malignant lesion and 1 was on a healthy volunteer [30]. In opposition with the first phase of the clinical trials, that applied solely the “Tandem scan” configuration, the phase 2 has tested the 2 different scan configurations – “Tandem Scan” and “fixed scan”- previously described. The Table 6 shows the obtained results in the 16 malignant lesions imaged by PAM using different scan configurations: 10 measured using the ‘tandem-scan’ configuration and 6 measured using the ‘fixed scan’ configuration [30].

In this last set of measurements made using “fixed scan” configuration, 5 out of 6 abnormality in the tissues were clearly visible in PAM images with high contrast with respect to the background and 1 lesion was visible with low to moderate contrast [30]. The average contrast for these 6 lesions was 7.1 on photoacoustic mammography and 3.1 on x-ray mammography [30].

By other side, in the “tandem scan” the photoacoustic contrast was 5, and in x-ray mammography was 2.7 [30].

The contrast was significantly higher ( $p < 0.05$ ) in “fixed scan” configuration than for the ‘tandem scan’ configuration as is illustrated in Fig. 16. Although the average size deviation was smaller for the ‘fixed scan’ configuration (-33%) than for the ‘tandem scan’ configuration (-41%), results were not significantly different and, with -33%, the average size underestimation was still substantial [30].

	“Tandem Scan”	“Fixed Scan”
<b>N° of patients</b>	10	6
<b>Photoacoustic abnormalities with confined high contrast</b>	10 (9 patients)	7 (5 patients)
<b>Scattered photoacoustic contrast</b>	1 (1 patient)	0
<b>Photoacoustic abnormalities with low-moderate contrast</b>	0	1 (1 patient)
<b>Average contrast (50% threshold)</b>	5	7.2*
<b>Average size deviation (50% threshold)</b>	-41%	-33%

**Table 6.** Overview of the measurements results for the 2 scan configurations (only for the malignant lesions). \*This value is significantly different ( $p < 0.05$ ) from the value in the ‘tandem scan’ configuration [30].

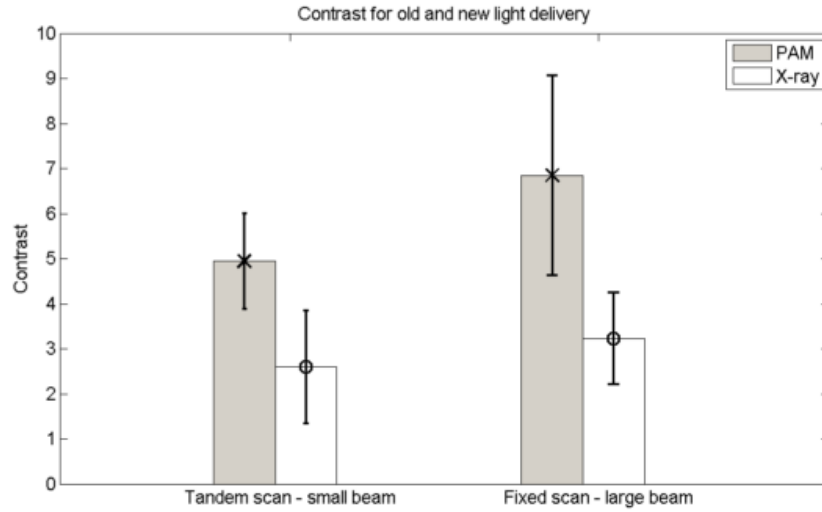


**Fig. 16.** The average contrast of the lesions on PAM (gray) and x-ray mammography (white) is compared between the two different image configurations. There is a significant increase in contrast for PAM when the image configuration is changed from ‘tandem scan’ to ‘fixed scan’ mode. Error bars indicate the plus and minus one standard deviation [30].

### Phase 3

Finalized the 2 first phases of the clinical trials the designers have focused their efforts in new steps to increase the measurement speed. In this pursuit, the phase 3 of clinical trials, in process, is being developed with a changed version of PAM considering a new acoustic reception scheme where 10 elements are activated at a time instead of 1 at a time and with a typical ROI of  $8 \times 8 \text{ cm}^2$  [34]. This new version made possible to decrease the measurement time to 10 minutes, even though the ROI is 4 times bigger [34].

## 2.1.3.7.5. Conclusions

### Phase 1

This first phase of the clinical trials helped the designers to make some important conclusions.

PAM visualized breast malignancies in women with a high imaging contrast and that performance seems to be independent of mammographic breast density as shown in Fig. 15. According with the designers, this behavior can be theoretical explained by the expectation that neither the total hemoglobin concentration nor the oxygen saturation is significantly different between the four BI-RADS breast density scales [29].

Although the results are limited, those have shown that cysts did not manifest in confined high-contrast regions [29]. The explanation is that the cysts are mainly water and water is not a prominent source for the photoacoustic signal. Even if cysts appear in PAM images, they would probably appear edge-enhanced due to the limited bandwidth of the transducers [28, 29].

Finally, the main disadvantage detected at this point was that lesion size determined by PAM was smaller than the determined by histopathology as shown in

Table 5. The designers suggested 2 main explanations for this fact. The primary explanation is related with the breast positioning and the amount of compression applied, both are varying between the different imaging modalities [29]. By other side, the level of the threshold to define the high contrast region influences the estimation of the lesion's extension. The optimal threshold still needed at this point future evaluations in a large number of patients.

## **Phase 2**

This second phase of the clinical trials helped the designers to make some important conclusions concerning the optimal scan configuration and about the lesion sizes underestimation by PAM.

The “fixed scan” configuration has shown to provide better contrast than “tandem scan”. The designers explained this improvement with 2 technical reasons: The primary reason is that in photoacoustic imaging, the amplitude of the generated pressure wave is proportional to the local absorption coefficient of the tissue and the local value of laser fluence [30]. And this is very relevant in “fixed scan” configuration because although the laser fluence at the breast surface was decreased, the total amount of energy per pulse was increased and as it is known that for a broader laser beam, more of this light power will be delivered inside a turbid medium [30]. The second reason is that a broad beam has much better penetration than a single narrow beam [30].

In general this new scan configuration has the advantage of providing a better distribution of the total fluence by the reasons already presented. Besides the artifacts due to the movement disappear in this “fixed scan” configurations as the illumination and ultrasound generation are the same for every acquisition. Therefore, the ultrasound generated in the tissues is measured by more elements and as a consequence the backprojection of the photoacoustic source will have more contributions, which will result in an improved signal to noise ratio [30].

The problem of lesion size underestimation, already reported in the phase 1, remained in the second phase. Besides the reason already reported of the threshold for the high contrast delimitation, still 50%, the designers added other one - the limited scan size of the system, more visible in the “Tandem scan” configuration, only a limited number of signals were used to reconstruct the lesion, consequently it might cause shape and size deviations, which can be simply overcome by extending the measurement area [30].

The step from ‘tandem scan’ to ‘fixed scan’ already made possible to reduce the number of averages per acquisition (from 90 to 30-60) while gaining image contrast. This leads clearly to the main conclusion that the designers could take from this phase of clinical trials: the measurement area can be increased without increasing the scan time [30].

Phase 3 has no results yet as it is still going; it will be finished only at 2014.

### 2.1.3.8. Assessments Studies

So far, 3 studies were conducted to assess the viability of clinical implementation of PAM: *Hilgerink, 2009; Haakma W., 2011; Roelvink, J., 2012* [31-33].

In December of 2009 Hilgerink presented the work titled “Implemented Scenarios and predicted performance of the Twente Photoacoustic Mammoscope as an alternative imaging modality in Breast Cancer Diagnosis” [31]. In this study Hilgerink proposed two research questions: What is the appropriate position for PAM in a diagnostic track, and does PAM perform equally or better compared to existing breast imaging modalities? And how can the implementation criteria be translated into development goals for the PAM, in order to improve its position with respect to alternative imaging techniques? In order to answer the research questions Hilgerink applied the methods Analytic Hierarchy Process (AHP) and the House of Quality to solve the first and the second questions respectively. The AHP selection is justified by the fact that it derives a assessment of a new technology through transversal discussions, considering social, cultural and technology context, between stakeholders with diverging backgrounds and therefore with diverse opinions about the relevance of the criteria for technology development. To achieve the best performance from the most important criteria (calculated through AHP) the author applied the methods of House of Quality using a comparison to justify the choice- House of Quality method is frequently used to link customers desires to engineering possibilities so in this case it is very intuitive to regard the experts as customers. To build the AHP framework, Hilgerink carried on a literature research based on the guidelines from different cancer institutions in Netherlands and some discussions with professionals to get the relevant criteria. The cost subcriteria resulted from an interview with the investment Medisch Spectrum Twente. The effectiveness subcriteria were provided from the radiology department of Medisch Spectrum Twente. The Patient comfort subcriteria was obtained from websites of the different cancer institute’s and societies. Finally, the safety/risk subcriteria were provided from a medical physicist of Medisch Spectrum Twente. According with the results obtained by the author the most important criterion in the design of a diagnostic breast imaging device is sensitivity, which is mainly determined by the performance of PAM concerning visualization of mass margins, mass shape and vascularization. The work finishes with some general conclusions to the designers namely improvements in the quality of the reconstruction algorithm, detector sensitivity, detector bandwidth and in the number of wavelength applied by the system. Moreover, from the overall performance on the costs, effectiveness, patient comfort and safety/risks criteria assessed, it can be concluded that PAM will be the most preferred alternative in the majority of scenarios. The exception is for the most negative scenario, in which MRI is wins over PAM. Therefore, from the overall results the author states that when implemented for diagnostic use, PAM use can be feasible and useful in if positioned at the start of the diagnostic track, as a substitute for the combined use of X-ray mammography and ultrasound.

In July, 2011, Haakma W. presented the work “Expert Elicitation to Populate Early Health Economic Models of Medical Diagnostic Devices in Development” [32].

In this work, the author purposed to address the following methodological research question: Is expert elicitation a valid approach to characterize uncertainty regarding the diagnostics performance of photoacoustics mammography in an early stage of development? In the pursuit of the answer, the author worked over PAM and used expert elicitation as the method to gather the knowledge and beliefs of experts regarding its performance. This procedure culminated in the quantification of probability distributions for the different performance parameters. For the expert elicitation 18 experienced radiologists (specialized, in examining images of breasts) were asked to estimate the importance of different tumor characteristics in the examination of images of breasts. Following this, the performance of visualizing these characteristics, namely TPR and TNR was estimated for both MRI and PAM based on existing MRI data (with a TPR of 263 out of 292, and a TNR of 214 out of 308) and specified the mode (the most likely value), the lower, and the upper boundaries within a 95% confidence interval. From those estimations it is possible to get the relevant values of sensitivity and specificity. The Table 7 shows the overall values that resulted from the elicitation. The author differentiated the results by experts' category in early adopters, majority and overall, being the early categories characterized by their broad experience in research. According with the comparison between those results and the ones obtained to MRI, in general, PAM is expected to perform worse than MRI. However, PAM in terms of mechanical properties and visualization of oxygen saturation its performance is expected to be better. In terms of methodology the author stated that the obtained results showed that this typology of elicitation is useful to guide the designers among the uncertainty during the development and experimental stages of a new technology.

	Early Adopters			Majority			Overall		
	Lower	Upper	Mode	Lower	Upper	Mode	Lower	Upper	Mode
<b>Sensitivity (%)</b>	67.7	91.9	81.7	51.2	74.3	67.4	58.9	85.1	75.6
<b>Specificity (%)</b>	70.2	88.4	79.1	40.8	70.7	58.5	52.2	77.6	66.5

**Table 7.** Values of sensitivity and specificity resulted from expert elicitation [32].

Later, in August 2012, Roelvink presented the work titled “Patient preferences versus professional preferences in population screening technology: Patient centered decision making in the population screening for Breast Cancer” [33]. In the present context where patient centered decision making is gaining attention, even in the preventive field of population screening for breast cancer, Roelvink purposed to address the following research questions: Which breast cancer screening technology is most preferred by women and professionals in population based screening for breast cancer? Do these preferences influence each other or the intention to adhere in the population screening for breast cancer? To address these questions the author selected as methodology the AHP, also used by Hilgerink. In the considered scenarios the author included PAM besides the standard of care technologies (FFDM). The obtained results indicated that the effectiveness of a screening technology is the most important factor in the choice for a screening technology for both health care professionals as patients, by other side, comfort is valued as the least important factor in screening technology. The

overall results analysis allowed to conclude that PAM is preferred over FFDM by both professionals and patients if it performs at least equally as good as FFDM in terms of effectiveness. The results also indicated that although the patients' opinion is important in the adherence to the population screening, the opinion of the professional (Radiologist) is valued as the most important one. An important final note that the results allowed to take is that PAM could be a suitable screening technology in the future for patients with dense breasts.

## 2.2. Standard of Care

One can divide the breast cancer clinical pathway in 4 different stages: Screening, diagnosis (Early diagnosis, late diagnosis and pathological diagnosis), treatment and follow up as Fig. 17. The purpose of this section is to describe the standard of care procedures for those stages.

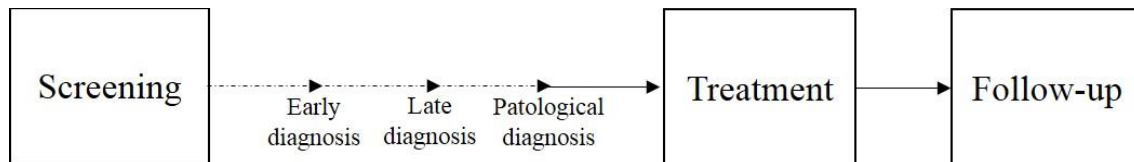


**Fig. 17.** Clinical pathway of breast cancer.

### 2.2.1. Screening

The breast cancer screening procedure is regulated by national and international official institutions that define the target groups considered at risk, the interval and periods of screening and the typology of procedure to be made.

In Europe the guidelines for breast cancer screening and diagnosis are gathered in the manual *European Guidelines for Quality Assurance in Breast Cancer Screening and Diagnosis*, a document supported by European commission and built with the collaboration from the International Agency for Research on Cancer (IARC) [35]. These guidelines are generally adopted by all the EU counties. However each country can adopt some particular norms.

According with the guidelines the general screening public policy should be directed to women 50-69 employing two-yearly mammography (SFM / FFDM) [35]. 2 views of each breast (medio lateral oblique plus cranio- caudal) is the recommended procedure, more effective than single oblique view screening [35]. The following table shows the adopted periods and intervals of screening of some countries.

	Netherlands	Portugal	UK	IARC Guidelines
Age-eligible national population	50-75	45-69	50-70	50-69
Screening Interval	2	2	3	2

**Table 8.** Adopted periods and intervals of screening in the general population [2]



Recently, the National Institute for Health and Care Excellence (NICE) has published guidelines for the high to moderate risk screening groups and for the BRCA 1, BRCA2, TP53 gene carriers [36]. According to this institution, for the different risk groups considered, the screening should be performed in an annual basis as described in the Table 9.

Age	Group	Imaging Modality
40-69	BRCA 1 /BRCA 2	MRI
40-59	HR	FFDM/SFM
40-49	MR	FFDM /SFM
30-49	HR / BRCA1 /BRCA2	MRI
20-49	TP53	MRI

**Table 9.** NICE guidelines for the moderate to high risk screening. HR- high risk; MR- moderate risk;

### 2.2.2. Diagnosis

The diagnosis can be done in two different moments and then named *Early diagnosis* or *Late Diagnosis*, followed by *pathological diagnosis*.

When after the screening procedures, there is a need for further assessment the European guidelines suggest the adoption of the following procedures for *early diagnosis*: Repeat views (medical), Cranio-caudal view, other views or Ultrasound [35]. When the diagnosis is still unclear MRI is the procedure adopted for *late diagnosis* [35]. According with the guidelines of European Society for Medical Oncology (ESMO) the final *Pathological diagnosis* should be based on core needle biopsy obtained by manual, or preferably by ultrasound or stereotactic, guidance [37]. A core needle biopsy must be obtained before any surgical operation [37]. The *final pathological diagnosis* should be made according to the World Health Organization (WHO) classification and the tumor–node–metastases (TNM) staging system (Appendix II) [37] [35].

### 2.2.3. Treatment

After the *pathological diagnosis* and before the treatments pre-operative assessments are performed. According with the Portuguese guidelines, that follow the IARC recommendations, the pre-operative assessments by stage are the set of procedures that Table 10 shows. The definition of treatments to be performed in each case of breast cancer is in the most of the cases very complex. The Table 11 shows a simplified possible combination of treatments by stage according with ESMO guidelines.

	Mammography	Pathologic Revision	Axilar US	Hemogram	Liver Function Tests	RX (Thorax)	ECG	Bone Scintigraphy	ECO/TAC (hepatic)
<i>0 (DCIS)</i>	X	X							
<i>Stage I cT1 N0 M0 ; II A cT2 N0 M0 &lt;3cm</i>	X	X		X	X	X	X	X*	X*
<i>Stage II A cT0 N1 M0 cT1 N1 M0 ; IIB cT2 N1 M0 &lt;3cm-</i>	X	X	X	X	X	X	X	X	X
<i>Stage IIA cT2 N0 M0 cT2 N1 M0 &gt;3 cm ; IIB cT3 N0 M0</i>	X	X	X	X	X	X	X	X	X
<i>Stage III A cT0 N2 M0 cT1 N2 M0 cT2 N2 M0 cT3 N2 M0 ; Stage IIIB cT4 N1-3 M0 cT1-4 N3 M0</i>	X	X	X	X	X	X	X	X	X

**Table 10.** Pre-Operative assessments by stage. Adapted from [38]

	Neoadjuvant chemotherapy	Mastectomy (Total)	Breast Reconstruction	Lumpectomy	Axillary dissection (ALND) / Sentinel lymph node biopsy (SLNB)- Guidelines until [II, A]	Radiotherapy	Hormone Therapy	Adjuvant chemotherapy
<i>O(DCIS)</i>				X		X <sup>1</sup>	X (50%) <sup>2</sup>	
<i>I</i>				X	X	X	X (50%)	
<i>II</i>				X	X	X	X (50%)	
<i>III</i>	X	X	X		X	X	X (50%)	X
<i>IV</i>							X (50%) Palliative	X Palliative

**Table 11.** Treatments stage of breast cancer. Adapted from [37, 39] [38].

<sup>1</sup> If the tumor is <10 mm the probabilities of recurrence is considered very low so the radiotherapy may be omitted

<sup>2</sup> Might be considered in 50% of the cases

#### 2.2.4. Follow-Up

In the current IARC guidelines it is recommended two types of follow-up: an extended version and a limited version (still the most used) that can be adopted according to the risk evaluation of recurrence.

Type	1	2	3
<b>Limited (Annual)</b>	History taking	Physical examination	Mammography
<b>Extended (Annual)</b>	Chest x-ray	Blood analysis	Scintigraphy

**Table 12.** Set of annual procedures by type of follow up [40].

### 2.3. Health Technology Assessment

In this second part of the *literature review* a methodological overview is presented about the techniques involved in health technology assessment.

The adoption of new technologies is generally associated with big raises in the healthcare costs in the developed countries. The official public institutions, as FDA, have the role of regulation new drugs and new medical devices, however HTA methodology applications remains limited [41]. Nowadays, this typology of assessments is decentralized being also made by the private sector with the transversal contribution of the technology designers, the industry and physicians. Their contribute is essentially focused in the development, adoption, utilization and choice of new technologies [41].

Moreover, nowadays there is a great debate between two perspectives of the healthcare role in the economy - leveraging economic growth through R&D spending or to have a stricter control of healthcare budgets [42]. In this context, several attempts have been made to apply the health technology assessment methodologies to earlier stages of technology development and implementation [42]. The final goals of these methods are: support governments in making decisions and to give information to biomedical product designers and to anticipate further development and market access [42].

According with *Ijzerman et al*, the HTA can be done in 4 different consecutive stages of the progress of technology development (as illustrated in Fig. 18) dependently in the level of uncertainty about product's technical value:

- Basic research (where there is still no evidence on mechanisms and proof of principle);
- Translational research (in the end of which it is possible to have defined prototype);
- Clinical research;
- Market access.

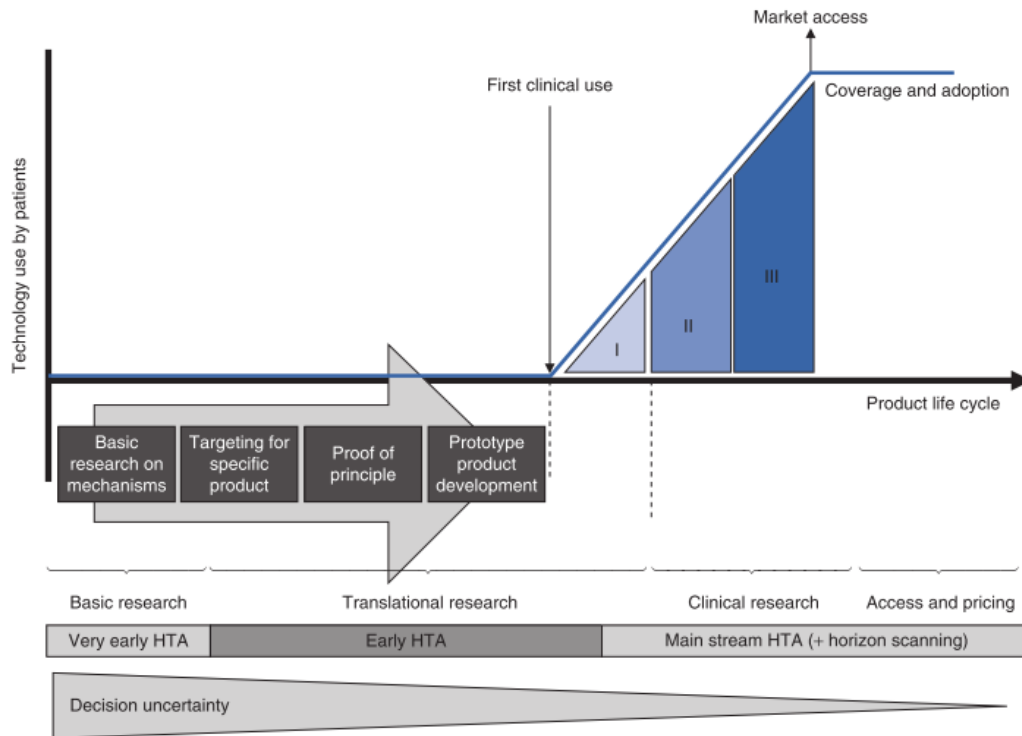


**Fig. 18.** Flowchart of stages in medical product development [42].

### 2.3.1. Methodologies

In order to get accurate answers to the questions associated with a new health device, commonly, a very large number of patients would be needed to participate in a randomized trial during big periods of time. The HTA methodologies try to minimize the time and the resources necessary to find the proper answers. In the different stages of HTA there are several methods and tools that can be applied.

Common HTA methodology include *Multi-Criteria decision methods*, *Health impact assessment*, *Strategy business care*, *Pay-back from research analysis*, *Coinjoint analysis*, *Real options analysis*, *Health Economic modeling*, *Horizon Scanning systems*, *Clinical trial simulation* and *Value-of-information analysis* [42].

In general the HTA methods can be supported by: Clinical database/registries, Case series/cohort studies, Epidemiological and Surveillance Studies and Quantitative Analysis (meta-analysis) [41].

#### 2.3.1.1. Health Economic Modeling

Health economic evaluations are extremely important today and have added a whole new dimension to health technology assessment. In the most of the cases the evaluations are made through evaluation models, which are useful as an alternative to long and expensive economic trials [41]. Two model techniques are used- Markov models and Discrete Event simulation (DES) [43]. Markov models are currently the most used because they needs less detailed data and are computationally more efficient:

the DES requires two levels of simulation to estimate the costs and the utilities of interest. Besides DES require also two levels to quantify decision uncertainty, normally through probabilistic sensitivity analysis. Generally DES is a more flexible, but more complicated decision modeling technique. According to some studies, the obtained results indicate that the use of DES may be beneficial only when the available data demonstrates particular characteristics [44].

### 2.3.1.1.1. Economic Evaluation Methods

Common useful economic evaluation methods are *cost-effectiveness analysis* (CEA), *cost-utility analysis* (CUA), *cost-benefit analysis* (CBA) and *cost-minimization analysis* (CMA) [41].

These types of evaluations can be applied to any health intervention as a treatment, screening test, or primary prevention techniques. The health intervention typically reduce the incidence rate of disease or its complications, improve the quality of life lived with disease, or improve life expectancy, sometimes in combination [43]. The benefits of a health intervention are referred to as outcomes. Generally, the evaluations compare the status quo with a competing Alternative.

Each type of economic evaluation seeks to calculate a final ratio -  $\frac{Cost}{Outcome}$ . Additionally, it is calculated the incremental cost by unit of outcome gained – the ICER (Incremental cost-effectiveness ratio), which is yielded by (7). [43]. The threshold of acceptability of an ICER or the maximum value that it is considered acceptable to pay is called *willingness to pay* (WTP) for an additional unit of health gain [43]. There isn't a strict definition of WTP values, the choice of a certain value is dependent on social and political issues. The appraisal committee of the British institution NICE (National Institute for Health and Care Excellence) “does not use a fixed ICER threshold above which a technology would automatically be defined as not cost effective or below which it would. Given the fixed budget of the NHS, the appropriate threshold is that of the opportunity cost of programmes displaced by new, more costly technologies “ [45].

$$ICER: \frac{Cost A - Cost Standard of Care}{Effectiveness A - Effectiveness Standard of Care} \quad (7)$$

The outcome nature or the effectiveness measure is what defines the evaluation. The Table 13 gives an overview of the purposes of the different economic evaluations methods.

Method	CEA	CUA	CBA	CMA
<b>Description</b>	Compares alternatives with therapeutic effects measured in physical units; computes a <i>cost-effectiveness ratio</i>	Measures therapeutic consequences in utility units rather than physical units; computes a <i>cost-utility ratio</i>	Measures benefit in monetary units and computes a net gain	Finds the least expensive cost alternative
<b>Application</b>	Can compare competing alternatives that differ in clinical outcomes and use the same unit of benefit	Use to compare competing alternatives that are life extending	Can compare programs with different objectives	Use when benefits are the same
<b>Cost Unit</b>	Monetary currency	Monetary currency	Monetary currency	Monetary currency
<b>Outcome Unit</b>	Physical Units	QALYs	Monetary currency	Assume to be equivalent

**Table 13.** Overview of the different economic evaluations methods. Adapted from [46]

*Cost-effectiveness analysis* is a method of summarizing the health benefits and resources used by competing alternative with different safety and efficacy profiles [43]. Costs are measured in the chosen monetary currency, and outcomes are measured in terms of obtaining a specific therapeutic outcome. These outcomes are often expressed in physical units (e.g., lives saved, cases cured, life expectancy, or drop in blood pressure) [46].

*Cost-utility analysis* is a method for comparing treatment alternatives that integrates patient preference or quality of life when comparing competing treatment alternatives [46]. Cost is measured in the chosen monetary currency, and the outcome is measured in patient-weighted utilities rather than in physical units [46]. The most used utility measurement is the quality-adjusted life years (QALY's) gained, a common measure of health status used in CUA, combining morbidity and mortality data [46].

*Cost-benefit analysis* is a method that allows the identification, measurement, and comparison of the benefits and costs between competing alternatives [46]. The benefits realized from a program or treatment alternative are compared with the costs of providing it, both the costs and the benefits are measured and converted into the equivalent chosen monetary currency [46].

*Cost-minimization analysis* involves the determination of the least costly alternative when comparing two competing alternatives assumed to be equal performance [46]. Once this equivalency in outcome is confirmed, the costs can be identified, measured, and compared in monetary units [46]

One can say that CEA, that considers as outcome any physical unit, is a broader method that includes CUA, that considers as outcome QALY. Due to this fact, the generality of authors of health-economics works consider that designations of CEA and CUA should be used interchangeably [43]. In this thesis CEA it is the adopted designation.

### 2.3.1.1.1. Costs

Once the methodology of economic evaluation is chosen it is crucial to assess costs that heavily depend on the perspective of the evaluation.

The generality of the studies include the following perspectives: patient, provider, payer, and society. Costs from the perspective of patients are essentially what patients pay for a product or service—that is, the portion not covered by insurance or by the government [46]. Costs from the provider’s perspective are the actual expense of providing a product or service, regardless of what the provider charges [46]. These providers can be hospitals, or private-practice physicians. From this perspective, direct costs such as drugs, hospitalization, laboratory tests, supplies, and salaries of healthcare professionals can be considered, however, indirect costs can be of less importance to the provider [46]. Payers include insurance companies, employers, or the government. From this perspective, costs represent the charges for health-care products and services allowed or reimbursed by the payer [43]. The primary cost for a payer is of a direct nature, however, indirect costs, such as lost workdays, being at work but not feeling well and therefore having lower productivity, also can be considered to the total cost of healthcare to the payer. Finally, the perspective of society is the broadest of all perspectives because it is the only one that considers the benefit to society as a whole [46]. In this perspective, all direct and indirect costs are included. Costs from this perspective include patient morbidity and mortality and all the important consequences an individual could experience and the overall costs of giving and receiving medical care [46]. Generally in countries with nationalized medicine, society is the most used perspective.

The evaluation can assess the value of the competing alternatives from single or multiple perspectives. However, clarification of the perspective is critical because the results of an economic evaluation depend heavily on the chosen perspective.

#### **2.3.1.1.1.2. Outcomes**

Among the considered outcomes in economic evaluations models, lives saved, cases cured, life expectancy, drop in blood pressure and QALY’s (Quality -adjusted life year) are some important examples. QALY’s is by far the most accepted and used outcome in CEA. This is also proved by the results obtained in the meta- analyses over CEA studies that have been performed. The meta-analyses description is made in the Appendix I.

The QALY was originally developed as a measure of health effectiveness for CEA as a method intended to aid decision-makers charged with allocating scarce resources across competing alternatives [47].

A QALY may be defined as a year of life that is lived in perfect health [43]. The quantification of a lifetime in terms of QALY’s depends on another concept, the concept of HRQL score or utilities.

A HRQL score is a number between 0 and 1 used to quantify a health state or an intervention in a certain moment. 1 represents perfect health and values near 0 represents preoccupied levels of morbidity. This concept may be simply thought of as a continuum of values ranging from perfect health to death.

The relation between QALY’s and HRQL score can be given by (8).

$$QALY's = Life\ expectancy * HRQLscore \quad (8)$$

Thus, if a medical intervention adds 10 years of life and each of these years is associated with an HRQL of 0.7, the medical intervention would have resulted in a gain of  $0.7 * 10$  years, i.e., 7 years of perfect health (7 QALYs) [43].

The usefulness of utilities and QALY's has been shown by a huge number of works. However the methodologies to calculate those preference scores are still a controversial issue.

The main reported methods to calculate the HRQL scores are *standard gamble* (SG), time trade-off (TTO), rating scale (RS), multiattribute utility (MAU) and person trade-off (PTO) [47].

*Standard gamble* is a controversial technique to derive HRQL scores. SG is designed to estimate the risk of death that a patient would be willing to accept in a gamble for perfect health [43]. In this technique, subjects must choose between a health state and a gamble in which there is a chance of perfect health or death [43]. The chance of death is changed until the decision between the health state and the gamble is perceived to be about equally desirable to the subject, the probability decided is the utility for that health state [43].

In the *time trade-off method*, also controversial and similar to SG, the patient is asked how much time in poor health would be willing to trade for perfect health [43]. Thus, the patient has to forgo future years of life in poor health in exchange for fewer years of life in perfect health, once the subject has decided how much time she would be willing to sacrifice for better health, the HRQL score is obtained by dividing the life expectancy in the state of illness by life expectancy in perfect health [43].

In the *rating scale* method, considered for many also controversial and inferior to SG or TTO, the subject is asked to rate the health state on a scale of 1 to 100, where 0 is the worst imaginable and 100 is the best imaginable [43]. In opposition to SG and TTO, RS involves a rating task rather than a choice task [47].

Some literature strongly argue with the use of *Person trade-off* method that is basically the elicitation of the values from experts [47]. In this method, individuals make hypothetical choices about competing alternatives. The paradigm of PTO involves asking representative members of the community to make judgments about the value of health outcomes for others [47].

Finally, *Multiattribute utility methods* are nowadays the most accepted to derive HRQL scores. MAU methods use score sheets to generate HRQL scores. These survey instruments may be completed using information from the medical literature and by people familiar with the studied health state [43]. Such a range of people can fill them out and get comparable scores because the categories are quite broad, once the instrument is completed, the researcher inputs the responses into a simple formula that produces an HRQL score suitable for use in CEA study [43]. An important example of MAU method is the Euroqol surveys. In fact, this is the method of choice in most contemporary CEA studies and it is the method recommended by the Panel on Cost-Effectiveness in Health and Medicine and by NICE [48]. The remaining problem is that different analysis give different results, due to the preference elicitation methods, to the choice of health attributes, and due to the manner in which interactions across the individual health attributes are modeled [47].



### 2.3.1.1.1.3. Discounting Costs and Outcomes

In health economic modeling the economic evaluations are made over extended time horizons, therefore it is necessary to forecast the overall cost and outcomes that an adoption of a certain competing alternative can bring in the future. That requires choosing a discount rate, which determines the value of future costs and benefits relative to current ones. The choice of discount rate can make a huge difference to the desirability of alternatives, especially when their costs and benefits occur over long periods [49].

In general terms discounting is the process of reducing any costs and consequences that may occur in the future back to their present value. The concept of discounting is not related with the concept of inflation and can be explained by some intuitive facts: The explanation for discount outcomes comes from the assumption that normally one is tempted to place a greater value on things if it is possible to have them now rather than in the future, by other side discounting costs can be explained similarly as costs seem less of a constraint if one only have to pay for them in the future [50].

According to some authors the reasons to valorize less the future (discounting) is due to three main factors: positive income growth expectation (due to inflation); awareness of risk because benefits in the future may not occur and pure time preference- the utility one gain from consuming something now relative to the future [49, 50].

The general formula for discounting future costs and outcomes is given by (9) and (9) respectively [43].

$$\frac{\text{Cost of future event}}{(1+\text{discount rate})^{\text{year in future}}} \quad (9)$$

$$\frac{\text{Outcome of future event}}{(1+\text{discount rate})^{\text{year in future}}} \quad (10)$$

Among the health economist researchers there is no agreement about which discount rate to use, as well as about whether to discount costs and outcomes (simultaneously) using the same discount rate(s) [46]. For instance, the Panel on Cost - Effectiveness in Health and Medicine bases the recommended discount rate on a rate of 3 percent [48] . Some authors consider that the discount rate should depend on regional or national data. Therefore the discount rate ( $D_t$ ) to use should be given by (11) [50].

$$D_t = \rho + g\varepsilon \quad (11)$$

Where,

$\rho$  – Pure time preference (1- 2%);

$g$ - Growth income (1-3%);

$\varepsilon$ - Elasticity marginal utility of income (1-3%);

By (11) and by other specific national data it yields the discount rates showed in Table 14.

Country	Discount Rate Costs (%)	Discount Rate Outcomes (%)
<i>Australia</i>	5	5
<i>England</i>	3.5	3.5
<i>France</i>	2.5- 5	2.5- 5
<i>Netherlands</i>	4	4
<i>Portugal</i>	5	5
<i>New Zeland</i>	3.5	3.5

**Table 14.** National discount rate [50].

In fact, HTA procedures, specifically CEA show nowadays an important relevance for the stakeholders and regulators to choose technologies or interventions among several options.

### 3. Research Question

As it has been shown in the previous sections, PAM is currently in the second phase of clinical trials. Therefore and according with Fig. 18 of *section 2.3*. one can consider that PAM is placed on the called *main stream HTA* – phase I.

The process of assessment of PAM has already passed through different stages. The previous assessment studies have focused on its performing levels in terms of sensitivity, specificity, safety, costs/time and comfort. However, the economic impact of PAM application in the different scenarios in the clinical pathway of breast cancer (screening and diagnostic track) are still uncertain, leading to the main research questions that this thesis will address:

What is the best scenario of application of PAM in the clinical pathway of breast cancer in the perspective of an economical evaluation?

The considered possible scenarios of application are the following:

- General Screening;
- Early Diagnosis;
- Late Diagnosis;
- High Risk Screening;
- Moderate Risk Screening;
- High breast density Screening;

## 4. Materials and Methods

In this chapter, different materials and methods used in this thesis shall be described.

A Markov model was developed in TREEAGE software (*TreeAge Software Inc., Williamstown, MA, USA*). The relevant data on accuracy, sensitivity and specificity of each diagnostic test and crucial probabilities were linked in the model, to costs and the primary outcome measure (QALY), yielding cost per quality-adjusted life-year (QALY). The applied performance data of PAM is an estimation of its sensitivity and specificity. Costs were based on Dutch and Portuguese national rates for hospital and physician services provided by official institutions. Utilities from the literature were applied to each health outcome in the model including the temporary health states. All costs and outcomes were discounted at 4% and 5% per year in the Dutch and in the Portuguese context respectively. The analysis was performed from the society perspective. The model estimated the *cost-effectiveness* associated with the integration of PAM in several scenarios further explained (divided in 3 groups: Group I, Group II and Group III).

**Background:** Expert elicitation studies about PAM performance

**Objective:** To evaluate the cost-effectiveness of PAM in different scenarios

**Design:** Markov Model with 2 years of cycle length

**Target Population:** Portuguese and Dutch woman in the regular screening-diagnostic pathway and in the High to moderate risk screening groups

**Time Horizon:** From 9 year to 29 years of tracking

**Perspective:** Society

**Interventions:** Breast cancer screening with PAM; Breast cancer early diagnosis with PAM; Breast cancer late diagnosis with PAM

**Outcome Measures:** Cost per quality-adjusted life year (QALY) gained

**Discount Rate:** 4% and 5% in the Dutch and Portuguese contexts

### 4.1. Cost-Effectiveness Analysis

The chosen economic evaluation method was *Cost-effectiveness Analysis* using QALY's as the outcome measure. The CEA was implanted in different clinical scenarios (further explained) for two social contexts - Portugal and Netherlands that have health system with different screening rules and costs and different values of breast cancer incidence and prevalence. The discount rate for costs and outcomes was 5% for the Portuguese scenarios and 4% in the Dutch scenarios, following the suggestions made by *Clark, 2010* [50].

## 4.2. The Markov Model design

Markov model was the chosen model design. In fact, this type of model is the most used in CEA analysis as proved in the CEA studies review in Appendix I: 28 out of the 35 studies considered in the meta-analysis used Markov models.

Markov models are recursive (repetitive) decision trees that are used for modelling conditions that have events that may occur repeatedly over time or for modelling predictable events that occur over time (e.g., screening for disease at fixed intervals) [51].

The designed Markov model to perform the CEA is shown in Fig. 19. At the final of every cycle the trial is allocated to one of the represented final Markov states:

- Screening (including early diagnosis, late diagnosis and biopsy as internal microstates);
- Treatment;
- Follow up;
- Local recurrence;
- Regional Recurrence;
- Distant Recurrence;
- Dead (absorbing state);

The pathway inside each Markov state is detailed in the Appendix III (Fig. 30, Fig. 31 Fig. 30, Fig. 32, Fig. 33, Fig. 34 and Fig. 35).



Sixteen scenarios were tested in the two studied contexts (32 combinations) in these two groups. The Table 15 and Table 16 show the specifications of each tested scenario in group I and II, respectively. Additionally to the described main scenarios, another group of scenarios (*Group III*) was tested. This group included 6 scenarios tested in the 2 contexts (12 combinations), presented in Table 17. The main difference between group III scenarios and the others is that the tested technology is not specifically PAM as it is not applied data about PAM accuracy. In opposition the purpose is to measure the *cost-effectiveness* for a hypothetical technology that has sensitivities or specificities 5% higher than the standard of care and the same cost of PAM use.

### *Group I*

Scenario	Context	Cycle Length (years)	Time Horizon (years)	Interval of ages	Replaced Technology
Screening	NL	2	25	50-75	FFDM
Screening	PT	2	24	45-69	FFDM
E. Diagnosis (Replacing US, FFDM and Clinical Examination)	NL	2	25	50-75	US +FFDM+CE
E. Diagnosis (Replacing US, FFDM and Clinical Examination)	PT	2	24	45-69	US +FFDM+CE
E. Diagnosis (Replacing US)	NL	2	25	50-75	US
E. Diagnosis (Replacing US)	PT	2	24	45-69	US
E. Diagnosis (Replacing FFDM)	NL	2	25	50-75	FFDM
E. Diagnosis (Replacing FFDM)	PT	2	24	45-59	FFDM
E. Diagnosis (Replacing US)	NL	2	25	50-75	US
E. Diagnosis (Replacing US)	PT	2	24	45-69	US
L. Diagnosis	NL	2	25	50-75	MRI
L. Diagnosis	PT	2	24	45-69	MRI

**Table 15.** Tested scenarios in the regular clinical pathway of breast cancer

**Group II**

Scenario	Context	Cycle Length (years)	Time Horizon (years)	Interval of ages	Replaced Technology
BRCA 1	NL	1	29	40-69	MRI
BRCA 1	PT	1	29	40-69	MRI
BRCA 2	NL	1	29	40-69	MRI
BRCA 2	PT	1	29	40-69	MRI
HRisk mam: dense	NL	1	19	40-59	FFDM
HRisk mam: dense	PT	1	19	40-59	FFDM
HRisk mam: non dense	NL	1	19	40-59	FFDM
HRisk mam: non dense	PT	1	19	40-59	FFDM
MRisk mam: dense	NL	1	9	40-49	FFDM
MRisk mam: dense	PT	1	9	40-49	FFDM
MRisk mam: non dense	NL	1	9	40-49	FFDM
MRisk mam: non dense	PT	1	9	40-49	FFDM
HRisk	NL	1	19	30-49	MRI
HRisk	PT	1	19	30-49	MRI
BRCA1	NL	1	19	30-49	MRI
BRCA1	PT	1	19	30-49	MRI
BRCA2	NL	1	19	30-49	MRI
BRCA2	PT	1	19	30-49	MRI
TP53	NL	1	29	20-49	MRI
TP53	PT	1	29	20-49	MRI

**Table 16.** Tested scenarios in the high risk screening groups



The high screening groups included in the tested scenarios are differentiated not just for the specifications shown above but also for the incidence and prevalence of each group. This issue will be described in further sections.

### Group III

Scenario	Context	Cycle Length (years)	Time Horizon (years)	Interval of ages	Replaced Technology
Screening (+ 5 % sen)	NL	2	25	50-75	FFDM
Screening (+ 5 % sen)	PT	2	24	45-69	FFDM
E. Diagnosis (+ 5 % sen)	NL	2	25	50-75	FFDM
E. Diagnosis (+ 5 % sen)	PT	2	24	45-69	FFDM
E. Diagnosis (+ 5 % sen)	NL	2	25	50-75	US
E. Diagnosis (+ 5 % sen)	PT	2	24	45-69	US
L. Diagnosis (+ 5 % sen)	NL	2	25	50-75	MRI
L. Diagnosis (+ 5 % sen)	PT	2	24	45-69	MRI
L. Diagnosis (+ 5 % spe)	NL	2	25	50-75	MRI
L. Diagnosis (+ 5 % spe)	PT	2	24	45-69	MRI
L. Diagnosis (+ 5 % sen & spe)	NL	2	25	50-75	MRI
L. Diagnosis (+ 5 % sen & spe)	PT	2	24	45-69	MRI

**Table 17.** Group of additional scenarios teste

## 4.4. Cancer Progression

At the beginning of every trial it was associated a health state to that person: healthy or with breast cancer, being associated with 1 of the 5 stages of breast. This attribution is a monte-carlo process based on probabilities distributions derived from the literature as will be further explained. As mentioned the *Roman* staging system was the adopted method to describe the different stages. The Table 18 shows the relation between each *Roman* breast cancer stage and the most important biological features in breast cancer: the diameter size of breast cancer and the number of lymph nodes that is involved with cancer.

Breast Cancer Stage and biological features		
Stage	Diameter Size (cm)	Number of Lymph nodes
<b>0</b>	<0.95	0
<b>I</b>	<2	[0, 4]
<b>II</b>	>= 2 & <5	[0, 4]
<b>III</b>	>= 5	[0,4]
<b>IV</b>	Any	>4

**Table 18.** The correspondence between roman staging system and the biological features of breast cancer. Adapted from [52] .

In the simulation, once the stage was set it was needed to track the initial cancer diameter size and the number of lymph nodes already involved. The association is made as the Table 19 shows. For instance, if it has been defined that one person has cancer in stage 2, the initial diameter size was set to 3.5 cm and the number of lymph nodes involved at this point was set to 0.

Breast Cancer Stage and biological features		
Stage	Diameter Size (cm)	Number of Lymph nodes involved
<b>0</b>	0.2	0
<b>I</b>	1.475	0
<b>II</b>	3.5	0
<b>III</b>	5	0
<b>IV</b>	5	5

**Table 19.** Initial association between the defined stage and the biological features.

At every cycle (1 or 2 years according with the scenario) the biological features were updated. The diameter size was updated by the version of *Gompertz growth function* (12) adapted by *Fryback et al, 2006* [52].

$$d(t) = d_0 e^{\ln\left(\frac{d_{max}}{d_0}\right)(1-e^{-\alpha t})} \quad (12)$$

where,

$d_0$ - 0.2 cm (as previous mentioned)

$d$  – [0.2 – 8] cm

$\alpha$ - growth parameter: gamma distribution ( $\mu=0.12$ ;  $\theta=0.012$ ), sampled for every trial;

The number of involved Lymph nodes was updated by the Schwartz's function, adapted from *Fryback et al, 2006* as well [52]. The function (13) yields the number of lymph nodes ( $n$ ) that has been involved in a certain period of time  $dt$ .

$$n(t) = b_1 + b_2 * V(t) + b_3 * V(t) * dt \quad (13)$$

where  $V$  is the volume of the primary cancer, ideally a sphere, with the volume being yield by  $V = \frac{\pi}{6} d^3$ . The parameters  $b_1$ ,  $b_2$ , and  $b_3$  are growing parameters that are respectively equal to 0.0058, 0.0053 and 0.0002 [52] .

The stage and the related biological features are updated ate every cycle of the model.

## 4.5. TreeAgePro

The computer implementation and simulation was made through the ©TreeAgePro 2013 software. Fig. 21 shows the interface of the program.

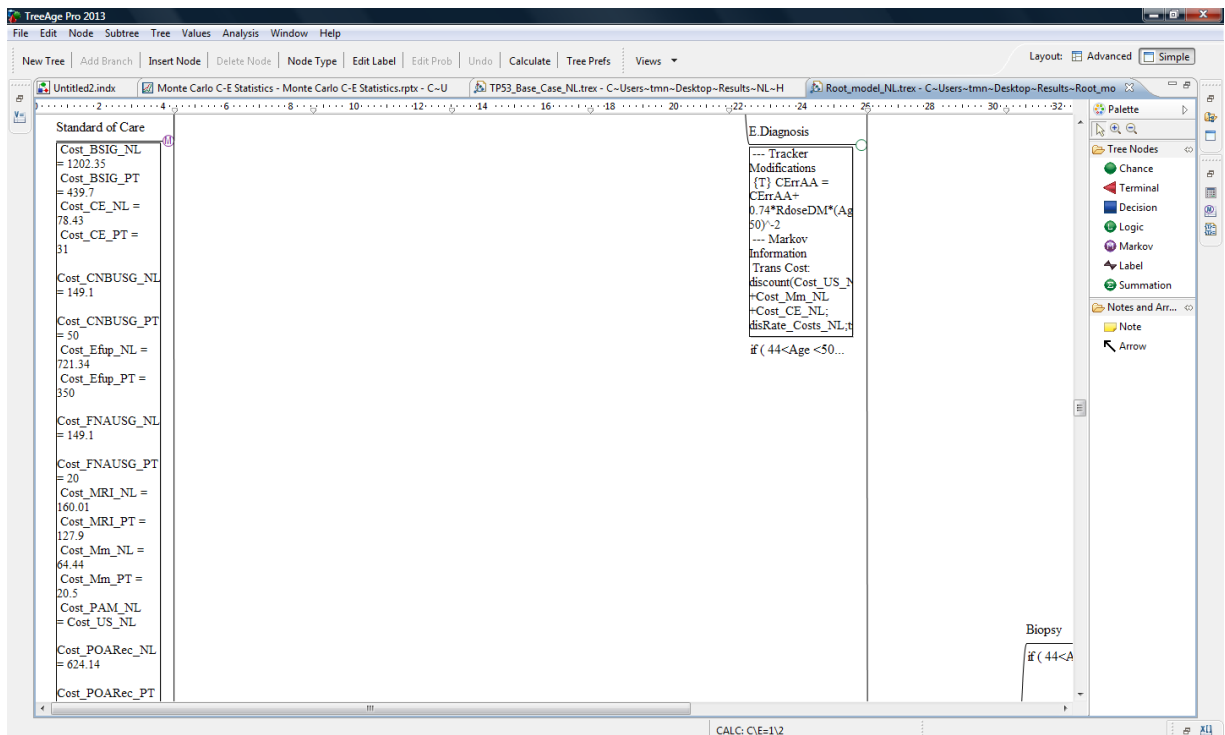


Fig. 21. TreeAgePro interface

## 4.6. Data required for the model

In this section it will be described the data applied in the model and the considered criteria for its choice.

### 4.6.1. Prevalence and Incidence

In order to quantify the expression of breast cancer among the population the model required the knowledge of the values of breast cancer *prevalence* (**P**) and breast cancer *incidence* (**I**). These values are context dependent. The *prevalence* is the proportion of a population found to have a condition at a time, while *incidence* is a measure of the risk of developing some new condition within a certain period of time. Both are normally expressed as a rate.

At the first cycle of the simulation for each trial the values of *prevalence* were applied, while for the next cycles the values of *incidence* were applied:

- If cycle=1 , the considered probability of having cancer was **P**- only in the **Group I** and **III** of scenarios;
- If cycle >1 , the considered probability of having cancer was **I**;

According with data provided by EUCAN the *1 year prevalence* is 12.82% and 5.44% for the Dutch and the Portuguese population respectively [53].

The considered values of *incidence* used in **Group I** and **III** are context and age dependent, as presented in the following table. The data were found in EUREG

database. For **Group II** the values of incidence (presented in Table 21) are determined by the risk of the target group.

Interval of ages (years)	Incidence (%)	
	<i>Netherlands</i>	<i>Portugal</i>
20-24	0.0023	0.0027
25-29	0.0125	0.0012
30-34	0.0367	0.0209
35-39	0.0715	0.0643
40-44	0.1381	0.0969
45-49	0.24800	0.1501
50-54	0.3017	0.1507
55-59	0.3181	0.1432
60-64	0.3602	0.1642
65-69	0.4145	0.2093
70-74	0.4562	0.1239

**Table 20.** Incidence values among the different interval of ages. The rates are for the all interval of ages (4 years) [54] .

Risk Group	Incidence (%)	Reference
40-69 BRCA1	1.800	[55]
40-59 HR	0.600	[36]
40-69 BRCA2	0.820	[55]
40-49 MR	0.567	[36]
30-49 HR	0.600	[36]
20-49 TP53	1.600	[56]
30-49 BRCA1	1.800	[55]
30-49 BRCA2	0.820	[55]

**Table 21.** Annual incidences for different groups at risk.

If some trial was associated with breast cancer in any cycle of the simulation, it was needed to initialize the tracker **stage**. That was made using the stage distribution at screening in the Netherlands that shows the proportion of found breast cancers by stage (Table 22). This distribution was assumed to be similar for the two studied contexts and for the different ages.

Roman Cancer Stage	
0	15.590%
1	65.744%
2	17.436%
3	0.923%
4	0.308%

**Table 22.** Stage distribution among the diagnosed cancers [57].

## 4.6.2. Mortality

According with the health state at any cycle, different mortality rates was considered. The mortality rates of a healthy person (stage=5) were derived from the general population lifetables (life-expectancy by age group) provided by WHO. These values are presented in Table 62 (Appendix IV).

The existing data about mortality for the different stages of breast cancer and for the different ages is very uncertain and incoherent. There are several methodologies and parameters to characterize the breast cancer mortality. The chosen approach to calculate that data was based on the 5-years-survival rate by stage and by age found from the 302 763 adult cases from the Surveillance, Epidemiology, and End Results (SEER) Program of the National Cancer Institute (NCI) in USA. The results were reported by *Lynn et al, 2001* and are presented in Table 63 (Appendix IV) [58]. For the model, as the used

cycle lengths were 1 year and 2 years, it was required the 1-year and 2-years mortality rate.

According with the Survival Parameter Conversion Tool, the survival and mortality rate can be modeled as following [59]:

$$S(t) = e^{ht} \quad (14)$$

$$M(t) = 1 - e^{ht} \quad (15)$$

The knowledge of the 5-years survival rate and (14) made possible to calculate the exponential parameter  $h$  for the different ages and stages –  $h(\text{age, stage})$ . The calculated values for  $h$  are shown in Table 64 (Appendix IV). Using (15) and the exponential parameter  $h$  matrix it was possible to calculate the mortality rates for the different cycle lengths internally in the model. This approach was used to calculate the mortality at all the states in the model with one exception: the mortality associates with the states *Local recurrence*, *Distant recurrence* and *Regional recurrence* were derived from *Auguste et al, 2011* (as shown in Table 23) [60] .

State	Biannual Mortality rates
<i>Local recurrence</i>	0.430
<i>Regional recurrence</i>	0.488
<i>Distant recurrence</i>	0.745

**Table 23.** Biannual mortality values for the different types of recurrence.

### 4.6.3. Clinical effectiveness data

The transition probabilities between most of the states in the model were conditioned by clinical effectiveness data, namely sensitivity and specificity values and by some probabilities obtained from breast cancer institutions. These values were used to represent the standard of care procedures and also the inset of PAM in the pathway.

Two criteria were followed to select the values of sensitivity and specificity among the found abundant literature:

- The experimental sample dimension (N): the biggest sample dimension as possible;
- The year of publishing- the most recent literature;

The transitions determined by the clinical effectiveness data (sensitivity and specificity) were calculated as the Table 24. shows: as the model tracked the breast cancer, the transition could be conditioned by stage. Based on their cancer stage and the performance of the device, patients at screening, for instance, either remain in screening (with true or false negative) or go to the diagnosis probability tree, when the screening is (true or false) positive.

Cancer stage (Roman stage)	$p(TP StateX)$	$p(FP StateX)$	$p(TN StateX)$	$p(FN StateX)$	$p(na StateX)$
<b>0 (DCIS)</b>	TP	0	0	FN	TP
<b>I</b>	TP	0	0	FN	TP
<b>II</b>	TP	0	0	FN	TP
<b>III</b>	TP	0	0	FN	TP
<b>IV</b>	TP	0	0	FN	TP
<b>V</b>	0	FP	TN	0	0
<b>(no cancer)</b>					

**Table 24.** State transitions determination based on clinical effectiveness data (sen. and spe.)

#### 4.6.3.1. Standard of Care

This section shows all the values that were used as transition probabilities between different states in the model for the considered standard of care pathway. First it will be shown the transitions between Screening and its internal micro states: Early Diagnosis, Late Diagnosis and Biopsy. Finally it will be shown the transitions from Treatment, follow-up and the different types of recurrence.

##### 4.6.3.1.1. Screening

Table 25 shows the values of sensitivity and specificity used to model the following transitions:

- Screening – E. Diagnosis;
- Screening – Screening;

Scenarios (Group of application)	Technology	Age Interval	Sensitivity	Specificity	TP (rate)	FP (rate)	FN (rate)	TN (rate)	N (Sample dimension)	Reference
I and III	FFDM	45-49	0.658	0.989	0.658	0.011	0.342	0.989	6000	[57] <sup>3</sup>
I and III	FFDM	50-54	0.678	0.990	0.678	0.010	0.322	0.990	6000	[57]
I and III	FFDM	55-59	0.766	0.993	0.766	0.007	0.234	0.993	6000	[57]
I and III	FFDM	60-64	0.800	0.993	0.800	0.007	0.200	0.993	6000	[57]
I and III	FFDM	65-69	0.843	0.992	0.843	0.008	0.157	0.992	6000	[57]
I and III	FFDM	70-74	0.821	0.990	0.821	0.010	0.179	0.990	6000	[57]
II (Dense)	FFDM	20-49	0.591	0.896	0.591	0.104	0.409	0.896	49528	[61]
II (Dense)	FFDM	50-64	0.609	0.911	0.609	0.089	0.391	0.911	49528	[61]
II (Not Dense)	FFDM	20-49	0.857	0.905	0.857	0.095	0.143	0.905	49528	[61]
II (Not Dense)	FFDM	50-64	0.667	0.932	0.667	0.068	0.333	0.932	49528	[61]
II	MRI	<i>Considered to be constant</i>	0.807	0.800	0.807	0.200	0.193	0.800	3571 average (pooled from 5 studies)	[62]

**Table 25.** Sensitivity and Specificity values of standard of care screening procedures

#### 4.6.3.1.2. Early Diagnosis

Table 26 shows the values of sensitivity and specificity used to model the following transitions:

- E. Diagnosis – Screening
- E.Diagnosis – L. Diagnosis
- E. Diagnosis – Biopsy

<sup>3</sup> Although SFM was also used, FFDM was the most used technology in the trials.

Scenarios (Group of application)	Technology	Age Interval	Sensitivity	Specificity	TP (rate)	FP (rate)	FN (rate)	TN (rate)	N (Sample dimension)	Reference
II	FFDM	20-29	0.833	0.889	0.833	0.111	0.167	0.889	11003	[63]
II	US	20-29	0.444	0.999	0.444	0.001	0.556	0.999	10849	[63]
II	CE	20-29	0.474	0.963	0.474	0.037	0.526	0.963	290330	[64]
II	<b>Combined<sup>4</sup> (FFDM + CE+ US)</b>	20-29	0.951	0.855	0.951	0.145	0.049	0.855	-	
II	FFDM	30-39	0.476	0.999	0.476	0.001	0.524	0.999	11003	[63]
II	US	30-39	0.667	0.997	0.667	0.003	0.333	0.997	10849	[63]
II	CE	30-39	0.474	0.963	0.474	0.037	0.526	0.963	290330	[64]
II	<b>Combined (FFDM + CE+ US)</b>	30-39	0.908	0.959	0.908	0.041	0.092	0.959	-	
II	FFDM	40-49	0.512	0.998	0.512	0.002	0.488	0.998	11003	[63]
II	US	40-49	0.732	0.995	0.732	0.005	0.268	0.995	10849	[63]
II	CE	40-49	0.474	0.963	0.474	0.037	0.526	0.963	290330	[64]
II	<b>Combined (FFDM + CE+ US)</b>	40-49	0.931	0.956	0.931	0.044	0.069	0.956	-	
I and III	US	45-49	0.732	0.995	0.732	0.005	0.268	0.995	10849	[63]
I and III	CE	45-49	0.474	0.963	0.474	0.037	0.526	0.963	290330	[64]
I and III	<b>Combined (FFDM + CE+ US)</b>	45-49	0.952	0.948	0.952	0.052	0.048	0.948	-	-
I and III	US	50-54	0.749	0.995	0.749	0.005	0.251	0.995	10849	[63]
I and III	CE	50-54	0.474	0.963	0.474	0.037	0.526	0.963	290330	[64]
I and III	<b>Combined (FFDM + CE+ US)</b>	50-54	0.957	0.949	0.957	0.051	0.043	0.949	-	-

<sup>4</sup> To calculate the combined sensitivity and specificity it was followed an approach suggested by *Auguste et al, 2011* that the overall result would be positive if either test is positive on its own. The main consequence of this approach the sensitivity increase as a result of combining the two tests – as all individual patients who test positive on either (but not necessarily both) test are considered a potential positive case leading to more false-positives, and so the specificity of the combined test is necessarily lower than the specificity of either test individually. The calculated values were yielded by the following formulas:  $1-Sen_{combinedXYZ} = (1-sen_X)*(1-sen_Y)*(1-sen_Z)$  ;  $Spe_{XYZ} = Spe_X * Spe_Y * Spe_Z$ .



I and III	US	55-59	0.749	0.995	0.749	0.005	0.251	0.995	10849	[63]
I and III	CE	55-59	0.474	0.963	0.474	0.037	0.526	0.963	290330	[64]
I and III	<b>Combined (FFDM + CE+ US)</b>	55-59	0.969	0.951	0.969	0.969	0.031	0.951	-	-
I and III	US	60-64	0.867	0.987	0.867	0.013	0.133	0.987	10849	[63]
I and III	CE	60-64	0.474	0.963	0.474	0.037	0.526	0.963	290330	[64]
I and III	<b>Combined (FFDM + CE+ US)</b>	60-64	0.986	0.944	0.986	0.056	0.014	0.944	-	-
I and III	US	65-69	0.867	0.987	0.867	0.013	0.133	0.987	10849	[63]
I and III	CE	65-69	0.474	0.963	0.474	0.037	0.526	0.963	290330	[64]
I and III	<b>Combined (FFDM + CE+ US)</b>	65-69	0.989	0.943	0.989	0.057	0.011	0.943	-	-
I and III	US	70-74	0.925	0.968	0.925	0.032	0.075	0.968	10849	[63]
I and III	CE	70-74	0.474	0.963	0.474	0.037	0.526	0.963	290330	[64]
I and III	<b>Combined (FFDM + CE+ US)</b>	70-74	0.993	0.923	0.993	0.077	0.007	0.923	-	-

**Table 26.** Sensitivity and Specificity values of early diagnosis standard of care procedures

#### 4.6.3.1.3. Late Diagnosis

Table 27 shows the values of sensitivity and specificity used to model the following transitions:

- L. Diagnosis – Biopsy
- L. Diagnosis – Screening

Scenarios (Group of application)	Technology	Age Interval	Sensitivity	Specificity	TP (rate)	FP (rate)	FN (rate)	TN (rate)	N (Sample dimension)	Reference
I, II and III	MRI	<i>Considered to be constant</i>	0.900	0.750	0.900	0.250	0.100	0.750	9298, average (pooled from 69 studies)	[65]

**Table 27.** Sensitivity and Specificity values of late diagnosis standard of care procedures

#### 4.6.3.1.4. Pathological diagnosis - Biopsy

It was assumed that biopsy is 100% accurate in determining if cancer is present. Positives go to treatment and negatives go back to screening.

#### 4.6.3.1.5. Treatment

While in treatment, 4 scenarios were considered possible to the patient: to die from cancer, to die from other causes, to remain in treatment or to be redirected to follow up. This last option was considered when the patient is for more than 4 years in treatment and the diagnosed cancer stage was different than IV. In this case the patient remained in treatment, in the context of palliative care.

#### 4.6.3.1.6. Follow up

As the patients entered the follow-up (it was considered the limited one for the season introduced in *section 2.2.4*) 7 options might be considered: to die from cancer; to die from other causes; to remain in follow up; to restart the normal screening pathway if the patient has already been in follow up for more than 5 years; to restart treatment procedures if the patient has been diagnosed with contralateral cancer (cancer in the other breast); to be diagnosed either local, or regional or distant recurrence from the primary cancer. The transition probabilities from the follow up state to the recurrence states (Table 28) and contralateral cancer were derived from the data provided by the Dutch institution *Integraal kankercentrum Zuid* that gathers the follow up information from thousands of woman every year [66].

Time after primary diagnosis (years)	Primary diagnosed stage	Local Recurrence	Regional Recurrence	Distant Recurrence	Contralateral Cancer
<= 2	0	0.0055	0.0030	0.0130	0.0840
>2 & <= 4	0	0.0092	0.0046	0.0199	0.0110
<= 2	I	0.0252	0.0074	0.1063	0.0053
>2 & <= 4	I	0.0217	0.0154	0.1398	0.0130
<= 2	II	0.0429	0.0180	0.3598	0.0000
>2 & <= 4	II	0.0165	0.0233	0.3002	0.0547
<= 2	III	0.0521	0.0232	0.2210	0.0151
>2 & <= 4	III	0.0323	0.0194	0.2154	0.0197

**Table 28.** Biannual transition probabilities from follow up to local, regional or distant recurrence and contralateral cancer [66] .

#### 4.6.3.1.7. Recurrence

From each of the 3 types of recurrence 4 options were considered to be possible: to die from cancer; to die from other causes; to remain with the current type of recurrence; or the health state to get worse and the recurrence to progress to one of the worse types (in case of Local or regional recurrence). The following table shows the mentioned transition probabilities.

From	To	
Local Recurrence	Regional Recurrence	0.040
Local Recurrence	Distant Recurrence	0.452
Regional Recurrence	Distant Recurrence	0.452

**Table 29.** Biannual transition probabilities between different types of recurrence [60].

#### 4.6.3.2. PAM

In order to obtain the *Cost-effectiveness* of PAM in the different scenarios it was essential to insert in the model the data on PAM accuracy, sensitivity and specificity and costs.

The results obtained by *Haakma W., 2011*, presented in Table 7 (2.1.3.8) were the root for this analysis. The overall results were considered the *base case* data (Sen- 0.756; Spe- 0.665), while the early adopters and majority values were considered the *best* (Sen- 0.817; Spe- 0.791) and *worst* (Sen- 0.674; Spe- 0.585) *scenario* values, respectively. Moreover, one of main conclusion of the work “Expert Elicitation to Populate Early Health Economic Models of Medical Diagnostic Devices in Development” is the expected worse performance of PAM in DCIS detection. This fact is explained by the fact that PAM functioning is based on angiogenesis detection (as mentioned before), however, there are tumor types without angiogenesis induction as some types of DCIS that doesn’t show vascularization [32]. Therefore, in the tests it was considered that PAM sensitivity is 20% lower for DCIS (Stage 0 in the model) than for the other cancer stages.

##### 4.6.3.2.1. Screening and Late Diagnosis

Table 30 shows the different values of PAM sensitivity and specificity. Those values were directly used for PAM at Screening and Late Diagnosis.

Stages	Worst Scenario (WS)	Base Case (BC)	Best Scenario (BS)
DCIS (0)	Sen-0.540; Spe- 0.585	Sen-0.605; Spe- 0.665	Sen-0.654; Spe- 0.791
I, II, III, IV	Sen-0.674; Spe- 0.585	Sen-0.756; Spe- 0.665	Sen-0.817; Spe- 0.791

**Table 30.** PAM sensitivity and specificity values applied in the model.

##### 4.6.3.2.2. Early diagnosis

Table 54 and Table 55 shows the different combinations of sensitivities and specificities for early diagnosis considering that PAM replaces FFDM and US, respectively. Those values were used to model the following transitions:

- E. Diagnosis – Screening;
- E. Diagnosis – L. Diagnosis;
- E. Diagnosis – Biopsy;

Scenarios (Group of application)	Stages	Technology	Age Interval	Sensitivity	Specificity	TP (rate)	FP (rate)	FN (rate)	TN (rate)	N (Sample dimension)	Reference
I	HA <sup>5</sup>	US	45-49	0.732	0.995	0.732	0.005	0.268	0.995	10849	[63]
I	HA	CE	45-49	0.474	0.963	0.474	0.037	0.526	0.963	290330	[64]
I	DCIS	<b>Combined (PAM WS + CE+ US)</b>	45-49	0.935	0.589	0.935	0.411	0.065	0.589	-	-
I	DCIS	<b>Combined (PAM BC + CE+ US)</b>	45-49	0.944	0.669	0.944	0.331	0.056	0.669	-	-
I	DCIS	<b>Combined (PAM BS + CE+ US)</b>	45-49	0.951	0.795	0.951	0.204	0.049	0.796	-	-
I	I,II,III, IV	<b>Combined (PAM WS + CE+ US)</b>	45-49	0.954	0.560	0.954	0.439	0.046	0.561	-	-
I	I,II,III, IV	<b>Combined (PAM BC + CE+ US)</b>	45-49	0.966	0.637	0.966	0.363	0.034	0.637	-	-
I	I,II,III, IV	<b>Combined (PAM BS + CE+ US)</b>	45-49	0.974	0.948	0.974	0.052	0.026	0.948	-	-
I	HA	US	50-54	0.749	0.995	0.749	0.005	0.251	0.995	10849	[63]
I	HA	CE	50-54	0.474	0.963	0.474	0.037	0.526	0.963	290330	[64]
I	DCIS	<b>Combined (PAM WS + CE+ US)</b>	50-54	0.939	0.589	0.939	0.411	0.061	0.589	-	-
I	DCIS	<b>Combined (PAM BC + CE+ US)</b>	50-54	0.948	0.669	0.948	0.331	0.052	0.669	-	-
I	DCIS	<b>Combined (PAM BS + CE+ US)</b>	50-54	0.954	0.796	0.954	0.204	0.046	0.796	-	-
I	I,II,III, IV	<b>Combined (PAM WS + CE+ US)</b>	50-54	0.957	0.561	0.957	0.439	0.043	0.561	-	-

<sup>5</sup> HA- Homogeneous accuracy was considered

		<b>CE+ US)</b>									
I	I,II,III, IV	<b>Combined (PAM BC + CE+ US)</b>	50-54	0.968	0.637	0.968	0.363	0.032	0.637	-	-
I	I,II,III, IV	<b>Combined (PAM BS + CE+ US)</b>	50-54	0.976	0.948	0.976	0.052	0.024	0.948	-	-
I	HA	US	55-59	0.749	0.995	0.749	0.005	0.251	0.995	10849	[63]
I	HA	CE	55-59	0.474	0.963	0.474	0.037	0.526	0.963	290330	[64]
I	DCIS	<b>Combined (PAM WS + CE+ US)</b>	55-59	0.939	0.589	0.939	0.411	0.061	0.589	-	-
I	DCIS	<b>Combined (PAM BC + CE+ US)</b>	55-59	0.948	0.669	0.948	0.331	0.052	0.669	-	-
I	DCIS	<b>Combined (PAM BS + CE+ US)</b>	55-59	0.954	0.796	0.954	0.204	0.046	0.796	-	-
I	I,II,III, IV	<b>Combined (PAM WS + CE+ US)</b>	55-59	0.957	0.560	0.957	0.439	0.043	0.561	-	-
I	I,II,III, IV	<b>Combined (PAM BC + CE+ US)</b>	55-59	0.968	0.637	0.968	0.363	0.032	0.637	-	-
I	I,II,III, IV	<b>Combined (PAM BS + CE+ US)</b>	55-59	0.976	0.948	0.976	0.052	0.024	0.948	-	-
I	HA	US	60-64	0.867	0.987	0.867	0.013	0.133	0.987	10849	[63]
I	HA	CE	60-64	0.474	0.963	0.474	0.037	0.526	0.963	290330	[64]
I	DCIS	<b>Combined (PAM WS + CE+ US)</b>	60-64	0.968	0.584	0.968	0.416	0.032	0.584	-	-
I	DCIS	<b>Combined (PAM BC + CE+ US)</b>	60-64	0.972	0.664	0.972	0.336	0.028	0.664	-	-
I	DCIS	<b>Combined (PAM BS + CE+ US)</b>	60-64	0.976	0.789	0.976	0.211	0.024	0.789	-	-
I	I,II,III, IV	<b>Combined (PAM WS +</b>	60-64	0.977	0.556	0.977	0.444	0.023	0.556	-	-

		<b>CE+ US)</b>									
I	I,II,III, IV	<b>Combined (PAM BC + CE+ US)</b>	60-64	0.983	0.632	0.983	0.368	0.017	0.632	-	-
I	I,II,III, IV	<b>Combined (PAM BS + CE+ US)</b>	60-64	0.987	0.940	0.987	0.060	0.013	0.940	-	-
I	HA	US	65-69	0.867	0.987	0.867	0.013	0.133	0.987	10849	[63]
I	HA	CE	65-69	0.474	0.963	0.474	0.037	0.526	0.963	290330	[64]
I	DCIS	<b>Combined (PAM WS + CE+ US)</b>	65-69	0.968	0.584	0.968	0.416	0.032	0.584	-	-
I	DCIS	<b>Combined (PAM BC + CE+ US)</b>	65-69	0.972	0.664	0.972	0.336	0.028	0.664	-	-
I	DCIS	<b>Combined (PAM BS + CE+ US)</b>	65-69	0.954	0.789	0.976	0.211	0.024	0.789	-	-
I	I,II,III, IV	<b>Combined (PAM WS + CE+ US)</b>	65-69	0.977	0.556	0.977	0.444	0.023	0.556	-	-
I	I,II,III, IV	<b>Combined (PAM BC + CE+ US)</b>	65-69	0.983	0.632	0.983	0.368	0.017	0.632	-	-
I	I,II,III, IV	<b>Combined (PAM BS + CE+ US)</b>	65-69	0.976	0.940	0.987	0.060	0.013	0.940	-	-
I	HA	US	70-74	0.925	0.968	0.925	0.032	0.075	0.968	10849	[63]
I	HA	CE	70-74	0.474	0.963	0.474	0.037	0.526	0.963	290330	[64]
I	DCIS	<b>Combined (PAM WS + CE+ US)</b>	70-74	0.982	0.573	0.982	0.427	0.018	0.573	-	-
I	DCIS	<b>Combined (PAM BC + CE+ US)</b>	70-74	0.984	0.650	0.984	0.349	0.016	0.651	-	-
I	DCIS	<b>Combined (PAM BS + CE+ US)</b>	70-74	0.986	0.774	0.993	0.078	0.007	0.922	-	-
I	I,II,III, IV	<b>Combined (PAM WS +</b>	70-74	0.987	0.545	0.987	0.455	0.013	0.545	-	-



		<b>CE+ US)</b>									
I	I,II,III, IV	<b>Combined (PAM BC + CE+ US)</b>	70-74	0.990	0.620	0.990	0.380	0.010	0.620	-	-
I	I,II,III, IV	<b>Combined (PAM BS + CE+ US)</b>	70-74	0.993	0.922	0.993	0.078	0.007	0.922	-	-

**Table 31.** Sensitivity and Specificity values of PAM+ CE+US at early diagnosis

Scenarios (Group of application)	Stages	Technology	Age Interval	Sensitivity	Specificity	TP (rate)	FP (rate)	FN (rate)	TN (rate)	N (Sample dimension)	Reference
I	HA	FFDM	45-49	0.658	0.989	0.658	0.011	0.342	0.989	6000	[57]
I	HA	CE	45-49	0.474	0.963	0.474	0.037	0.526	0.963	290330	[64]
I	DCIS	<b>Combined (PAM WS + CE+ FFDM)</b>	45-49	0.917	0.917	0.415	0.415	0.083	0.585	-	-
I	DCIS	<b>Combined (PAM BC + CE+ FFDM)</b>	45-49	0.929	0.665	0.929	0.335	0.071	0.665	-	-
I	DCIS	<b>Combined (PAM BS + CE+ FFDM )</b>	45-49	0.938	0.791	0.938	0.209	0.062	0.791	-	-
I	I,II,III, IV	<b>Combined (PAM WS + CE+ FFDM)</b>	45-49	0.941	0.557	0.941	0.443	0.059	0.557	-	-
I	I,II,III, IV	<b>Combined (PAM BC + CE+ FFDM)</b>	45-49	0.956	0.633	0.956	0.367	0.044	0.633	-	-
I	I,II,III, IV	<b>Combined (PAM BS + CE+ FFDM)</b>	45-49	0.967	0.753	0.967	0.247	0.033	0.753	-	-
I	HA	FFDM	50-54	0.678	0.990	0.678	0.010	0.322	0.990	6000	[57]
I	HA	CE	50-54	0.474	0.963	0.474	0.037	0.526	0.963	290330	[64]
I	DCIS	<b>Combined (PAM WS + CE+ FFDM)</b>	50-54	0.922	0.586	0.922	0.414	0.078	0.586	-	-

I	DCIS	<b>Combined (PAM BC + CE+ FFDM)</b>	50-54	0.933	0.667	0.933	0.334	0.067	0.666	-	-
I	DCIS	<b>Combined (PAM BS + CE+ FFDM)</b>	50-54	0.941	0.792	0.941	0.208	0.059	0.792	-	-
I	I,II,III, IV	<b>Combined (PAM WS + CE+ FFDM)</b>	50-54	0.945	0.556	0.945	0.442	0.055	0.558	-	-
I	I,II,III, IV	<b>Combined (PAM BC + CE+ FFDM)</b>	50-54	0.959	0.634	0.959	0.366	0.041	0.634	-	-
I	I,II,III, IV	<b>Combined (PAM BS + CE+ FFDM)</b>	50-54	0.969	0.754	0.969	0.246	0.031	0.754	-	-
I	HA	FFDM	55-59	0.766	0.993	0.766	0.007	0.234	0.993	6000	[57]
I	HA	CE	55-59	0.474	0.963	0.474	0.037	0.526	0.963	290330	[64]
I	DCIS	<b>Combined (PAM WS + CE+ FFDM)</b>	55-59	0.953	0.5871	0.953	0.413	0.047	0.587	-	-
I	DCIS	<b>Combined (PAM BC + CE+ FFDM)</b>	55-59	0.963	0.668	0.963	0.332	0.037	0.668	-	-
I	DCIS	<b>Combined (PAM BS + CE+ FFDM)</b>	55-59	0.979	0.794	0.979	0.206	0.021	0.794	-	-
I	I,II,III, IV	<b>Combined (PAM WS + CE+ FFDM)</b>	55-59	0.960	0.559	0.960	0.441	0.040	0.559	-	-
I	I,II,III, IV	<b>Combined (PAM BC + CE+ FFDM)</b>	55-59	0.970	0.636	0.970	0.364	0.030	0.636	-	-
I	I,II,III, IV	<b>Combined (PAM BS + CE+ FFDM)</b>	55-59	0.977	0.756	0.977	0.244	0.023	0.756	-	-
I	HA	FFDM	60-64	0.800	0.993	0.800	0.007	0.200	0.993	6000	[57]
I	HA	CE	60-64	0.474	0.963	0.474	0.037	0.526	0.963	290330	[64]
I	DCIS	<b>Combined (PAM WS + CE+ FFDM)</b>	60-64	0.962	0.587	0.962	0.413	0.038	0.587	-	-

I	DCIS	<b>Combined (PAM BC + CE+ FFDM)</b>	60-64	0.967	0.667	0.967	0.333	0.033	0.667	-	-
I	DCIS	<b>Combined (PAM BS + CE+ FFDM)</b>	60-64	0.971	0.793	0.971	0.207	0.793	0.029	-	-
I	I,II,III, IV	<b>Combined (PAM WS + CE+ FFDM)</b>	60-64	0.966	0.560	0.966	0.441	0.034	0.559	-	-
I	I,II,III, IV	<b>Combined (PAM BC + CE+ FFDM)</b>	60-64	0.974	0.667	0.967	0.333	0.033	0.667	-	-
I	I,II,III, IV	<b>Combined (PAM BS + CE+ FFDM)</b>	60-64	0.981	0.756	0.981	0.244	0.019	0.756	-	-
I	HA	FFDM	65-69	0.843	0.992	0.843	0.008	0.157	0.992	6000	[57]
I	HA	CE	65-69	0.474	0.963	0.474	0.037	0.526	0.963	290330	[64]
I	DCIS	<b>Combined (PAM WS + CE+ FFDM)</b>	65-69	0.968	0.587	0.968	0.413	0.032	0.587	-	-
I	DCIS	<b>Combined (PAM BC + CE+ FFDM)</b>	65-69	0.975	0.667	0.975	0.333	0.025	0.667	-	-
I	DCIS	<b>Combined (PAM BS + CE+ FFDM)</b>	65-69	0.986	0.793	0.986	0.207	0.014	0.793	-	-
I	I,II,III, IV	<b>Combined (PAM WS + CE+ FFDM)</b>	65-69	0.973	0.559	0.973	0.441	0.027	0.559	-	-
I	I,II,III, IV	<b>Combined (PAM BC + CE+ FFDM)</b>	65-69	0.980	0.635	0.980	0.365	0.020	0.635	-	-
I	I,II,III, IV	<b>Combined (PAM BS + CE+ FFDM)</b>	65-69	0.985	0.756	0.985	0.244	0.015	0.756	-	-
I	HA	FFDM	70-74	0.821	0.990	0.821	0.010	0.179	0.990	6000	[57]
I	HA	CE	70-74	0.474	0.963	0.474	0.037	0.526	0.963	290330	[64]
I	DCIS	<b>Combined (PAM WS + CE+ FFDM)</b>	70-74	0.957	0.586	0.957	0.414	0.043	0.586	-	-

I	DCIS	<b>Combined (PAM BC + CE+ FFDM)</b>	70-74	0.963	0.666	0.963	0.334	0.037	0.666	-	-
I	DCIS	<b>Combined (PAM BS + CE+ FFDM)</b>	70-74	0.967	0.756	0.981	0.244	0.019	0.756	-	-
I	I,II,III, IV	<b>Combined (PAM WS + CE+ FFDM)</b>	70-74	0.969	0.558	0.969	0.031	0.031	0.969	-	-
I	I,II,III, IV	<b>Combined (PAM BC + CE+ FFDM)</b>	70-74	0.977	0.634	0.977	0.366	0.023	0.634	-	-
I	I,II,III, IV	<b>Combined (PAM BS + CE+ FFDM)</b>	70-74	0.983	0.754	0.983	0.246	0.017	0.754	-	-

**Table 32.** Sensitivity and Specificity values of PAM+ CE + FFDM at early diagnosis

#### 4.6.4. Utilities

As shown in *section 2.3.1.1.1.2* the utilities are fundamental to measure the quality of a specific health state or an intervention in order to obtain the overall QALYS's.

The Markov model structure, previously described, is associated with the evaluation of the health states or inventions in the breast cancer clinical pathway listed in the Table 33. 2 criteria were considered for selecting the values from the literature that considers a great variety of values:

- Either the calculation method is a MAU method, considered the most accurate method to calculate utilities as explained in *section 2.3.1.1.1.2*;
- Or the Quality score of the source paper is at least 5 in the quality score (1- to 7 score) attributed in the Cost-effectiveness analysis registry provided by the TUFTS University [67].

Health State/Intervention	Utility value (0-1)	Source	Calculation method	Quality score (TUFTS CEA registry) from [67]
Screening	0.990	[68]	NF	6
False Negatives	0.450	[69]	MAU	NF
False Positives	0.890	[68]	NF	6
Diagnosed breast cancer, by stage	Depends on age and cancer stage (Table 34)	[70, 71]	NF	5
Follow-up	0.850	[72]	NF	5.5
Local Recurrence	0.700	[73]	MAU	5.5
Regional Recurrence	0.500	[73]	MAU	5.5
Distant Recurrence	0.300	[73]	MAU	5.5

**Table 33.** Information about the utilities applied in the analysis for the different Health states/Interventions considered.

	Breast Cancer Stages				
	0	1	2	3	4
20-21	0.950	0.900	0.800	0.700	0.300
22-23	0.950	0.900	0.800	0.700	0.300
24-25	0.950	0.900	0.800	0.700	0.300
26-27	0.950	0.900	0.800	0.700	0.300
28-29	0.950	0.900	0.800	0.700	0.300
30-31	0.950	0.900	0.800	0.700	0.300
32-33	0.950	0.900	0.800	0.700	0.300
34-35	0.950	0.900	0.800	0.700	0.300
36-37	0.950	0.900	0.800	0.700	0.300
38-39	0.950	0.900	0.800	0.700	0.300
40-41	0.950	0.900	0.800	0.700	0.300
42-43	0.950	0.900	0.800	0.700	0.300
44-45	0.950	0.900	0.800	0.700	0.300
46-47	0.950	0.900	0.800	0.700	0.300
48-49	0.950	0.900	0.800	0.700	0.300
50-51	0.936	0.886	0.786	0.686	0.286
52-53	0.936	0.886	0.786	0.686	0.286
54-55	0.936	0.886	0.786	0.686	0.286
56-57	0.916	0.866	0.766	0.666	0.266
58-59	0.916	0.866	0.766	0.666	0.266
60-61	0.915	0.865	0.765	0.665	0.265
62-63	0.915	0.865	0.765	0.665	0.265
64-65	0.915	0.865	0.765	0.665	0.265
66-67	0.908	0.858	0.758	0.658	0.258
68-69	0.908	0.858	0.758	0.658	0.258
70-71	0.898	0.848	0.748	0.648	0.248
72-73	0.898	0.848	0.748	0.648	0.248
74-75	0.898	0.848	0.748	0.648	0.248

**Table 34.** Utilities used in the analysis by stage of breast cancer and by age

#### 4.6.5. Costs

The costs used in the model depend on the context that is being analysed – Portugal and Netherlands. The majority of Portuguese costs were taken from *Portaria n.º 163/2013* published in 24 of April in *Diário da República, 1ª Série* [74]. The majority of Netherlands costs were taken from the 2012 tables of health Costs defined by NZA (Nederlandse Zorgautoriteit), the Dutch Healthcare Authority [75].

##### 4.6.5.1. Screening and Diagnosis

Table 35 shows the costs for the screening and diagnosis procedures applied in the model.

	<b>Netherlands</b>	<b>Portugal</b>
<b>FFDM</b> ( <i>bilateral and 2 incidences for breast</i> )	64.44 € (Ref. 086902 [75])	20.50 € (Ref. 13100 [74])
<b>Clinical Examination</b> ( <i>Oncology</i> )	78.43 € (Ref. 197005 [75])	31.00 € (Art. 15° [74])
<b>Ultrasound</b> ( <i>Breast</i> )	51.35 € (Ref. 086970 [75])	14.50 € (Ref. 17105 [74])
<b>MRI</b> ( <i>Breast</i> )	160.10 € (Ref. 085090 [75])	127.90 € (Ref. 18100 [74])
<b>Stereotactic core biopsy</b>	202.70 € [76]	330.00 € (Ref. 13147 [74])
<b>Fine needle aspiration, ultrasound-guided</b>	149.10 € [76]	20.00 € (Ref. 15161 [74])
<b>Core needle aspiration, ultrasound-guided</b>	149.10 € [76]	50.00 € (Ref. 15171 [74])
<b>PAM (aprox US)</b>	51.35 €	14.50 €
<b>Open surgical biopsy, Image Guided<sup>6</sup></b>	1203.95 € [76]	439.70 € (Ref. 17315 [74])
<b>TAC</b> ( <i>abdominal</i> )	160.01 € (Ref. 089042 [75])	84.50 € (Ref. 16070 [74])

**Table 35.** Costs for screening and diagnosis procedures.

It was considered that the biopsies after early diagnosis were made with Surgical biopsy- image guided (in 30% of the cases) , Core needle biopsy- ultrasound guided (in 17% of the cases), Stereotactic Biopsy (in 49% of the cases) and Fine needle aspiration-ultrasound guided (in 4% of the cases) [77]. After late diagnosis it was considered that the biopsies were made with Surgical biopsy- image guided (in 45% of the cases), Core needle biopsy-imaged guided US/MRI (in 45% of the cases) and Fine needle aspiration- ultrasound guided (in 10 % of the cases) [78].

#### 4.6.5.2. Pre-Operative Assessments

Table 36 shows the individual costs for the procedures made after the diagnosis of breast cancer that preceded the treatment of breast cancer – the pre-operative assessments. Table 37 shows the overall costs of pre-operative assessments by stage.

<sup>6</sup> US-guided or stereotactic-guided

	Netherlands	Portugal
<b>Basic ECG</b> (12 DER)	97.74 € (Ref. 039844 [75])	6.50 € (Ref. 40301 [74])
<b>Hemogram</b>	27.64 € (Ref. 075044 [75])	4.70 € (Ref. 075044 [74])
<b>LFT- Albumin</b>	3.45 € (Ref. 070486 [75])	2.60 € (Ref. 2503 [74])
<b>LFT – Alanine transaminase</b>	1.76 € (Ref. 074891 [75])	1.30 € (Ref. 21217 [74])
<b>LFT – Aspartate transaminase</b>	1.76 € (Ref. 070489 [75])	1.30 € (Ref. 21220 [74])
<b>LFT – Alkaline phosphatase</b>	1.76 € (Ref. 077121 [75])	11.70 € (Ref. 21938 [74])
<b>LFT - Total Bilirubin</b>	1.76 € (Ref. 074110 [75])	1.40 € (Ref. 21340 [74])
<b>LFT - Gamma-glutamyltransferase</b>	1.76 € (Ref. 072110 [75])	1.50 € (Ref. 22035 [74])
<b>TAC Thorax</b> (2 incidences)	195.83 € (Ref. 08542 [75])	9.00 € (Ref. 10406 [74])
<b>Bone Scintigraphy to the whole body</b>	132.54 € (Ref. 120094 [75])	90.00 € (Ref. 58150 [74])
<b>Additional TC of volumetric measurement to the liver</b>	160.01 € (Ref. 089042 [75])	14.1 € (Ref. 16347)
<b>X- Rays</b> (Thorax)	45.37 € (Ref. 085002 [75])	9.00 € (Ref. 10406)

**Table 36.** Costs of pre-operative procedures

Stage	Netherlands	Portugal
<b>0</b>	64.44 €	20.50 €
<b>I</b>	787.17 €	179.10 €
<b>II</b>	787.17 €	179.10 €
<b>III</b>	787.17 €	179.10 €
<b>IV</b>	787.17 €	179.10 €

**Table 37.** Overall costs of pre-operative assessments by stage

### 4.6.5.3. Treatments

Table 38 shows the individual costs of treatment procedures applied in the model. Further Table 39 and Table 40 shows the overall treatments costs by stage and by cycle in Netherlands and Portugal respectively.



	Netherlands	Portugal
<b>Radiotherapy</b> (Non ambulatory)	218.31 € [75]	3140.84 € [74]
<b>Excision of malign tumors</b> (< 3cm)	438.31 € [75]	52.10 € (Ref: 75800 [74])
<b>Excision of malign tumors</b> (> 3 cm)	9346.00 € (Ref. 15A13 [75])	93.40 € (Ref :75805 [74])
<b>Hormonal Therapy</b> (per cycle of 1 year)	793.20 € [79]	793.20 € [79]
<b>Nursing hospital days</b> (6-28)	34257.00 € (Ref. 15A019 [75])	-
<b>Nursing hospital</b> (Daily fee)	-	1570.42 € (average 13.8 days [74])
<b>Consult Medical Oncology</b>	200 € [79]	123.74 € (Q117 [80])
<b>Masectomy</b> (Total)	2187.31 € [79]	1588.50 € [74]
<b>Chemoterapy</b> (per cycle of 6 months)	1442.18 € [79]	914.39 € [74]
<b>Reconstruction</b>	69474.00 € (Ref. 15A016 [75])	7010.64 € (Ref. 564[74])

**Table 38.** Costs of treatment procedures.

Stage	Overall first cycle costs	Overall next cycle costs
<b>0</b>	38604.71 €	1722.08 €
<b>I</b>	47950.71 €	1722.08 €
<b>II</b>	65158.89 €	2178.30 €
<b>III</b>	170017.61 €	2498.50 €
<b>IV</b>	8267.24 €	2498.50 €

**Table 39.** Overall costs of treatment procedures by stage and cycle in Netherlands.

Stage	Overall first cycle costs	Overall next cycle costs
<b>0</b>	26193.90 €	1329.16 €
<b>I</b>	29378.55 €	1329.16 €
<b>II</b>	27336.40 €	1637.16 €
<b>III</b>	104852.30 €	1892.96 €
<b>IV</b>	5550.52 €	1892.96 €

**Table 40.** Overall costs of treatment procedures by stage and cycle in Portugal.

#### 4.6.5.4. Follow Up

As mentioned in *section 2.2.4* the IARC guidelines suggest two procedures combinations to carry the *follow up*. In the model here described it was considered only the *limited follow up*, under which physical examination, x-ray mammography and history taking are made at an annual basis. Table 41 shows the costs associated with the follow up.

Netherlands	Portugal
142.87 €	51.50 €

**Table 41.** Costs of *limited follow up* every year.

#### 4.6.5.5. Recurrence

Table 42 shows the treatments by type of recurrence and by stage of primary breast cancer. Table 43 and Table 44 show the overall costs of recurrence treatment by type and by primary stage of breast cancer for cycle in Netherlands and Portugal, respectively.

	0	1	2	3
<b>Local</b>	Excision (Lumpectomy)	Excision (Lumpectomy)	Hormone therapy (50%) + Excision (Lumpectomy) + Adjuvant Chemotherapy (4 cycles)	Excision (Lumpectomy) + Hormone Therapy (50%) + Adjuvant Chemotherapy (4 cycles) + Radiotherapy
<b>Regional</b>	Excision (Lumpectomy)	Excision (Lumpectomy)	Hormone therapy (50%) + Excision (Lumpectomy) + Adjuvant Chemotherapy (4 cycles)	Excision (Lumpectomy) + Hormone Therapy (50%) + Adjuvant Chemotherapy (4 cycles) + Radiotherapy
<b>Distant (metastized)</b>	Palliative treatments of diagnosed primary stage 4			

**Table 42.** List of treatments by type of recurrence and primary stage of breast cancer. From [81] and [38].

	Primary Cancer Stage			
	0	1	2	3
<b>Local Recurrence (First cycle)</b>	438.31 €	438.31 €	6561.94 €	8749.25 €
<b>Local Recurrence (Next cycle)</b>	0 €	0 €	793.20 €	793.20 €
<b>Regional Recurrence (First cycle)</b>	438.31 €	438.31 €	6561.94 €	8749.25 €
<b>Regional Recurrence (Next cycle)</b>	0 €	0 €	793.20 €	793.20 €
<b>Distant Recurrence (First cycle)</b>	8267.24 €			
<b>Distant Recurrence (Next cycle)</b>	2498.50 €			

**Table 43.** Costs of recurrence treatment in Netherlands by type and primary stage of breast cancer for cycle. The next cycle costs includes only the hormone therapy costs.

	Primary Cancer Stage			
	0	1	2	3
<b>Local Recurrence (First cycle)</b>	52.10 €	52.10 €	4502.86 €	7643.70 €
<b>Local Recurrence (Next cycle)</b>	0 €	0 €	793.20 €	793.20 €
<b>Regional Recurrence (First cycle)</b>	52.10 €	52.10 €	4502.86 €	7643.70 €
<b>Regional Recurrence (Next cycle)</b>	0 €	0 €	793.20 €	793.20
<b>Distant Recurrence (First cycle)</b>	5550.52 €			
<b>Distant Recurrence (Next cycle)</b>	1892.96 €			

**Table 44.** Costs of recurrence treatment in Portugal by type and primary stage of breast cancer for cycle. The next cycle costs includes only the hormone therapy costs.

#### 4.6.5.6. PAM

According with the designers the costs of PAM use were estimated to be identical to the costs of US - 51.35 and 14.50 in the Dutch and Portuguese context, respectively. These were the values used in the CEA. In other perspective, the designers estimations for the costs of the whole equipment is 400.000 € [82].

### 4.7. Simulations

In CEA and similar analysis, the most efficient calculation method is generally the roll back analysis (expected values); however, it is also possible to evaluate decision trees using simulation, sometimes referred to *microsimulation* [83]. The calculation and simulation method to run the markov model was *microsimulation*. *Microsimulation* in decision trees approximates an expected value by “sampling” a representative distribution of paths through the model’s chance events; In this type of simulation the purpose is to utilize as many “trials” as time allows, in order to improve the expected value estimation, ensuring even small probability paths are “sampled” proportionally [83]. At the decision node (Scenario X vs Standard of care), each trial is repeated for each strategy, to facilitate strategy comparison. For each run in the different scenarios it was performed a *microsimulation* with 100.000 trials. The choice of this value was the result of a “trade-off” between the simulation time and the accuracy of the simulation. *Microsimulation* was also be used to explore the variability through Monte Carlo analysis. As mentioned in 4.6.3.2 a deterministic sensitivity analysis was also performed through the use of different values of PAM efficiency: Best scenario, Base case, worse scenario (as presented in 4.6.3.2).

## 5. Results

The results acquired in this thesis will be described. The chapter is divided into 3 main sections: one for the results acquired from the simulation made with scenarios of **Group I** (*section 5.1*), other for the results acquired from the simulation made with scenarios of **Group II** (*section 5.2*) and other for the results acquired from the simulation made with scenarios of **Group III** (*section 5.3*).

### 5.1. Group I

This section presents the results acquired with scenarios of Group I that consider the regular screening and diagnosis pathway of the general population. Table 45 shows the overall results obtained for the different simulations: It is presented the results by scenario (**Best scenario**, base case and worse scenario) at in terms of costs and effectiveness separately and the correspondent CE ratio ( $\frac{Cost}{Effectiveness}$ ), as explained in 2.3.1.1.1. Finally, for each Scenario it is presented the ICER relatively to the respective mean standard of care values (also previously introduced in 2.3.1.1.1.) and the optimal frequency of CE ratio among the 100.000 microsimulations performed in each scenario.

Scenario and context	Costs (€)					Effectiveness (QALY's)					Cost-effectiveness (€/QALY's)		Optimal frequency
	Mean	Std Deviation	Minimum	Median	Maximum	Mean	Std Deviation	Minimum	Median	Maximum	CE ratio	ICER	
Standard of Care NL	13117.933	34682.346	64.440	546.065	236849.595	13.601	2.984	0.000	14.799	14.815	964.483	-	-
Standard of Care PT	3465.627	14185.451	20.500	158.486	147217.965	12.732	2.005	0.000	13.327	13.341	272.198	-	-
Screening NL	<b>13476.750</b>	<b>34732.174</b>	<b>51.350</b>	<b>771.752</b>	<b>236912.245</b>	<b>13.536</b>	<b>2.992</b>	<b>0.000</b>	<b>14.799</b>	<b>14.824</b>	<b>995.623</b>	<b>5520.262</b>	<b>0.310</b>
	14018.551	34434.022	51.350	1494.269	236971.258	13.260	3.236	0.000	14.799	14.824	1057.206	2641.109	0.182
	13215.928	33816.120	51.350	1104.271	236971.258	13.364	3.187	0.000	14.799	14.824	988.920	413.481	0.190
Screening PT	<b>3622.626</b>	<b>14408.531</b>	<b>14.500</b>	<b>209.239</b>	<b>147208.935</b>	<b>12.630</b>	<b>2.134</b>	<b>0.000</b>	<b>13.327</b>	<b>13.348</b>	<b>286.827</b>	<b>1539.206</b>	<b>0.380</b>
	3785.573	14257.190	14.500	438.073	147258.181	12.428	2.364	0.000	13.327	13.348	304.600	1052.454	0.101
	3553.844	13960.946	14.500	313.775	147208.935	12.529	2.260	0.000	13.327	13.356	283.649	434.567	0.119
E. Diagnosis (Replacing US, FFDM and Clinical Examination) NL	<b>12660.442</b>	<b>33867.909</b>	<b>64.440</b>	<b>546.065</b>	<b>236656.945</b>	<b>13.518</b>	<b>3.099</b>	<b>0.000</b>	<b>14.799</b>	<b>14.815</b>	<b>936.572</b>	<b>-5511.940</b>	<b>0.182</b>
	12428.824	33579.75	64.440	546.065	236793.722	13.462	3.156	0.000	14.799	14.824	923.252	-4057.619	0.135
	11854.262	32531.704	64.440	546.065	236352.794	13.432	3.213	0.000	14.799	14.824	882.539	-7477.343	0.144
E. Diagnosis (Replacing US, FFDM and Clinical Examination) PT	<b>3360.769</b>	<b>13931.039</b>	<b>20.500</b>	<b>158.486</b>	<b>1471814.645</b>	<b>12.680</b>	<b>2.129</b>	<b>0.000</b>	<b>13.327</b>	<b>13.348</b>	<b>265.049</b>	<b>-2016.500</b>	<b>0.130</b>
	3215.295	13636.313	20.500	158.486	147196.907	12.628	2.194	0.000	13.327	13.348	241.262	-2407.038	0.088
	3101.71	13327.682	20.500	158.486	147317.466	12.726	2.188	0.000	13.327	13.348	243.730	-60652.833	0.105
E. Diagnosis (Replacing US) NL	<b>13120.619</b>	<b>34805.184</b>	<b>64.440</b>	<b>546.065</b>	<b>237313.878</b>	<b>13.539</b>	<b>3.071</b>	<b>0.000</b>	<b>14.799</b>	<b>14.815</b>	<b>969.098</b>	<b>43.323</b>	<b>0.050</b>
	13080.168	34703.912	64.440	546.065	236986.373	13.529	3.082	0.000	14.799	14.824	966.824	-524.514	0.050
	13005.732	34627.371	64.440	546.065	236820.423	13.508	3.100	0.000	14.799	14.824	962.817	-1206.462	0.049
E. Diagnosis (Replacing US) PT	<b>3463.342</b>	<b>14171.653</b>	<b>20.500</b>	<b>158.486</b>	<b>147383.221</b>	<b>12.697</b>	<b>2.068</b>	<b>0.000</b>	<b>13.327</b>	<b>13.348</b>	<b>272.769</b>	<b>65.286</b>	<b>0.004</b>
	3487.402	14175.567	20.500	158.486	147317.466	12.689	2.062	0.000	13.327	13.348	274.837	-506.395	0.005
	3398.334	14021.654	20.500	158.486	147317.466	12.678	2.095	0.000	13.327	13.348	268.050	-1246.167	0.006
E. Diagnosis (Replacing FFDM) NL	<b>13039.915</b>	<b>34606.007</b>	<b>64.440</b>	<b>546.065</b>	<b>254728.161</b>	<b>13.581</b>	<b>3.019</b>	<b>0.000</b>	<b>14.799</b>	<b>14.815</b>	<b>960.159</b>	<b>-3900.900</b>	<b>0.153</b>
	13098.791	34643.167	64.440	546.065	254728.161	13.515	3.092	0.000	14.799	14.824	969.204	-222.581	0.127
	13323.354	34997.604	64.440	546.065	248457.241	13.493	3.116	0.000	14.999	14.824	987.427	1902.046	0.122
E. Diagnosis (Replacing FFDM) PT	<b>3505.716</b>	<b>14344.236</b>	<b>20.500</b>	<b>158.486</b>	<b>151228.332</b>	<b>12.729</b>	<b>2.023</b>	<b>0.000</b>	<b>13.327</b>	<b>13.341</b>	<b>275.412</b>	<b>13363.00</b>	<b>0.153</b>
	3494.396	14276.721	20.500	158.486	147209.774	12.679	2.098	0.000	13.327	13.348	275.605	-542.811	0.124
	3458.413	14223.284	20.500	158.486	147259.021	12.670	2.107	0.000	13.327	13.348	272.961	116.355	0.118
L. Diagnosis NL	<b>12854.331</b>	<b>34272.201</b>	<b>64.440</b>	<b>546.065</b>	<b>248841.495</b>	<b>13.592</b>	<b>2.993</b>	<b>0.000</b>	<b>14.799</b>	<b>14.815</b>	<b>945.728</b>	<b>-29289.111</b>	<b>0.053</b>
	13313.988	35027.554	64.440	546.065	247787.261	13.551	3.054	0.000	14.799	14.815	982.510	3921.100	0.053

	12971.403	34467.808	64.440	546.065	237076.639	13.571	3.032	0.000	14.799	14.815	955.818	-4884.333	0.049
L. Diagnosis PT	<b>3472.050</b>	<b>14229.585</b>	<b>20.500</b>	<b>158.486</b>	<b>147167.710</b>	<b>12.727</b>	<b>2.030</b>	<b>0.000</b>	<b>13.327</b>	<b>13.348</b>	<b>272.809</b>	<b>1284.600</b>	<b>0.008</b>
	3452.217	14191.700	20.500	158.486	142831.898	12.726	2.019	0.000	13.327	13.348	271.230	-3352.500	0.007
	3531.118	14316.624	20.500	158.486	147267.211	12.723	2.030	0.000	13.327	13.341	277.538	-7276.778	0.007

**Table 45.** Overall results from scenarios of Group I: Best scenario, **base case** and **worse scenario**

With the results from Table 45 it was possible to distinguish the scenarios in which PAM is either dominated or not dominated. The tested scenarios were then classified as follows and illustrated in Fig. 22:

- Lower effectiveness and higher costs – Strict dominated (SD);
- Lower effectiveness and lower costs – Dominated (D);
- Higher effectiveness and lower costs – Not dominated (ND);
- Higher effectiveness and higher costs – Not dominated, requiring willingness to pay analysis (NDWTP);

## ICER CLASSIFICATION

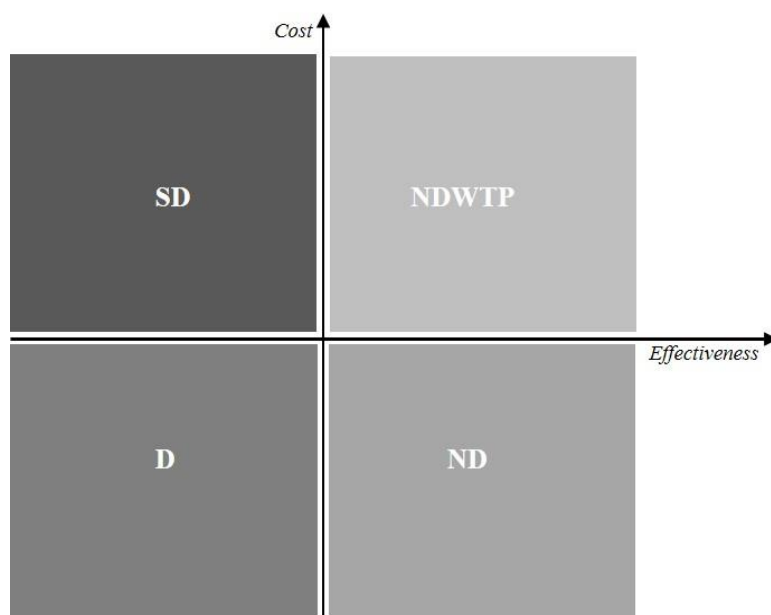


**Fig. 22.** Scenarios classification system in terms of dominance

The concept of WTP has been previously introduced in 2.3.1.1.1. Table 46 shows the status of dominance for the scenarios of Group I.

Scenario	Context	
	NL	PT
Screening (BS)	<i>SD</i>	<i>SD</i>
Screening (BC)	<i>SD</i>	<i>SD</i>
Screening (WS)	<i>SD</i>	<i>SD</i>
E. Diagnosis , Replacing US (BS)	<i>SD</i>	<i>SD</i>
E. Diagnosis , Replacing US (BC)	<i>D</i>	<i>D</i>
E. Diagnosis, Replacing US (WS)	<i>D</i>	<i>D</i>
E. Diagnosis , Replacing FFDM (BS)	<i>D</i>	<i>D</i>
E. Diagnosis, Replacing FFDM (BC)	<i>D</i>	<i>SD</i>
E. Diagnosis, Replacing FFDM (WS)	<i>SD</i>	<i>D</i>
E. Diagnosis, Replacing US, FFDM and Clinical Examination (BS)	<i>D</i>	<i>D</i>
E. Diagnosis, Replacing US, FFDM and Clinical Examination (BC)	<i>D</i>	<i>D</i>
E. Diagnosis, Replacing US, FFDM and Clinical Examination (WS)	<i>D</i>	<i>D</i>
L. Diagnosis (BS)	<i>D</i>	<i>SD</i>
L. Diagnosis (BC)	<i>SD</i>	<i>D</i>
L. Diagnosis (WS)	<i>D</i>	<i>D</i>

**Table 46.** Status of dominance of PAM versus Standards of care in all the scenarios of group I. *D*- Dominated; *SD* – Strict dominated; *ND* – Not Dominated; *NDWTP*- dominated, requiring willingness to pay analysis;

As Table 46 shows the majority of scenarios of group I have been dominated or strict dominated by the standard of care.

## **5.2. Group II**

This section presents the results acquired with scenarios of Group II, that test the scenarios including the different groups at moderate to high risk of breast cancer. Table 46 shows the overall results obtained for the different simulations (following the same logical explained in *section 5.1*).



	<i>Costs</i>					<i>Effectiveness</i>							
Scenario and context	Mean	Std Deviation	Minimum	Median	Maximum	Mean	Std Deviation	Minimum	Median	Maximum	CE ratio	ICER	Optimal frequency
Standard of Care NL	4997.184	14081.726	160.010	3461.510	282430.753	15.110	3.689	0.000	16.914	16.827	330.720	-	-
Standard of Care PT	3060.184	8128.227	127.900	2229.367	145865.614	13.535	3.163	0.000	14.990	15.000	<b>226.094</b>	-	-
BRCA 1 (40-69) NL	<b>3278.611</b> 4796.268 3981.144	<b>13987.418</b> 14297.378 14071.393	<b>51.350</b> 51.350 51.350	<b>1628.881</b> 3168.343 2336.291	<b>272201.341</b> 262833.450 261772.306	<b>15.354</b> 14.050 12.835	<b>2.294</b> 3.011 2.253	<b>0.000</b> 0.000 0.000	<b>15.965</b> 15.285 13.587	<b>16.325</b> 16.196 15.873	<b>213.535</b> 341.171 310.179	<b>-7043.332</b> -189.543 -446.611	<b>0.180</b> 0.180 0.150
BRCA 1 (40-69) PT	<b>1465.591</b> 1862.110 1652.668	<b>8395.214</b> 8058.696 8255.768	<b>14.500</b> 14.500 14.500	<b>453.832</b> 937.876 677.194	<b>158173.431</b> 152439.703 145686.858	<b>13.709</b> 12.588 11.473	<b>1.961</b> 2563 1.933	<b>0.000</b> 0.000 0.000	<b>14.233</b> 13.627 12.113	<b>14.701</b> 14.589 14.294	<b>106.907</b> 147.974 144.049	<b>-9164.328</b> -1265.126 -682.597	<b>0.178</b> 0.180 0.144
Standard of Care NL	4107.236	9664.566	160.010	3459.200	283541.748	15.184	3.589	0.000	16.814	16.827	270.498	-	-
Standard of Care PT	2549.863	5559.261	127.900	2228.348	158457.977	13.624	3.039	0.000	14.990	15.000	187.160	-	-
BRCA 2 (40-69) NL	<b>2413.693</b> 3843.431 3062.234	<b>9798.507</b> 9410.937 9411.407	<b>51.350</b> 51.350 51.350	<b>1624.736</b> 3163.600 23330.875	<b>262156.235</b> 261720.767 261114.449	<b>15.455</b> 14.143 12.895	<b>2.069</b> 2.871 2.142	<b>0.000</b> 0.000 0.000	<b>15.965</b> 15.285 13.587	<b>16.325</b> 16.006 15.706	<b>156.176</b> 298.056 237.474	<b>-6249.236</b> -253.415 -456.532	<b>0.176</b> 0.179 0.145
BRCA 2 (40-69) PT	<b>914.091</b> 1356.932 1126.146	<b>5714.385</b> 5387.532 5397.538	<b>14.500</b> 14.500 14.500	<b>452.994</b> 936.738 675.757	<b>145582.382</b> 158110.574 158052.398	<b>13.788</b> 12.655 11.532	<b>1.768</b> 2.451 1.819	<b>0.000</b> 0.000 0.000	<b>14.233</b> 13.627 12.113	<b>14.701</b> 14.415 14.311	<b>66.296</b> 107.225 97.654	<b>-9974.220</b> -1231.095 -680.553	<b>0.177</b> 0.177 0.140
Standard of Care NL	1673.842	7468.455	64.440	1154.255	343091.908	11.669	1.006	0.000	11.821	12.102	143.443	-	-
Standard of Care PT	626.878	4216.312	20.500	328.113	145595.072	11.820	0.971	0.000	11.964	11.977	53.035	-	-
HRisk mam: dense (40-59) NL	<b>1838.865</b> 2996.445 2337.548	<b>7838.133</b> 7627.929 7383.345	<b>51.350</b> 51.350 51.350	<b>1268.060</b> 2480.530 1818.560	<b>260537.176</b> 270904.959 343055.185	<b>12.741</b> 12.349 11.435	<b>1.363</b> 2.079 1.541	<b>0.000</b> 0.000 0.000	<b>13.003</b> 13.003 11.821	<b>13.017</b> 13.023 12.102	<b>144.327</b> 242.647 204.421	<b>153.939</b> 1945.004 2836.350	<b>0.978</b> 0.917 0.054
HRisk mam: dense (40-59) PT	<b>670.98</b> 1061.252 840.180	<b>4348.429</b> 4367.942 4303.868	<b>14.500</b> 14.500 14.500	<b>362.623</b> 758.633 543.332	<b>145582.382</b> 145309.976 145309.976	<b>11.728</b> 11.396 10.529	<b>1.223</b> 1.833 1.384	<b>0.000</b> 0.000 0.000	<b>11.964</b> 1.964 10.877	<b>11.982</b> 11.986 11.145	<b>57.212</b> 93.125 79.797	<b>479.370</b> 1024.467 165.222	<b>0.981</b> 0.925 0.077
HRisk mam: non dense (40-59) NL	<b>1838.665</b> 3021.677 2339.198	<b>7882.336</b> 7922.099 7458.476	<b>51.350</b> 51.350 51.350	<b>1268.119</b> 2480.569 1820.289	<b>262256.177</b> 257482.816 261531.856	<b>11.540</b> 11.230 10.176	<b>1.362</b> 2.073 1.335	<b>0.000</b> 0.000 0.000	<b>13.003</b> 13.003 10.507	<b>13.023</b> 13.023 11.921	<b>144.322</b> 244.611 229.874	<b>153.896</b> 1970.519 445.650	<b>0.343</b> 0.025 0.016

HRisk mam: non dense (40- 59) PT	<b>659.185</b> 1042.001 839.339	<b>4222.276</b> 4185.857 4311.293	<b>14.500</b> 14.500 14.500	<b>362.608</b> 757.788 543.367	<b>145526.976</b> 145199.224 145582.382	<b>11.727</b> 11.402 9.378	<b>1.222</b> 1.819 1.171	<b>0.000</b> 0.000 0.000	<b>11.964</b> 11.964 9.668	<b>11.982</b> 11.982 11.033	<b>56.211</b> 91.388 89.501	<b>347.387</b> 993.117 87.003	<b>0.452</b> 0.025 0.015
<b>Standard of Care NL</b>	1108.200	6124.197	51.350	697.068	172309.555	6.651	0.394	0.000	6.692	6.990	166.622	-	-
<b>Standard of Care PT</b>	571.222	3749.645	20.500	215.461	105442.504	6.360	0.360	0.000	6.397	6.675	89.815	-	-
MRisk mam: dense (40-49) NL	<b>1113.448</b> 1851.847 1485.827	<b>5607.448</b> 5924.789 6068.223	<b>51.350</b> 51.350 51.350	<b>746.284</b> 1451.133 1063.754	<b>172296.465</b> 170160.735 172296.465	<b>7.296</b> 7.208 6.601	<b>0.506</b> 0.757 0.557	<b>0.000</b> 0.000 0.000	<b>5.948</b> 7.361 6.692	<b>7.391</b> 7.391 6.990	<b>154.474</b> 256.916 225.091	<b>8.136</b> 1335.093 7552.540	<b>0.008</b> 0.036 0.103
MRisk mam: dense (40-49) PT	<b>435.220</b> 686.112 584.076	<b>3167.149</b> 3291.112 3674.251	<b>14.500</b> 14.500 14.500	<b>218.767</b> 443.391 324.649	<b>103879.159</b> 106815.12 105436.504	<b>6.980</b> 6.894 6.313	<b>0.454</b> 0.704 0.520	<b>0.000</b> 0.000 0.000	<b>7.037</b> 7.037 6.397	<b>7.065</b> 7.065 6.753	62.352 99.523 92.520	-219.358 215.150 273.489	<b>0.007</b> 0.031 0.154
MRisk mam: non dense (40- 49) NL	<b>1120.247</b> 1813.489 1485.989	<b>5581.297</b> 5514.377 6124.289	<b>51.350</b> 51.350 51.350	<b>756.284</b> 1415.133 1064.295	<b>172296.465</b> 171283.724 169147.995	<b>6.550</b> 6.520 5.880	<b>0.484</b> 0.748 0.457	<b>0.000</b> 0.000 0.000	<b>7.361</b> 7.361 5.948	<b>7.391</b> 7.391 6.841	<b>153.489</b> 251.489 252.119	<b>18.562</b> 1259.445 489.999	<b>0.444</b> 0.018 0.009
MRisk mam: non dense (40- 49) PT	<b>441.200</b> 712.084 560.012	<b>3249.838</b> 3570.904 3400.430	<b>14.500</b> 14.500 14.500	<b>218.767</b> 443.391 443.391	<b>13879.159</b> 106793.505 106793.505	<b>6.289</b> 6.200 6.010	<b>0.469</b> 0.701 0.701	<b>0.000</b> 0.000 0.000	<b>7.037</b> 7.037 7.037	<b>7.065</b> 7.065 7.065	63.245 103.260 81.208	<b>-211.075</b> 262.802 -20.914	<b>0.554</b> 0.023 0.009
<b>Standard of Care NL</b>	3218.360	7264.656	160.10	2732.892	261392.429	12.238	2.274	0.000	13.003	13.023	262.981	-	-
<b>Standard of Care PT</b>	2049.670	4158.640	14.500	1813.886	157934.485	11.287	2.032	0.000	11.964	11.982	181.596	-	-
HRisk (30-49) NL	<b>1789.145</b> 2993.727 2331.029	<b>7302.950</b> 7531.846 7320.489	<b>51.350</b> 51.350 51.350	<b>1264.756</b> 2479.039 1818.357	<b>263733.508</b> 260570.654 262075.651	<b>12.137</b> 11.315 10.212	<b>1.197</b> 1.755 1.281	<b>0.000</b> 0.000 0.000	<b>12.346</b> 11.821 10.507	<b>12.467</b> 12.148 12.238	<b>147.413</b> 260.580 228.264	<b>-14150.644</b> -243.373 -437.972	<b>0.109</b> 0.109 0.091
HRisk (30-49) PT	<b>656.708</b> 1057.823 854.036	<b>4158.640</b> 4341.629 4461.463	<b>14.500</b> 14.500 14.500	<b>362.070</b> 755.650 541.900	<b>145585.895</b> 143044.167 105758.076	<b>11.169</b> 10.427 9.411	<b>1.089</b> 1.574 1.132	<b>0.000</b> 0.000 0.000	<b>11.360</b> 10.877 9.668	<b>11.463</b> 11.233 11.074	<b>58.797</b> 101.450 90.749	<b>-11804.763</b> -1153.310 -637.332	<b>0.110</b> 0.108 0.087
<b>Standard of Care NL</b>	4109.897	12138.192	160.010	2736.706	262353.631	12.160	2.393	0.000	13.003	13.023	387.985	-	-
<b>Standard of Care PT</b>	2585.619	7087.246	127.900	1815.160	155289.983	11.226	2.142	0.000	11.964	11.982	230,324	-	-
BRCA1 (30- 49) NL	<b>2685.918</b> 3920.927 3263.608	<b>12122.917</b> 12306.435 12357.759	<b>51.350</b> 51.350 51.350	<b>1270.477</b> 2428.176 1823.873	<b>262201.531</b> 278811.636 267038.626	<b>12.052</b> 11.241 10.154	<b>1.455</b> 1.901 1.428	<b>0.000</b> 0.000 0.000	<b>12.346</b> 11.821 10.507	<b>12.467</b> 12.148 11.968	<b>222.861</b> 358.806 321.411	<b>-13184.991</b> -205.626 -421.879	<b>0.114</b> 0.114 0.096
BRCA1 (30- 49) PT	<b>1210.678</b> 1615.771	<b>7187.895</b> 7226.246	<b>14.500</b> 14.500	<b>363.028</b> 758.144	<b>145751.456</b> 145437.525	<b>11.098</b> 10.364	<b>1.313</b> 1.699	<b>0.000</b> 0.000	<b>11.360</b> 10.877	<b>11.463</b> 11.233	<b>109.090</b> 155.902	<b>-10741.727</b> -1125.114	<b>0.113</b> 0.115

	1386.193	7244.604	14.500	542.558	155199.100	9.355	1.281	0.000	9.668	11.074	71.619	-147.549	0.092
<b>Standard of Care NL</b>	3392.501	8359.167	160.010	2734.408	273864.032	12.220	2.312	0.000	13.003	13.023	277.619	-	-
<b>Standard of Care PT</b>	<b>2137.265</b>	<b>4744.726</b>	<b>127.900</b>	<b>1814.515</b>	<b>143184.550</b>	<b>11.290</b>	<b>2.029</b>	<b>0.000</b>	<b>11.964</b>	<b>11.982</b>	<b>189.306</b>	<b>-</b>	<b>-</b>
BRCA2 (30-49) NL	<b>1964.050</b> 3137.541 2479.407	<b>8312.056</b> 8394.198 8213.365	<b>51.350</b> 51.350 51.350	<b>1268.064</b> 2481.166 1817.990	<b>262109.129</b> 261147.927 261114.449	<b>12.112</b> 11.297 10.199	<b>1.286</b> 1.798 1.315	<b>0.000</b> 0.000 0.000	<b>12.346</b> 11.821 10.507	<b>12.500</b> 12.022 11.968	<b>162.157</b> 277.732 243.103	<b>-13226.398</b> -276.230 -451.803	<b>0.107</b> 0.110 0.050
BRCA2 (30-49) PT	<b>741.373</b> 1130.853 904.436	<b>4670.781</b> 4785.647 4711.290	<b>14.500</b> 14.500 14.500	<b>362.381</b> 755.467 541.419	<b>142447.405</b> 145324.472 145199.224	<b>11.158</b> 10.419 9.402	<b>1.131</b> 1.591 1.151	<b>0.000</b> 0.000 0.000	<b>11.360</b> 10.877 9.668	<b>11.463</b> 11.233 11.074	<b>66.443</b> 108.538 96.196	<b>-10574.939</b> -1155,467 -652,981	<b>0.110</b> 0.109 0.089
<b>Standard of Care NL</b>	4440.781	11498.719	160.010	3384.610	270593.075	13.712	5.035	0.000	16.814	16.831	323.861	-	-
<b>Standard of Care PT</b>	2652.608	6412.576	127.900	2207.556	184850.613	12.327	4.358	0.000	14.990	15.000	215.187	-	-
TP53 (20-49) NL	<b>2940.497</b> 4237.096 3606.715	<b>11574.120</b> 11515.573 11549.986	<b>51.350</b> 51.350 51.350	<b>1635.964</b> 3115.001 2324.616	<b>261498.378</b> 260506.223 260539.702	<b>13.881</b> 12.441 11.886	<b>3.058</b> 4.579 3.498	<b>0.000</b> 0.000 0.000	<b>14.946</b> 15.285 13.587	<b>16.229</b> 16.293 15.619	<b>211.836</b> 340.575 303.442	<b>-8877.420</b> -160.256 -456.772	<b>0.233</b> 0.238 0.226
TP53 (20-49) PT	<b>1180.508</b> 1685.437 1422.732	<b>6415.269</b> 6810.157 6607.014	<b>14.500</b> 14.500 14.500	<b>465.484</b> 941.511 692.723	<b>145381.196</b> 129675.681 145324.472	<b>12.409</b> 11.187 10.691	<b>2.644</b> 3.949 2.975	<b>0.000</b> 0.000 0.000	<b>13.324</b> 13.627 12.113	<b>14.478</b> 14.534 14.255	<b>95.133</b> 150.660 133.077	<b>-17952.439</b> -848.396 -751.758	<b>0.230</b> 0.235 0.220

**Table 47.** Overall results from scenarios of Group II: Best scenario, **base case** and **worse scenario**

Scenario	Context	
	NL	PT
BRCA 1 (40-69) (BS)	<i>ND</i>	<i>ND</i>
BRCA 1 (40-69) (BC)	<i>D</i>	<i>D</i>
BRCA 1 (40-69) (WS)	<i>D</i>	<i>D</i>
BRCA 2 (40-69) (BS)	<i>ND</i>	<i>ND</i>
BRCA 2 (40-69) (BC)	<i>D</i>	<i>D</i>
BRCA 2 (40-69) (WS)	<i>D</i>	<i>D</i>
HRisk mam: dense (40-59) (BS)	<i>NDWTP</i>	<i>NDWTP</i>
HRisk mam: dense (40-59) (BC)	<i>NDWTP</i>	<i>NDWTP</i>
HRisk mam: dense (40-59) (WS)	<i>SD</i>	<i>SD</i>
HRisk mam: non dense (40-59) (BS)	<i>SD</i>	<i>SD</i>
HRisk mam: non dense (40-59) (BC)	<i>SD</i>	<i>SD</i>
HRisk mam: non dense (40-59) (WS)	<i>SD</i>	<i>SD</i>
MRisk mam: dense (40-49) (BS)	<i>NDWTP</i>	<i>ND</i>
MRisk mam: dense (40-49) (BC)	<i>NDWTP</i>	<i>NDWTP</i>
MRisk mam: dense (40-49) (WS)	<i>SD</i>	<i>SD</i>
MRisk mam: non dense (40-49) (BS)	<i>SD</i>	<i>D</i>
MRisk mam: non dense (40-49) (BC)	<i>SD</i>	<i>D</i>
MRisk mam: non dense (40-49) (WS)	<i>SD</i>	<i>SD</i>
HRisk (30-49) (BS)	<i>D</i>	<i>D</i>
HRisk (30-49) (BC)	<i>D</i>	<i>D</i>
HRisk (30-49) (WS)	<i>D</i>	<i>D</i>
BRCA1 (30-49) (BS)	<i>D</i>	<i>D</i>
BRCA1 (30-49) (BC)	<i>D</i>	<i>D</i>
BRCA1 (30-49) (WS)	<i>D</i>	<i>D</i>
BRCA2 (30-49) (BS)	<i>D</i>	<i>D</i>
BRCA2 (30-49) (BC)	<i>D</i>	<i>D</i>
BRCA2 (30-49) (WS)	<i>D</i>	<i>D</i>
TP53 (20-49) (BS)	<i>ND</i>	<i>ND</i>
TP53 (20-49) (BC)	<i>D</i>	<i>D</i>
TP53 (20-49) (WS)	<i>D</i>	<i>D</i>

**Table 48.** Status of dominance of PAM versus Standards of care in all the scenarios of group II. *D*- Dominated; *SD* – Strict dominated; *ND* – Not Dominated; *NDWTP*- dominated, requiring willingness to pay analysis;

The presented results suggest that in both contexts PAM use in *HRisk mam: dense (40-59)* (vide Fig. 23 and Fig. 24 for the Dutch and the Portuguese context respectively) and *MRisk mam: dense (40-49)* (vide Fig. 25 and Fig. 24 for the Dutch and the Portuguese context respectively) scenarios is not dominated simultaneously for the base case and best scenario of values. However the CE acceptability is dependent on the WTP analysis for all these cases with exception of the Portuguese best scenario where there is an absolute non dominance (vide Fig. 27). Additionally, PAM use for *BRCA1 (40-69)*, *BRCA2 (40-69)* and *TP53 (20-49)* carriers only appeared not dominated with the best scenario of values.

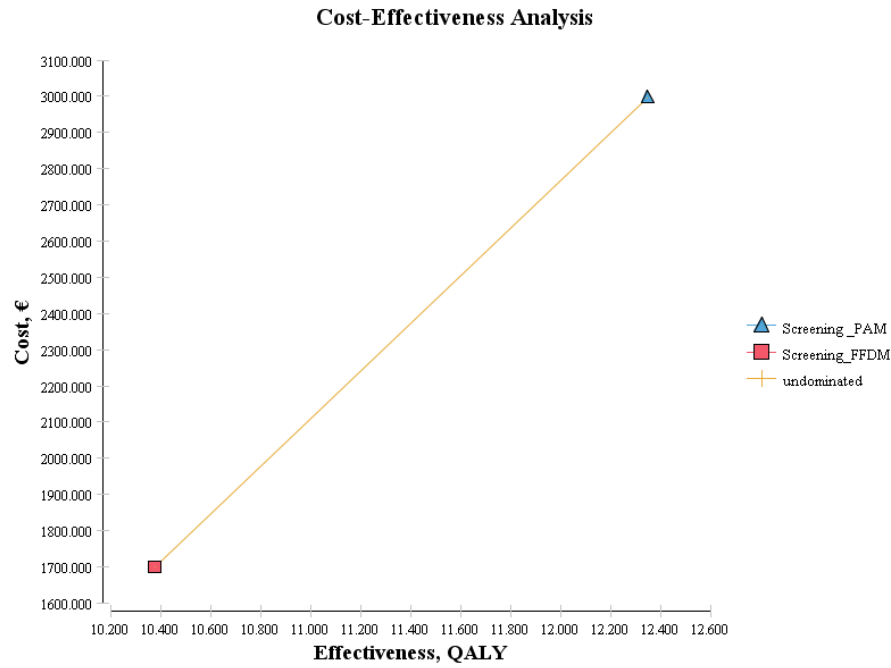


**Fig. 23.** Cost- effectiveness ratio of the scenario *HRisk mam: dense (40-59) NL base case*

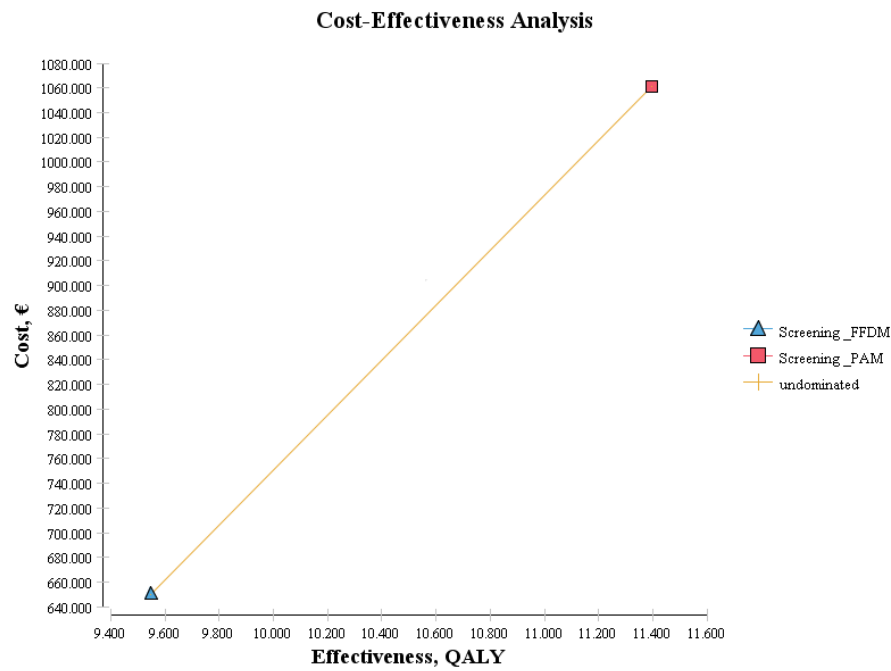


**Fig. 24.** Cost- effectiveness ratio of the scenario *HRisk mam: dense (40-59) PT base case*

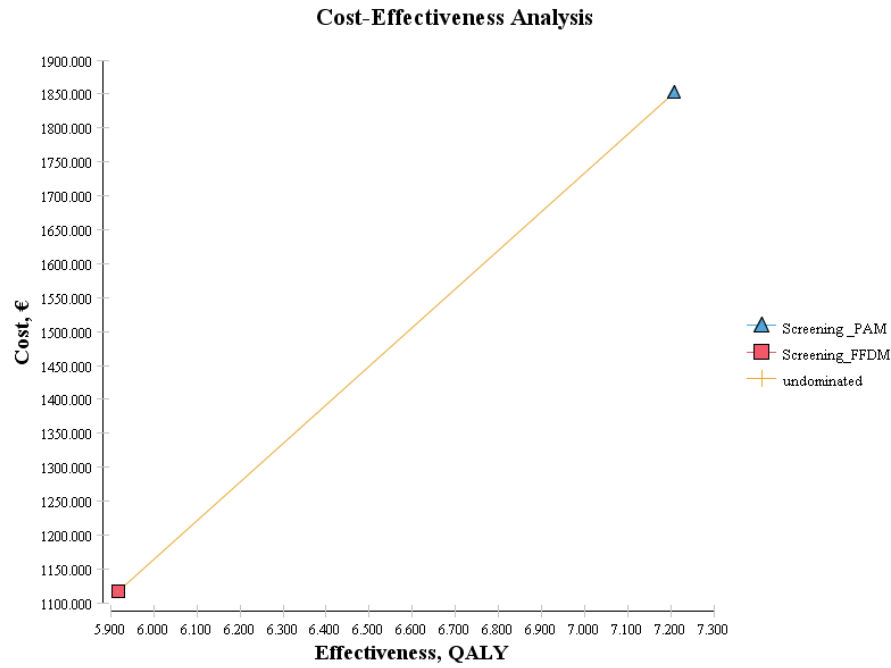


**Fig. 25.** Cost- effectiveness ratio of the scenario *MRisk mam: dense (40-49) NL base case*

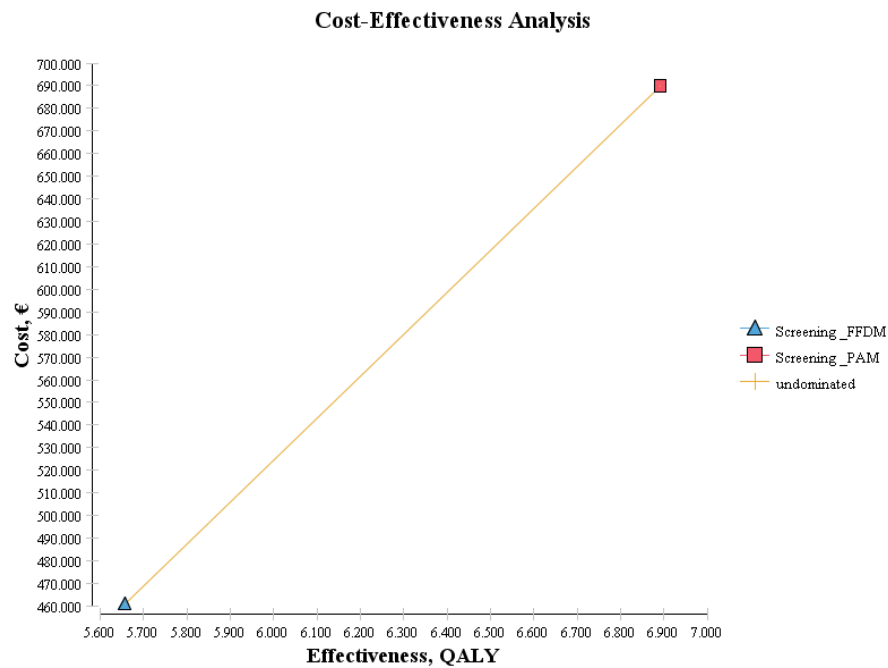


**Fig. 26.** Cost- effectiveness ratio of the scenario *MRisk mam: dense (40-49) PT base case*

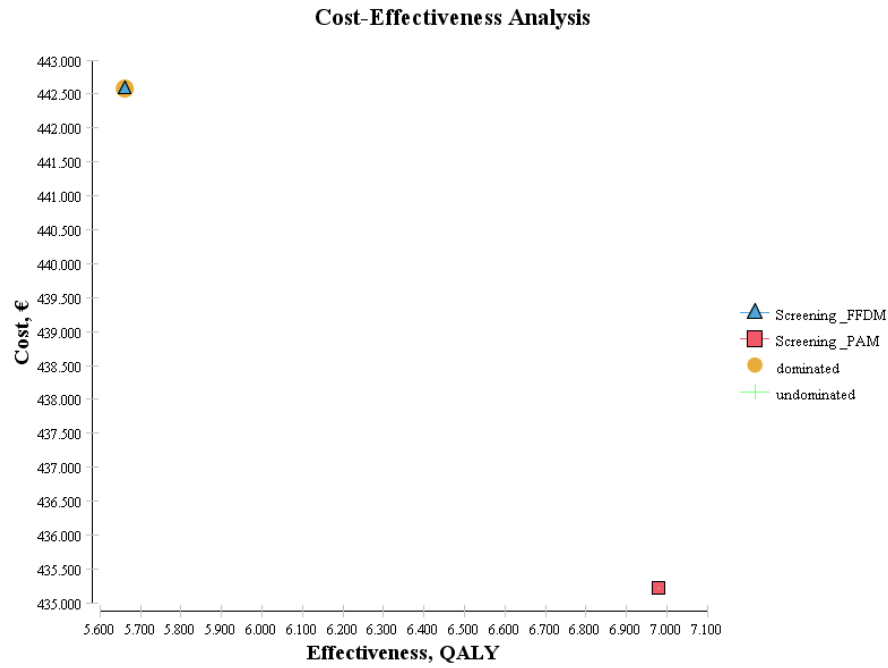


**Fig. 27.** Cost- effectiveness ratio of the scenario *MRisk mam: dense (40-49) PT best scenario*

### 5.3. Group III

This section presents the results acquired with scenarios of Group III, that test scenarios in which it is assumed to use an hypothetical technology with 5% better effectiveness than the standard of care for the regular clinical pathway of breast cancer. Table 49 shows the overall results obtained for the different simulations (following the same logical explained in *section 5.1*).

	Costs (€)					Effectiveness (QALY's)					Cost-effectiveness (€/QALY's)		
Scenario and context	Mean	Std Deviation	Minimum	Median	Maximum	Mean	Std Deviation	Minimum	Median	Maximum	CE ratio	ICER	Optimal frequency
Standard of care NL	9786.669	25950.844	64.440	733.957	229312.797	18.774	4.500	0.000	20.572	20.747	521.88	-	-
Standard of care PT	2682.831	11479.238	20.500	158.486	105758.219	12.883	1.827	0.000	13.327	13.341	208.246	-	-
Screening (+ 5 % sen) NL	9595.104	25661.149	51.350	584.865	229274.154	18.799	4.462	0.000	20.572	20.747	510.405	-7662.600	0.002
Screening (+ 5 % sen) PT	2641.978	11450.800	14.500	112.100	105752.219	12.889	1.811	0.000	13.327	13.341	140.538	-6808.833	0.001
E. Diagnosis (+ 5 % sen, repl US) NL	9792.002	25937.707	64.440	733.957	169468.706	18.774	4.501	0.000	20.572	20.800	521.572	5.333 <sup>7</sup>	0.002
E. Diagnosis (+ 5 % sen, repl US) PT	2727.777	11574.148	20.500	158.486	104971.655	12.884	1.849	0.000	13.327	13.341	211.916	4086.000	0.965
E. Diagnosis (+ 5 % sen, repl FFDM) NL	9767.500	25780.061	64.440	733.957	229070.249	18.783	4.508	0.000	20.572	20.747	520.572	-1742.636	0.231
E. Diagnosis (+ 5 % sen, repl FFDM) PT	2660.984	11318.824	20.500	158.486	103373.910	12.896	1.843	0.000	13.327	13.341	206.662	-3121.000	0.997
L. Diagnosis (+ 5 % sen) NL	9902.157	26214.021	64.440	733.957	164493.154	18.796	4.539	0.000	20.572	20.800	527.946	6416.000	0.012
L. Diagnosis (+ 5 % sen) PT	2727.665	11555.397	20.500	158.486	104532.925	12.891	1.857	0.000	13.327	13.341	211.923	3736.167	0.966
L. Diagnosis (+ 5 % spe) NL	9871.037	26070.640	64.440	733.957	164493.154	18.788	4.534	0.000	20.572	20.572	526.231	5273.000	0.012

<sup>7</sup> The ICER is not a real number due to the null difference between the effectiveness of standard of care and the scenario tested [E. Diagnosis (+ 5 % sen, repl US) NL]. For this reason the presented value is the cost difference between the 2 strategies.



L. Diagnosis (+ 5 % spe) PT	2792.470	11698.046	20.500	158.486	102796.828	12.889	1.869	0.000	13.327	13.341	217.043	6449.353	0.967
L. Diagnosis (+ 5 % sen & spe) NL	9834.407	26160.592	64.440	733.957	163568.922	18.779	4.546	0.000	20.572	20.582	524.598	1539.935	0.059
L. Diagnosis (+ 5 % sen & spe) PT	2693.858	11466.651	20.500	158.486	103850.499	12.899	1.859	0.000	13.327	13.341	209.297	918.917	0.966

**Table 49.** Overall results from scenarios of Group III.

Table 50 shows the status of dominance for the scenarios of Group III following the classification explained in *section 5.1*.

Scenario	Context	
	NL	PT
Screening (+ 5 % sen)	<i>ND</i>	<i>ND</i>
E. Diagnosis (+ 5 % sen, repl US)	<i>ND</i>	<i>NDWTP</i>
E. Diagnosis (+ 5 % sen, repl FFDm)	<i>ND</i>	<i>ND</i>
L. Diagnosis (+ 5 % sen)	<i>NDWTP</i>	<i>NDWTP</i>
L. Diagnosis (+ 5 % spe)	<i>NDWTP</i>	<i>NDWTP</i>
L. Diagnosis (+ 5 % sen & spe)	<i>NDWTP</i>	<i>NDWTP</i>

**Table 50.** Status of dominance of optimized hypothetical technology versus Standards of care in all the scenarios of group III. *D- Dominated; SD – Strict dominated; ND – Not Dominated; NDWTP- dominated, requiring willingness to pay analysis;*

As expected the increased efficiency of an optimized hypothetical technology (with PAM costs) induces better overall effectiveness. As Table 50 all the tested scenarios of group III were not dominated. However 4 scenarios require willingness to pay analysis:

- E. Diagnosis (+ 5 % sen, replacing US) in the Portuguese context (vide Fig. 28).
- L. Diagnosis (+ 5 % sen) in the Dutch and Portuguese context ;
- L. Diagnosis (+ 5 % spe) in the Dutch and Portuguese context (vide Fig. 29 for the Portuguese context).
- L. Diagnosis (+ 5 % sen & spe) in the Dutch and Portuguese context.

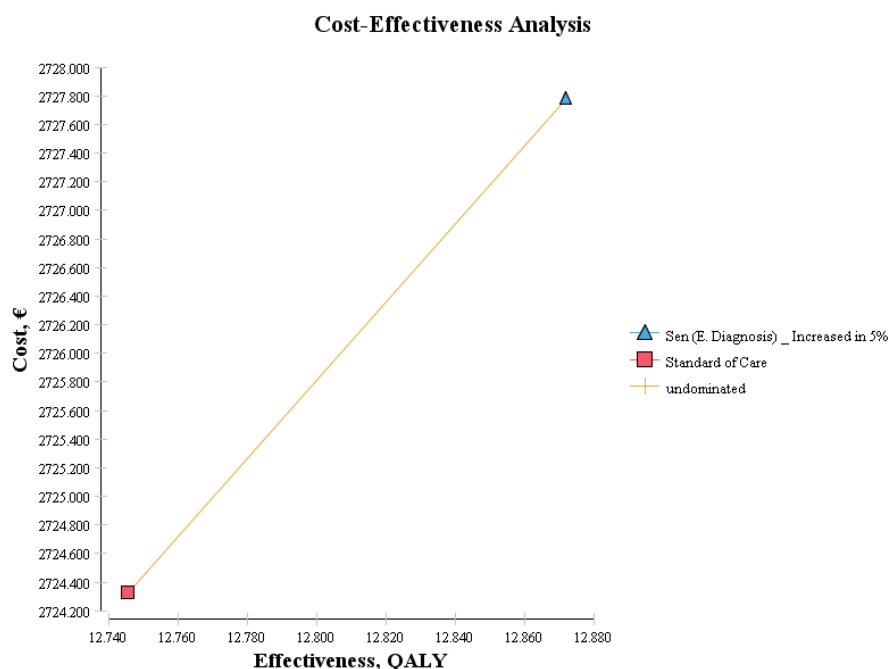


**Fig. 28.** Cost- effectiveness ratio of the scenario E. Diagnosis (+ 5 % sen, replacing US) in the Portuguese context

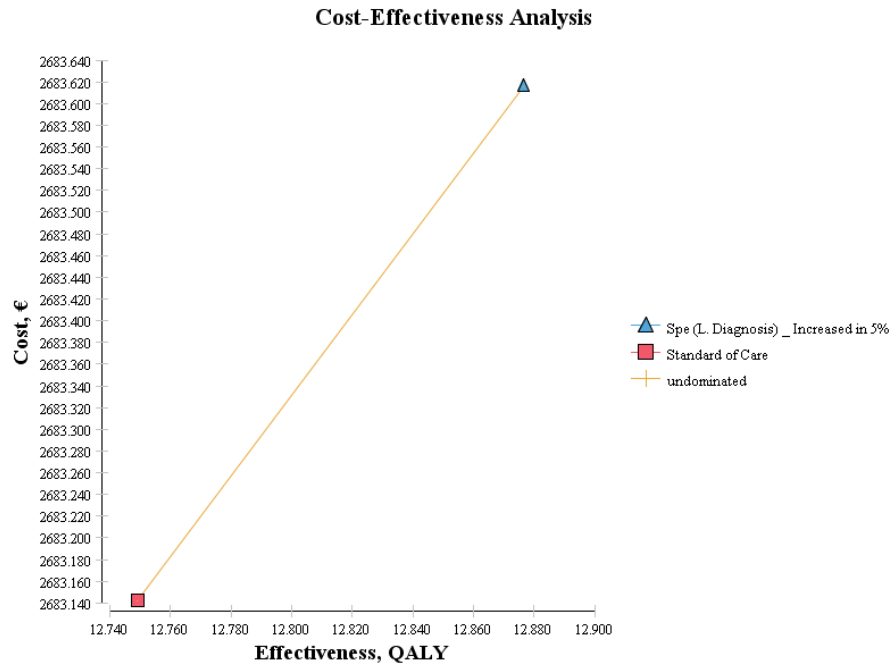


**Fig. 29.** Cost-effectiveness ratio of the scenario L. Diagnosis (+ 5 % spe) in the Portuguese context.

## 6. Discussion

In this section the overall results shall be discussed. In *section 6.1* it will be discussed the criteria to analyze the overall results. In *6.2* it will be discussed the results acquired from the simulation made with scenarios of Group I, in *section 6.3* it will be discussed the results acquired from the simulation made with scenarios of Group II. In *section 6.4* it will be discussed the results acquired from the simulation made with scenarios of Group III. In *section 6.5* the assumptions and limitations of the model are discussed. Finally in *section 6.6* some other possible scenarios to test are presented.

### 6.1. Criteria

Among the papers included in the meta-analysis (Appendix I) one of the main discussion issues is about the acceptable WTP ratio to consider in the result analysis leading to the following questions: Does the chosen cost-effectiveness ratio capture all societal preferences for selecting priorities in the decision making process, especially innovation [45]? What should be threshold for ICER? Some authors consider a fixed random value- 20000, 30000 or even 50000 monetary units (euro or dollar) per QALY, without a strict argumentation for such choice. Some other authors consider that the WTP threshold must be linked with the social context. For instance *Williams, 2004* suggested that a ‘common sense’ value for the threshold would be to set it equal to the GDP per capita (in Netherlands is 35900 € per capita and in Portugal is 15600 € per capita) [84, 85]. This approach was followed to perform the WTP analysis.

### 6.2. Group I

The results of Group I of scenarios indicate that PAM is not effective for the regular screening and diagnosis pathway of the general population. As Table 45 shows the generality of optimal frequencies of CE ratio is very short for this group of scenarios, being 0.380 the maximum value registered. In fact, considering only the base case among the 5 different scenarios in the 2 contexts (10 situations), 6 are strict dominated (lower mean effectiveness and higher mean cost) and 4 are dominated (lower mean effectiveness and lower mean cost).

### 6.3. Group II

The results of Group II of scenarios show 2 out of 10 scenarios whose base and best case are not dominated. This occurs in both contexts (vide Table 48 for *HRisk mam: dense (40-59)* and *MRisk mam: dense (40-49)*). Some of the results require a WTP analysis, performed as follows.

	Obtained ICER and (CE optimal frequency)	
	Netherlands	Portugal
<i>HRisk mam: dense (40-59) BS</i>	153.939 (0.978)	479.370 (0.981)
<i>HRisk mam: dense (40-59) BC</i>	1945.004 (0.917)	1024.467 (0.925)
<i>MRisk mam: dense (40-49) BC</i>	1335.093 (0.036)	215.150 (0.007)
<i>MRisk mam: dense (40-49) BS</i>	8.136 (0.008)	ND (does not require WTP analysis)

**Table 51.** WTP analysis of relevant scenarios of group II: Netherlands - WTP =35900 € per QALY; Portugal - WTP =15600 € per QALY.

As Table 51 shows, all the scenarios requiring WTP analysis have ICER's below the respective thresholds. Moreover, in the case of *HRisk mam: dense (40-59)* the optimal frequencies of the CE ratio is really high, from 0.925 to 0.981. This means that 0.925 to 0.981 of the performed microsimulations (100.000) using PAM are more cost-effective than the ones performed by the standard of care procedures. In opposite, in *MRisk mam: dense (40-49)* scenario the values of CE optimal frequency are very low - from 0.007 to 0.036. This means that in this scenario the costs in an individual (microsimulation) basis are generally higher than the cost of the standard of care, however this incremental costs are accepted by the WTP threshold, as explained. These facts makes these scenarios (*HRisk mam: dense (40-59)* and *MRisk mam: dense (40-49)*) the most viable and probable scenarios of PAM application. These results were expected and are linked to one of the great advantages that PAM presents over FFDM and US – the constant performance for different levels of breast density.

#### 6.4. Group III

The purpose of testing the Group III of scenarios was different than the previous groups. In this case, one was not testing the cost-effectiveness of a specific medical device with certain levels of effectiveness. In opposition it was tested a hypothetical technology with 5% higher effectiveness than the respective standard of care and the same estimated costs of PAM. Therefore, it was previously expected a higher effectiveness in the scenario application, the doubt was in the overall costs: 7 out of the 12 tested situations presented a higher mean costs than the standard of care, requiring a willingness to pay analysis, performed as Table 52).

	Obtained ICER and (CE optimal frequency)	
	Netherlands	Portugal
E. Diagnosis (+ 5 % sen, repl US)	ND (does not require WTP analysis)	4086.000 (0.965)
L. Diagnosis (+ 5 % sen)	6416.000 (0.012)	3736.167 (0.966)
L. Diagnosis (+ 5 % spe)	5273.000 (0.012)	6449.353 (0.967)
L. Diagnosis (+ 5 % sen & spe)	1539.935 (0.059)	918.917 (0.966)

**Table 52.** WTP analysis of relevant scenarios of group III: Netherlands - WTP =35900 € per QALY; Portugal - WTP =15600 € per QALY.

Although the ICER's of group III (the highest is 6449.353 € per QALY) are higher than the ICER's of Group II ((the highest is 1945.004 € per QALY), as Table 52 shows the incremental costs are still below the national WTP thresholds. These results might have special relevance for PAM designers because it shows that for a device with PAM costs and a small improvement in terms of effectiveness the market/health cycle introduction is acceptable in terms of cost- effectiveness.

## 6.5. Model Assumptions and Limitations

In this HTA exercise some limitations were faced and some assumptions were considered that can have some impact on the model outcomes. The data selection is an important factor for the model reliability: the major challenge is the quantification of the effectiveness of the standard of care devices in a unique and absolute way. Moreover the utility values are also hard to assess uniformly by the same method. The same happens with costs because these might vary over a broad range in each context. An important assumption is associated with the fact that the model tracks only the period of regular screening of the different groups of the model and not the entire life. This is due to the adopted methodology that pursuits to match with the regulated period of screening in the different contexts and for the different groups of risk. Due to inaccessibility to Portuguese data the model assumed that the breast cancer stage distribution in Portugal is identical to the Dutch one. The model does not consider the self-assessment and autonomous clinical appointments scheduling, which might be considered an important limitation of the model. Finally the performed simulations were made either with 2 years or with 1 year of model cycle length which might be considered by some health economists a big extended cycle length for a proper trial tracking.

## **6.6. Possible extra scenarios**

The fact that PAM doesn't use ionizing radiation is one its great advantages. Some health devices studies, as *Lowry, et al, 2012*, consider the effect of ionizing radiation in health, associating some special utilities and risk to each exposure [86]. Two types of excess risk models were used: Excess Absolute Risk (EAR) and Excess Relative Risk (EER). Therefore, 2 possible extra scenarios of scenarios to test could be 2 different situations in which theses 2 different models of risk would be applied simultaneously in PAM scenario and in the standard of care.

## 7. Conclusion

In a broad perspective which considers the best scenario (BS) individually the overall results indicate that the PAM application in 5 of the tested scenarios of Group I and II may be cost-effective in both contexts. However if the analysis to the Group I and II of scenarios is restricted to the base case (BC) scenarios, the group of viable scenarios of PAM use shortens to 2, namely HRisk mam: dense (40-59) and MRisk mam: dense (40-49). The PAM application in these two groups of high and moderate risk of breast cancer with dense breasts presented acceptable ICER ratios. Therefore, the future PAM design and development should continue to pursue a constant effectiveness in dense and non dense breasts because it is the major competitive advantage that PAM has while compared with FFDM. The results of Group III showed that an increased sensitivity and specificity in 5% of a medical device with the same costs of PAM can become cost-effective (above the WTP thresholds) in the all points of the screening and diagnosis pathway of breast cancer. This results are special relevant for late diagnosis where the obtained ICER's are the lowest- 1539.935 and 918.917 €/QALY for Portugal and Netherlands respectively, making late diagnosis one of the most interesting clinical scenarios of application in the context of a future performance improvement. This fact should stimulate the designers to keep improving the device. This fact should stimulate the designers to keep improving the device.

However the presented results are from a CEA perspective. If the analysis is made in a budget impact analysis perspective considering the equipment costs, the conclusion might be different.

The conducted study did not intend to provide a definitive judgment about the economic viability and introduction of PAM in the screening and diagnostic pathway of breast cancer. Instead, it aimed to give a generic idea on the cost-effectiveness consequences of PAM in the different scenarios. Moreover, it also aimed to give a methodological overview of early health technology assessment on advising whether or not to continue with the development of a certain technology when limited data is available on the technology itself and its intended market. Although it is very clear that this kind of health economic modeling doesn't give enough information so the decision maker can uniquely base the decision on its results, this project demonstrates that this type of early stage modeling can be useful in the constructive technology assessments of a new medical technology. Moreover the technology designers can be provided with a comprehensive advice based on data about the further actions to be taken in anticipation of a final assessment of the new technology.



# Appendixes

## Appendix I

This appendix presents the results of the performed meta-analyses over *Cost-effectiveness analyses* in the breast cancer diagnostic pathway papers found in PUBMED and published after the year 2000. The main objective of this meta-analysis was to acquire a methodological overview of CEA procedures.

The search was performed at May, 2013. The searched combination terms were “Breast Cancer” + “Cost-effectiveness” and “Breast Cancer” + “Cost-Utility”.

There were found 663 papers. Of those 480 were eliminated from the review by reading the title, 83 were eliminated by reading the abstract and finally 65 were eliminated by reading the whole paper. As a result of the sifting, 35 papers were considered in the review. 2 other papers, found by other means, were added to the review.

The 37 papers analyzed were then divided in two groups: one group (A) that gathers the studies that use as outcome QALYs and other group (B) that gathers the studies that use any other outcome.

The data of each group is showed in 3 tables: The first shows an overview of the methodology applied in the studied (the perspective used in the cost, Markov model/DES, the time horizon considered and the simulation platform used); The second shows the competing alternatives that are being analyzed and the obtained results; the final table shows the costs and outcomes discount rates applied and the type of sensitivity analysis performed.

## Group A- CEA studies using QALYS as outcome

The following 3 tables gather the data of 15 CEA studies that considers QALY as outcome.

Affiliation of First author	Perspective	Time-dependent Model	Markov	Discrete Event Model	Time Horizon	Simulation Platform	Author (s)
Centre for Health Informatics and Multiprofessional Education (CHIME), Royal Free and University College Medical School, London, UK	Payers (National Health Service)	X Cohort			10 years	NF	Taylor et al 2005 [73]
Departments of Radiology Stanford University School of Medicine, USA	Society	X Cohort	-		25 years	C++	Plevritis et al 2006 [78]
Center for Risk Analysis, Harvard School of Public Health, Boston, MA , USA	Payers	-	X		25 years	NF	Stout et al 2006 [87]
Centre for Health Economic Research and Evaluation (CHERE), University of Technology Sydney, Australia	Payers (National Health Service)	X Microsimulation	-		10 years	NF	Norman et al 2007 [88]
The Dartmouth Institute for Health Policy and Clinical Practice, Dartmouth Medical School, Lebanon, USA	Society	-	X		Life Expectancy	TreeAge Pro	Tosteson 2008 [89]

Department of Radiology, Institute for Technology Assessment, Massachusetts General Hospital, Boston, USA	Society (quasisocietal )	X Cohort	-	Life expectancy	TreeAge pro	Pandharipande et al 2008 [90]
Roche Company, Ljubljana, Slovenia	Payers (National Health Service)	X Cohort	-	Life Expectancy	NF	Rojnik 2008 [91]
Department of Hematology and Oncology, School of Medicine, Winship Cancer Institute, Emory University, Atlanta, USA	Payer	X Microsimulation	-	25 years	NF	Moore et al 2009 [68]
Erasmus MC, Department of Public Health, Rotterdam, The Netherlands	Society	X Microsimulation	-	40 years	Fortram (Miscan)	De Gelder et al 2009 [92]
Department of Medicine, Division of Biostatistics, The Dan L. Duncan Cancer Center at Baylor College of Medicine, Houston, USA	Society	X Microsimulation	-	59 years	NF	Ahern et al 2009 [93]
Massachusetts General Hospital Institute for Technology Assessment, Boston, USA	Society	X NF	-	Life Expectancy	NF	Lee 2010 [94]
Department of Community Medicine and School of Public Health, Li Ka Shing Faculty of Medicine, The University of Hong Kong, China	Society	X Cohort	-	50 years	TreeAge Pro	Leung 2010 [70]
Health Economics Unit on behalf of West Midlands Health Technology Assessment Collaboration, School of Health and Population Science, University of Birmingham,	Payers (National Health Service)	-	X	1 year	NF	Auguste et al 2011 [60]

<b>Birmingham, UK</b>							
<b>Basic Medical Sciences Department, Biomedical Research Institut of Lleida -University of Lleida, Lleida, Catalonia, Spain</b>	Payers (National Health Service)	X Cohort	-	40 years	NF	Carles et al 2011 [95]	
<b>Massachusetts General Hospital Institute for Technology Assessment, Boston, USA</b>	Society	X Microsimulation	-	45 years	C++	Chubiz [96]	2013

Table 53. Methodological Overview of the group A.

Standard of care	Competing alternatives	Tested group	Scenarios: applied <i>technologies</i> , (interval between tests- starting age)	Scenarios with dominance	Cost-Effectiveness Threshold – applied or suggested	Author (s)
<b>SFM Screening without CAD</b>	CAD- SFM	Cohort of 1000 patients in the breast cancer-diagnosed state at the age of 50 years	CAD-SFM (1 time, 50 yrs) Double reading SFM (1 time, 50 yrs)	£36.030 per QALY £102.330 per QALY	£ 30.000 per QALY	Taylor et al 2005 [73]
<b>SFM</b>	SFM, MRI	USA Female 25-year- old BRCA1/2 mutation carriers, born in 1980	(A) BRCA 1 mutation carriers: SFM + MRI ( 1 yr, 35-64) (B) BRCA 2 mutation carriers: SFM + MRI ( 1 yr, 35-54)	(A) \$55.420 per QALY;	\$ 100. 000 per QALY	Plevritis et al 2006 [78]
<b>No screening</b>	SFM	General USA female population	SFM (5 yrs, 55-70)	ICER per QALY \$ 27.000	\$ 50.000 per QALY	Stout et al 2006 [87]
<b>No screening</b>	MRI, SFM	Cohort of 1.000 BRCA1 mutation carriers aged either 30–39 or 40–49 years	SFM (1 yr, 30-39) vs MRI (1 yr, 30-39) vs SFM + MRI (1 yr, 30-39) SFM (1 yr, 40-49) vs MRI (1 yr, 40-49) vs SFM + MRI (1 yr, 40-49)	MRI- dominated at both scenarios (A) SFM (1 yr, 30-39): ICER = £5.240 per QALY SFM + MRI (1 yr, 30-39): ICER = £13.486 per QALY (B) SFM (1 yr, 40-49): ICER =£ 2.913 per QALY SFM + MRI (1 yr, 40-49): ICER = £ 7.781 per QALY	£20. 000 per QALY	Norman et al 2007 [88]

<b>Annual Mammography (SFM)</b>	Dual modalities with MRI and FFDM or MRI and SFM	General female population.	U.S. SFM (1 yr -40 yrs) VS FFDM (1 yr- 40 yrs) VS FFDM + SFM (1 yr- (40-50), 50 yrs) VS FFDM + SFM (1 yr, (RDBreasts/ RNDBreasts &<50 yrs),( RNDBreasts &>50 yrs))	FFDM (1 yr- 40 yrs): \$ 331.000 per QALY; FFDM + SFM (1 yr- (40-50), 50 yrs): \$ 26.500 per QALY; FFDM + SFM (1 yr, (RDBreasts/ RNDBreasts &<50 yrs),( RNDBreasts &>50 yrs)) : \$ 84.500 per QALY;	NF	Tosteson 2008 [89]
<b>No assessment procedure</b>	SLN Biopsy, MR lymphangiography	Hypothetical cohort of postmenopausal women 61 years old with a common profile of early clinically node-negative breast cancer	MR lymphangiography SLN Biopsy Combined MR lymphangiography and SLN Biopsy	ICER by order: \$ 37.244 per QALY \$ 153.00 per QALY	\$50.000–\$100. 000 per QALY	Pandharipande et al 2008 [90]
<b>No screening</b>	SFM	General Slovenian Population	SFM( 1 yr, 40-65/ 40-70/ 40-75/ 40-80/45-65/45-70/45-75/45-80/50-65/50-70/50-75/50-80) VS SFM( 2 yr, 40-65/ 40-70/ 40-75/ 40-80/45-65/45-70/45-75/45-80/50-65/50-70/50-75/50-80) VS SFM( 3 yr, 40-65/ 40-70/ 40-75/ 40-80/45-65/45-70/45-75/45-80/50-65/50-70/50-75/50-80)	SFM( 3 yr, 40-70/ 40-75/ 40-80/45-65/45-70/50-65): 4.307€ per QALY-41.815€ per QALY); SFM (2 yr, 40-80): >41.815 € per QALY;	\$50.000 per QALY	Rojnik 2008 [91]
<b>Annual screening with FFDM</b>	MRI	High risk population ( 10.000 )	FFDM (1 yr, for 25 yrs) vs MRI (1 yr, for 25 yrs)	ICER - \$ 179.599 per QALY	\$50.000 per QALY	Moore et al 2009 [68]
<b>No Screening</b>	SFM	Hypothetical cohort with 1.000.000 Swiss women	OSP (40 % participation rate) OSP (80 % participation rate) SFM ( 2 yrs, 50-69) – 80% participation rate OSP (20 % participation rate) + SFM ( 2 yrs, 50-69) – 60 % participation rate OSP (40 % participation rate) + SFM ( 2 yrs, 50-69) – 40 % participation rate	25.418 € per QALY 25.541 € per QALY 12.424 € per QALY 12.601 € per QALY 27.599 € per QALY	NF	De Gelder et al 2009 [92]
<b>No Screening</b>	SFM, CBE	Cohort of 500.000 women with 20 years old	SFM ( 2 yrs, 40-79) + CBE (2 yrs, 41-79) SFM ( 2 yrs, 40-79) + CBE (1 yrs, 40-79) SFM ( 2 yrs, 40-59) + SFM ( 2 yrs, 60-79) + CBE (1 yrs, 40-79) SFM ( 1 yrs, 40-79) + CBE (1 yrs, 40-79) SFM ( 1 yrs, 40-79) + CBE (2 yrs, 20-39) + CBE (2 yrs, 40-79)	ICER by order: \$35.500 per QALY \$90.100 per QALY \$169.500 per QALY \$367.100 per QALY \$3.939.000 per QALY	\$50.000 per QALY	Ahern et al 2009 [93]
<b>Annual Mammography (SFM)</b>	Single and dual modalities with MRI and SFM .	Cohort of 25-year-old BRCA1 mutation carriers	SFM (1 yr, 25) VS MRI (1 yr, 25) VS SFM +MRI (1 yr, 25)	SFM (1 yr, 25) : \$ 16. 751 per QALY; SFM +MRI (1 yr, 25): \$ 69.125 per QALY	\$100.000 per QALY	Lee 2010 [94]
<b>No screening</b>	SFM	General population in	SFM (2 yr, 50-69 yrs) VS	SFM (2 yr, 40-69 yrs) : \$ 61.800 per QALY	\$50.000 per QALY	Leung 2010 [70]

		Hong Kong		SFM (2 yr, 50-79 yrs) VS SFM (2 yr, 40-69 yrs) VS SFM (2 yr, 50-79 yrs)		SFM (2 yr, 50-79 yrs): \$ 178.899 per QALY		
<b>Recurrence diagnosis with conventional work-up procedures</b> <sup>8</sup>	PET and PET/CT	Cohort of 10000 women in follow up with ages between 50 and 75		Follow up with PET Follow up with PET/CT Follow up with PET/CT with conventional work-up	combined	ICER by order: £29.300 per QALY £31.000 per QALY £42.100 per QALY	£20.000 per QALY (NICE), also considered thresholds of £30.000 per QALY and £40.000 per QALY	Auguste et al 2011 [60]
<b>No Screening</b>	SFM	Cohort of 100.000 spanish women		SFM( 2 yRs, 50-69) SFM( 2 yrs, 45-69) SFM( 1 yr, 45-69) SFM( 1 yr, 40-69) SFM( 1 yr, 40-74)		ICER by order:  4.469 € per QALY 9.694 € per QALY 12.633 € per QALY 16.411 € per QALY 24.975 € per QALY 26.720 € per QALY	30.000 € per QALY	Carles et al 2011 [95]
<b>Annual mammography (FFDM) starting at age of 25 (DM25) or starting at age of 30 (DM30)</b>	Dual modalities with MRI and FFDM	BRCA1 and BRCA2 Gene Mutation Carriers		FFDM /MRI (alt 6-month- 25 yr) VS MRI( 1 yr- 25 yr) VS MRI+FFDM ( 1 yr- 25, 30 yrs) VS FFDM/MRI (alt 6-month- 30 yrs )		FFDM/MRI (alt 6- month- 30 yrs):  Group of BRCA1 carriers (ICER – \$ 74.200 per QALY), Group of BRCA2 carriers (ICER – \$ 215.700 \$ per QALY)		Chubiz 2013 [96]

**Table 54.** Overview of the results of group A

Discounting Rate (Costs)	Discounting Rate (QALY's or similar effectiveness measure)	Sensitivity analysis (Type)	Author (s)
3.5 %	1.5 %	Univariate, bounded: Costs and discount rates Probabilistic sensitivity analysis : prevalence of the breast cancer, sensitivity, specificity and costs	Taylor et al 2005 [73]
None in the base case (SA: 2- 5%)	None in the base case (SA: 2- 5%)	Univariate and Multivariate bounded : Cost of mammographic screening (\$), Ovarian cancer survival improvement (%), breast cancer utility, utilization rates after MRI, MRI detection threshold (cm), rates of mammogram opaque (%), Ovarian risk by age (%), MRI screening cost (\$), discount rate (%) , breast cancer by Age 70 (%)	Plevritis et al 2006 [78]
3%	3%	Univariate, bounded: level of population participation in the alternative screening scenarios and values of utilities	Stout et al 2006 [87]
3.5 %	3.5 %	Univariate, bounded: Costs, utilities Probabilistic sensitivity analysis: Costs, utilities	Norman et al 2007 [88]
3%	3%	Univariate, Bounded: Costs of MRI, prevalence of dense breasts	Tosteson 2008 [89]
3%	3%	Univariate, bounded: Sensitivity of SLN biopsy	Pandharipande et al 2008 [90]

<sup>8</sup> Conventional work-up is considered to be consisted of ultrasound, bone scintigraphy, X-rays, CT and measurement of serum tumour markers

		after false negatives findings at MR lymphangiography; MR lymphangiography sensitivity and specificity; transition probabilities from nonmetastatic to metastatic disease states; costs of each SLN biopsy setting considered; Bivariate, bounded: MR lymphangiography sensitivity and MR lymphangiography specificity / MR lymphangiography sensitivity and SLN biopsy sensitivity / post-SLN biopsy and post-axillary lymph node dissection utilities	
3%	3%	Univariate, Bounded: All parameters of the model; Probabilistic Sensitivity Analysis: All parameter of the model except costs and incidence	Rojnik 2008 [91]
5%	5 %	Univariate, bounded: individual costs, probabilities and utilities; Probabilistic sensitivity analysis: individual costs, probabilities and utilities;	Moore et al 2009 [68]
3 %	3 %	Univariate, bounded: false-negative rate of OS compared to MSP	De Gelder et al 2009 [92]
3%	3%	Univariate, bounded: Sensitivity and Specificity	Ahern et al 2009 [93]
3%	3%	Univariate, Bounded: Sensitivity and Specificity of MRI, Sensitivity and Specificity of SFM, mortality Risk and utilities	Lee 2010 [94]
3%	3%	NA	Leung 2010 [70]
0% (Time Horizon of the simulation is 1 year)		Univariate, bounded: Sensitivity, specificity, cost and prevalence of recurrence; Probabilistic sensitivity analysis: Sensitivity, specificity, treatment costs and prevalence of recurrence;	Auguste et al 2011 [60]
3%	3%	Multivariate, bounded: all cost Univariate, bounded: follow up times, ratio of screening/background non-invasive tests, screening attendance rates, cost of invasive tests for screen-detected tumors	Carles et al 2011 [95]
3%	3%	Univariate, bounded: time costs, costs, MRI performance (sensitivity and specificity), SFM and FFDM performance (sensitivity and specificity), breast cancer risk Multivariate, bounded: MRI performance and SFM and FFDM performance	Chubiz 2013 [96]

**Table 55.** Discount rates and sensitivity analyses approaches in the group A

## Group B- CEA studies using other units as outcome

Affiliation of First author and Country	Perspective	Time-dependent Markov Model	Discrete Event Model	Time Horizon	Simulation Platform	Author (s)
Wesley PET Centre & Southern X-ray Clinics, Wesley Hospital, Australia	Health Care Payer	-	X	NF	NF	Miles 2001 [97]
Cancer Registry of Norway	Society	X Cohort	-	Life Expectancy	NF	Wang et al 2001 [98]
INSERM U379, Paoli-Calmettes Institute, France	Society	-	X	NF	NF	Sevilla et al 2002 [99]
Department of Surgery, University of Minnesota, USA	Health Care Payer	-	X	NF	NF	Morris et al 2003 [100]
CAST—Centre for Applied Health Services Research and Technology Assessment, University of Southern Denmark	Society	X Cohort	-	Remaining Life time of the cohort	NF	Sorensen et al 2003 [101]
Registre des Tumeurs du Doubs, C.H.U. Saint Jacques, France	Society	X Cohort	-	20 years	NF	Arveux et al 2003 [102]
Department of Medical Oncology, Hospital de la Santa Creu i Sant Pau, Universitat Autònoma de Barcelona, Spain	Society	-	X	NF	TreeAge Pro	Balmana et al 2004 [103]
Department of Public Health, Erasmus MC, University Medical Center Rotterdam, Netherlands	Society	X Microsimulation		27 years	NF	Groenewoud et al 2004 [79]
Department of Oncology, Georgetown University Medical Center, and Cancer Control Program, Lombardi Cancer Center, Washington, DC, USA	Society	X Microsimulation		Life Expectancy	NF	Mandelblatt et al 2004 [104]
Faculty of Medicine, Memorial	Society	-	X	[initial diagnostic studies	MD@	Sloka et al 2005 [105]



University of Newfoundland, Canada					until final procedure of all treatment modalities]		
Department of Radiology, University of California, Davis School of Medicine, Sacramento, USA	Society	X Microsimulation	-	39 years	TreeAge Pro	Lindfors et al 2006 [106]	
Division of Breast Surgery, Iwate Prefectural Central Hospital, Japan	Payers	X Cohort	-	15 years	NF	Ohnuki et al 2006 [107]	
National Collaborating Centre for Primary Care (NICE), UK	Payers	X Cohort	-	Life expectancy	Excel	NICE 2006 [108]	
MRC Health Services Research Collaboration, Department of Social Medicine, University of Bristol, Bristol, UK	Payers (National Health Service)	-	X	Life expectancy	NF	Griebsch 2006 [109]	
Swiss Institute for Medical Decision Support (SIMEDES), MuttENZ, Switzerland	Payers (Third-party payer)	X Cohort	-	Life expectancy	NF	Neeser et al 2007 [110]	
Department of Public Health, Erasmus MC, University Medical Center Rotterdam, The Netherlands	Society	X Microsimulation	-	100 years	Fortram (Miscan)	Okonkwo et al 2008 [111]	
NHMRC Centre for Clinical Research Excellence in Renal Medicine, Children's Hospital at Westmead, Australia	Payers (National Health Service)	X Cohort	-	Life expectancy	TreeAge Pro	Wong 2008 [112]	
Department of Preventive Medicine and Public Health, School of Medicine, Ajou University, Suwon, South Korea	Payers (National Health Service)	X NF	-	55 years	NF	Lee et al 2009 [113]	
Department of Health and Ageing, Australian Government, Australia	Society	X Microsimulation	-	Life expectancy	TreeAge Pro	Australian Government 2009 [114]	

Massachusetts General Hospital Institute for Technology Assessment, Boston, USA	Society	X Microsimulation	-	Life expectancy	C++	Lowry 2012 [86]
Laboratory of Radiologic Sciences, University of Rio de Janeiro, Brasil	Payers	X Microsimulation	-	30 years	TreeAge Pro	Peregrino et al 2012 [115]
Division of Clinical Imaging, Tohoku University Graduate School of Medicine, Sendai, Miyagi Japan	Society	X Cohort	-	10 years	TreeAge Pro	Sato et al 2012 [116]

**Table 56.** Methodological Overview of the group B

The following 3 tables gather the data of 17 CEA studies that considers any other outcome different than QALY.

Standard of care	Competing alternatives	Tested group	Scenarios: applied <i>technologies</i> ( <i>interval between tests- starting age</i> )	Scenarios with dominance	Cost-Effective Threshold(s)	Author (s)
No staging	FDG-PET	General Australian female population	Axillary staging of breast cancer	\$ 550.08 per patient examined	NF	Miles 2001 [97]
No screening	SFM	Norway women aged 50-69 years old – Based on the results of the first round of screening (1996-1997)	SFM (2 yrs, 50-69)	3.750 \$ per LYG - 86.045 \$ per LYG	NF	Wang et al 2001 [98]
DS as prime strategy for performing a mutation search on the entire BRCA1 gene sequence	Combined modalities between DHPLC, SSCP, DGGE, HA, FAMA and PTT	‘Theoretical’ population sample (n=10000 individuals) with a 15% risk of harbouring a deleterious mutation	DHPLC + DS vs SSCP + DS vs DGGE + DS vs HA +DS vs FAMA + DS vs HA <sub>11</sub> + DS <sub>21</sub> + DS <sub>11</sub> (if needed) vs HA <sub>11</sub> +DHPLC <sub>21</sub> + DS vs HA <sub>11</sub> +SSCP <sub>21</sub> + DS vs HA <sub>11</sub> +DGGE <sub>21</sub> + DS vs FAMA <sub>11</sub> + DS <sub>21</sub> + DS <sub>11</sub> (if needed) vs FAMA <sub>11</sub> + DHPLC <sub>21</sub> +DS vs FAMA <sub>11</sub> + SSCP <sub>21</sub> +DS vs FAMA <sub>11</sub> + DGGE <sub>21</sub> + DS vs FAMA <sub>11</sub> + HA <sub>21</sub> + DS vs PTT <sub>11</sub> + DS <sub>21</sub> + DS <sub>11</sub> (if needed) vs PTT <sub>11</sub> + DHPLC <sub>21</sub> +DS vs PTT <sub>11</sub> + SSCP <sub>21</sub> +DS vs PTT <sub>11</sub> + DGGE <sub>21</sub> + DS vs PTT <sub>11</sub> + HA <sub>21</sub> + DS	DHPLC + DS: 1218.3 € per mutation detected and a ICER of 9668.9 €;  PTT <sub>11</sub> + HA <sub>21</sub> + DS : 971.3 € per mutation detected and a ICER of 971.3 €; PTT <sub>11</sub> + DHPLC <sub>21</sub> + DS: 1038.5 € per mutation detected and a ICER of 1873.3 €;  FAMA <sub>11</sub> + DHPLC <sub>21</sub> +DS: 1563.6 € per	NF	Sevilla et al 2002 [99]

					mutation detected and a ICER of 18140.0 €;		
					FAMA + DS: 4795.8 € per mutation detected and a ICER of 163173.3 €		
Traditional Methods: Classification of masses as cystic or solid on the basis of physical examination, mammography, and ultrasonography, followed by aspiration for cystic masses and fine needle aspiration biopsy for solid masses. Open Biopsy is needed if examinations have discordant results	Triple test score <sup>9</sup> to traditional methods	General USA female population	Triple test score vs Traditional Evaluation		Triple test score: \$ 925 per mass detected and \$2925 per Breast Cancer Detected  Traditional Evaluation: \$1793 per mass evaluated and \$5670 per Breast Cancer Detected	NF	Morris et al 2003 [100]
NA	A 3 year systematic training programme in breast self-examination.	10.000 Danish woman from 40 to 69 years old based on the population of Ribe County, Denmark considering a participation rate of 25 %	40-49 / 50-59/ 60-69		40-49 : ICER of 106 € per person with increased knowledge, ICER of 180 € per person with a regular BSE and ICER of 142 € per person with a correct technique;  50-59 : ICER of 644 € per person with increased knowledge, ICER of (-881) € per person with a regular BSE and ICER of 236 € per person with a correct technique;  60-69 : ICER of 87 € per person with increased knowledge, ICER of 93 € per person with a regular BSE and	NF	Sorensen et al 2003 [101]

<sup>9</sup> Triple test score (TTS)- In an effort to streamline diagnosis among the 40% of patients whose masses had discordant triple test results. Each element of the triple test received a score of 1 for a benign result, 2 for suspicious or indeterminate findings, or 3 for a malignant result. These component scores were added together for a total TTS. The minimum score of 3 indicated all three component tests were negative, while the maximum score of 9 indicated all three tests were positive for malignancy. In our prior study of 484 patients, we found that a score of 3 or 4 always predicted benign histology on subsequent open biopsy. A score of 6 through 9 always predicted malignant histology on subsequent open biopsy. For a score of 5 (8% of masses evaluated), neither benign nor malignant histology dominated.

						ICER of 194 € per person with a correct technique;
No screening	SFM (Single view)	Cohort of french women aged 50–65 years – Based on the Bas-Rhin screening programme.	SFM (2 yrs, 50-65)	131.023 French Francs per LYG	NF	Arveux et al 2003 [102]
No screening	Combined procedures: Genetic study (SSCP PTT); Genetic counseling; Genetic study of the index case Clinical breast examination Annual SFM	Spanish woman with family history of breast cancer: Hereditary breast and ovarian cancer (HBOC) syndrome	Single scenario with 3 different intervention groups. The first step for all groups is the genetic study procedure with SSCP and PTT  <b>Group 1:</b> females from high-risk families without an identified mutation : GC + GSIC + CBE + SFM( 1 yr – 30 to 80);  <b>Group 2:</b> BRCA1 or BRCA2 female mutation carriers: GC + determination of genetic status + GSIC +CBE + SFM( 1 yr – 30 to 80);  <b>Group 3 :</b> Female nonmutation carriers from families with a pathological BRCA1 or BRCA2 gene mutation: GC + GSIC + determination of genetic status;	4.294 € per LYG	NF	Balman a et al 2004 [103]
No screening	Combined scenarios with LCNB and NLBB	Nonpalpable (screen-detected) breast lesions in Dutch women	Mass screening with NLBB as diagnostic work-up for palpable and nonpalpable breast lesions; ‘  (B) Mass screening with LCNB replacing NLBB as diagnostic work-up for nonpalpable lesions, followed by NLBB if the core biopsy indicates normal breast tissue or a high-risk lesion.	(A) £ 1.515 per LYG ; (B) £ 1.459 per LYG;	NF	Groene woud et al 2004 [79]
No screening	SFM	Hypothetical cohort of 40-year-old African American women	SFM(2 yrs, 40-60)	ICER – \$85.755 per LYG	NF	Mandelblatt et al 2004 [104]
Staging ALND with MRM /BCS+RT/BCS+RT+ALND	ALND FDG-PET	1000 Canadian 55-year-old woman presenting with stage I or II breast cancer (target stages for foregoing ALND)	FDG-PET  If node status is positive:  MRM (ALND) / BCS +RT/BCS+RT+ALND  If node status is negative:  MRM /BCS+RT + follow up with FDG-PET – if positive (ALND), if negative (repeat FDG-PET follow up)	\$ (-) 695 per person for an Increase in life expectancy of 7.4 days	NF	Sloka et al 2005 [105]
FFDM Screening without Computer-aided Detection of Breast Cancer (CAD)	CAD-FFDM	32.000 hypothetical woman from age 40–79 years	FFDM (CAD) Vs FFDM Vs Observation without screening	Incremental MCLYS:  FFDM- Observation without screening: \$ 16 .023  \$FFDM(CAD)-FFDM: \$ 19.058	\$50 .000– \$100 .000 per LYG	Lindfors et al 2006 [106]

<b>No screening</b>	SFM + CBE	Cohort of 400 000 asymptomatic Japanese women aged 30, 40, 50, 60 and 70	CBE ( 1 yr,30-39/40-49/ 50-59/60-69/70-79) SFM + CBE ( 1 yr,30-39/40-49/ 50-59/60-69/70-79) SFM + CBE ( 2 yr,30-39/40-49/ 50-59/60-69/70-79)	Dominated [3.394.310 - 11.387.100] Yen per LYG  [2.025.070- 7.967.840] Yen per LYG	NF	Ohnuki et al 2006 [107]
<b>NA</b>	FFDM, MRI	High risk Cohort	FFDM (1 yr, 30-49) vs MRI + FFDM (1 yr, 30-49) No screening MRI (1 yr, 30-49)	Population aged 40-49: ICER (A-C) = £ 11.226 ICER (B-A) = £29.622  Population aged 30-39: ICER (A-C) = £ 16.746 ICER (B-A) = £ 36.919	£20.000	NICE 2006 [108]
<b>Annual Mammography (SFM)</b>	CE-MRI	Women (aged from 35-49 years old) at a high familial risk of breast cancer: tested carriers of a BRCA1, BRCA2 or TP53 mutation or are at a 50% risk of having inherited such a mutation	SFM (1yr-35 yrs) VS CE-MRI (1yr-35 yrs) VS CE-MRI+ SFM (1yr-35 yrs).	CE-MRI: Group of BRCA1 carriers (ICPC - £6.489 );  CE-MRI+ SFM: General group (ICPC- £ 22.388 ), BRCA2 carriers (£14.366)	NF	Griebsohn 2006 [109]
<b>OSP with SFM</b>	SFM	Hypothetical cohort of Swiss women aged either 40-50, or 50-60, or 60-70, or 70-80	MSP :  SFM ( 2 yrs, 40-50) SFM ( 2 yrs, 50-60) SFM ( 2 yrs, 60-70) SFM ( 2 yrs, 70-80)	MSP strategies over OSP:  ICER of \$73.018 per LYG ICER of \$75602 per LYG ICER of \$90.635 per LYG ICER of \$118.193 per LYG	NF	Neeser et al 2007 [110]
<b>No Screening</b>	SFM, CBE	Cohort of 1.000.000 Indian women with 40 years old	CBE (once in lifetime,50 yrs) CBE (once in lifetime ,40 yrs) CBE (5 yrs ,50-70 yrs) SFM (once in lifetime,50yrs) CBE (5 yrs ,40-60 yrs) SFM (once in lifetime,40yrs) CBE (2 yrs ,50-70 yrs) CBE (2 yrs ,40-60 yrs) CBE (1 yr ,40-60 yrs) SFM (2 yrs,50-70 yrs) SFM (2 yrs,40-60 yrs)	ICER by order:  \$1.251 per LYG  \$1.549 per LYG  \$3.108 per LYG  \$19.257 per LYG	\$2.820 per LYG (GDP per capita)	Okonkwo et al 2008 [111]
<b>No screening</b>	SFM	Women on dialysis therapy with a starting age of 50 years	SFM (1 yr, 50-70 yrs)	SFM (1 yr, 50-70 yrs): 109.852 \$/LYG per LE gained	\$50,000/LYG	Wong 2008 [112]

No Screening	SFM	General female population of Korea	SFM (3 yrs, 45-65) SFM (3 yrs, 40-65) SFM (2 / 3 yrs, 40-65) SFM (2 yrs, 40-65) SFM (2 yrs, 40-70) SFM (2 yrs, 40-75) SFM (2 yrs, 35-75) SFM (1 yrs, 35-65) SFM (1 yrs, 35-75) SFM (2 yrs, 30-75)	ICER by order: \$ 100.007 per Case found \$ 154.502 per Case found \$ 173.694 per Case found \$ 197.257 per Case found \$ 233.886 per Case found \$ 268.519 per Case found \$ 291.341 per Case found \$ 421.635 per Case found \$ 464.666 per Case found \$ 763.560 per Case found	NA	Lee et al 2009 [113]
No screening	FFDM	General Australian population	FFDM (2 yrs, 45-69/50-74/45-74/40-69/50-79/40-74/45-79/40-79) VS FFDM (2 yrs, 50-69 for 40 yrs) <sup>10</sup> VS FFDM (2 yrs, 50-69 for 20 yrs) <sup>11</sup> VS FFDM (1 yr, 50-69) VS FFDM (3 yrs, 50-69)	FFDM (2 yrs, 45-69/50-74/45-74/40-69/50-79/40-74/45-79/40-79): 37.873 \$ - 52.318 \$ per LYG);  FFDM (2 yrs, 50-69 for 40 yrs): 23.713 \$ per LYG FFDM (2 yrs, 50-69 for 20 yrs) : 38.302 \$ per LYG; FFDM (1 yr, 50-69): 55.411 \$ per LYG; FFDM (3 yrs, 50-69) : 30.602 \$ per LYG	NF	Australian Government 2009[114]
NA	FFDM, and dual modalities with MRI and SFM	SFM and BRCA1 and BRCA2 Gene Mutation Carriers	FFDM (1 yr – 25/30/35/40 yrs) VS SFM (1 yr – 25/30/35/40 yrs) VS FFDM + MRI (1 yr – 25/30/35/40 yrs) VS SFM + MRI (1 yr – 25/30/35/40 yrs) VS FFDM/MRI (alt 1 yr - 25/30/35/40 yrs ) VS SFM/MRI (alt 1 yr- 25/30/35/40 yrs ) VS MRI+FFDM (1 yr-25, 30 yrs ) VS MRI+SFM ( 1 yr-25, 30 yrs	FFDM/MRI (alt 1 yr - 25/30): Group of BRCA2 carriers (LE- 77.63 yrs/ 77,58 yrs)  FFDM/MRI (alt 1 yr- 30): Group of BRCA1 carriers (LE 72.52 yrs)	NF	Lowry 2012 [86]

<sup>10</sup> FFDM (2 yrs, 50-69 for 40 yrs) – This scenario follows the cohort of 50-69 for 40 years with a screening interval of 2 years, i.e, a women with a starting age of 50 is followed until the age of 90.

<sup>11</sup> FFDM (2 yrs, 50-69 for 20 yrs) – This scenario follows the cohort of 50-69 for 20 years with a screening interval of 2 years, i.e, a women with a starting age of 50 is followed until the age of 70.

<b>No Screening</b>	CE-MRI, SFM, FFDM	Cohort of 100.000 women with 50 years old	SFM ( 2 yrs, 50-69) FFDM ( 2 yrs, 50-69) (C) CE-MRI ( 2 yrs, 50-69)	13.573,072 R\$ per LYG	NF	Peregrino et al 2012 [115]
<b>Biennial screening with FFDM (with double reading)</b>	CAD	Hypothetical population comprised women aged 50 who have undergone biennial breast cancer screening with mammography and palpation	CAD- FFDM (2 yr, 50) Vs FFDM (2 yr, 50) with double reading	ICER - 310,805 JPY per LYG	6.000.000 yen per LYG	Sato et al 2012 [116]

**Table 57.** Overview of the results of group B

Discounting Rate (Costs)	Discounting Rate (QALY's or similar measure)	Sensitivity analysis (Type)	Author (s)
NA	NA	Bivariate, bounded : Specificity and Prevalence of axillary metastases	Miles 2001 [97]
4.5 %	4.5 %	Univariate, Bounded: Mortality reduction, cost per screen, positive predictive value (PPV) and discount rate	Wang et al 2001 [98]
8%	20 %	Univariate, bounded: prevalence of deleterious mutations and Sensitivity Ranges of each technique	Sevilla et al 2002 [99]
NA	NA	Univariate, bounded: Resource costs (every single component) and the effect of the misclassification of masses on TTS	Morris et al 2003 [100]
3 %	3 %	Univariate, bounded: Participation rates and Odds ratio (on learning BSE technique)	Sorensen et al 2003 [101]
3 %	3 %	Univariate, bounded: Participation rates and Odds ratio (on learning BSE technique)	Sorensen et al 2003 [101]
5%	-	Univariate, Bounded: Discount rate on Costs (fixed and variable) and compliance	Arveux et al 2003 [102]
5% over the current net value	-	Univariate, bounded: discount rate, probability of having BRCA mutation, percentage of negative lymph nodes and risk of breast cancer	Balmana et al 2004 [103]
3%	3%	Univariate, Bounded: Sensitivity of LCNB; Probability of nonmalignant diagnosis of a nonpalpable	Groenewoud et al 2004 [79]

		lesion after Diagnostic mammography/further assessment; Proportion of nonpalpable suspicious breast lesions at screening by mammography and LCNB costs	
3%	3%	Univariate, bounded: Utilities, attendance rate	Mandelblatt et al 2004 [104]
The cost of capital equipment is discounted over the expected lifetime of the equipment at a rate of 6%.	NA	Univariate, bounded: PET cost PET, specificity PET sensitivity, Prevalence of node positivity and Patient selection of BCS over MRM	Sloka et al 2005 [105]
3%	3%	Univariate, bounded: cost of CAD, the rates of cancer detection with CAD, the stage distribution of breast cancers diagnosed with CAD.	Lindfors et al 2006 [106]
3%	3%	Univariate and Multivariate bounded : Costs of the screening, sensitivity and specificity of the screening strategies	Ohnuki et al 2006 [107]
3.5 %	3.5 %	Univariate and Multivariate bounded: Costs, incidence; Probabilistic sensitivity analysis : All variables	NICE 2006 [108]
3.5 %	-	Univariate, bounded: Costs	Griebsch 2006 [109]
3% ( Inflation rate of 1.4 % was also considered)	1.5 %	Univariate deterministic : Breast Cancer mortality, incidence of Breast Cancer, cost of initial tumour treatment, and other costs such as biopsy or the MSP ; Probabilistic sensitivity analyses: Breast Cancer mortality, incidence of Breast Cancer, cost of initial tumour treatment, and other costs such as biopsy or the MSP	Neeser et al 2007 [110]
3%	3%	Univariate, bounded: incidence rate, attendance rate, Sensitivity of CBE,	Okonkwo et al 2008 [111]
5%	5%	Univariate, Bounded: Estrogen receptor positivity, discount rate, relative prevalence of cancers, age-specific screening test accuracies, stage distribution of cancers,, probability of clinical diagnosis, participation rate of screening, stage and age specific survival after treatment, relative risk reduction in breast cancer-specific mortality in the screened population and costs	Wong 2008 [112]
3%	3%	Univariate, bounded: the MST in the preclinical state, the sensitivities and the specificities of the mammography, costs, and discount rates	Lee et al 2009 [113]
3%	3%	Univariate, Bounded: Discount rate, indirect costs associated with breast cancer treatment, the progression rate of DCIS to invasive cancer and utilities	Australian Government 2009[114]
0%	0%	Univariate, Bounded: MRI test performance, Cumulative incidence, FFDM test performance from dense	Lowry 2012 [86]



		breast group, radiation risk	
0 %	0 %	Univariate, bounded: Increase of 50 % in the cost of the equipment used in the strategy most cost- effective - SFM	Peregrino et al 2012 [115]
3%	3%	Univariate, bounded: Costs, Sensitivity and Specificity of CAD, Number of annual examinees, discount rate; Multivariate: Sensitivity and Specificity of CAD	Sato et al 2012 [116]

**Table 58.** Discount rates and sensitivity analyses approaches in the group B

## Appendix II

### Breast Tumors Clinical Classification (TNM)

<i>TX</i>	Primary tumor cannot be assessed.
<i>TO</i>	No evidence of primary tumor found.
<i>Tis</i>	Carcinoma in situ: intraductal carcinoma, or lobular carcinoma in situ, or Paget disease of the nipple with- no tumor (Note: Paget disease associated with a tumor is classified according to the size of the tumor.)
<i>T1</i>	Tumor < 2 cm in greatest dimension
<i>T1a</i>	<0.5 cm in greatest dimension
<i>T1b</i>	0.5 cm but <1 cm in greatest dimension
<i>T1c</i>	>1 cm but not >2 cm in greatest dimension
<i>T2</i>	Tumor >2 cm but not >5 cm in greatest dimension
<i>T3</i>	Tumor >5 cm in greatest dimension
<i>T4</i>	Tumor of any size with direct extension to chest wall or skin
<i>T4a</i>	Extension to chest wall
<i>T4b</i>	Edema (including peau d'orange), or ulceration of the skin of the breast, or satellite skin nodules confined to the same breast
<i>T4c</i>	Findings of both 4a and 4b
<i>T4d</i>	Inflammatory carcinoma

**Table 59.** TNM – Breast cancer classification system – TN specification. From [117].

**Note:** Chest wall includes ribs, intercostal muscles, and serratus anterior muscle, but not pectoral muscle. Inflammatory carcinoma of the breast is characterized by diffuse, brawny induration of the skin with an erysipeloid edge, usually with no underlying palpable mass. If the result of skin biopsy is negative and no localized measurable primary cancer is found, the T category is pTX when pathologically staging a clinical inflammatory carcinoma (e.g., T4d). Dimpling of the skin, nipple retraction, or other skin changes, except those considered as T4b and 4d, may occur in T1, T2, or T3 cases without affecting the classification.

<i>NX</i>	Regional lymph nodes cannot be assessed.
<i>N0</i>	No regional lymph node metastasis
<i>N1</i>	Metastasis to movable ipsilateral axillary node(s)
<i>N2</i>	Metastasis to ipsilateral axillary node(s) fixed to one

**Table 60.** TNM – Breast cancer classification system – M specification. From [117].

### Breast Cancer Staging – Roman System

<i>Stage 0</i>	Carcinoma in situ of the breast (ductal carcinoma in situ [DCIS] lobular carcinoma in situ [LCIS])
<i>Stage I</i>	T1, N0, M0 <2 cm in diameter, does not touch the skin, does not touch the muscles, and has not invaded the lymph nodes anywhere.
<i>Stage II</i>	>2 cm in diameter but <5 cm in diameter, does not touch the skin, and does not touch the muscles. or Any size <5 cm but has spread to the lymph nodes in the axilla
<i>Stage IIa</i>	T0–1, N1, M0; T2, N0, M0
<i>Stage IIb</i>	T2, N1, M0; T3, N0, M0
<i>Stage III</i>	>5 cm in diameter and/or Spread to lymph nodes fixed to one another, or to the surrounding tissue (e.g., skin, muscle, blood vessels) or Breast cancers of any diameter that involve skin, the ribs of the chest wall, or the internal mammary lymph nodes beneath the middle part of the ribs No spread to other organs No spread to bones away from the chest area No spread to lymph nodes far from the breast
<i>Stage IIIa</i>	T0-2, N2, M0, or T3, N1-2, M0
<i>Stage IIIb</i>	T4, N (any), M0; T(any), N3, M0
<i>Stage IV</i>	T(any), N(any), M1 Any size tumor, metastasized to organs or lymph nodes away from the breast

**Table 61.** Breast cancer *Roman* Staging System. From [117].

## Appendix III

The following figures show the pathway inside each of the Markov states included in the model.

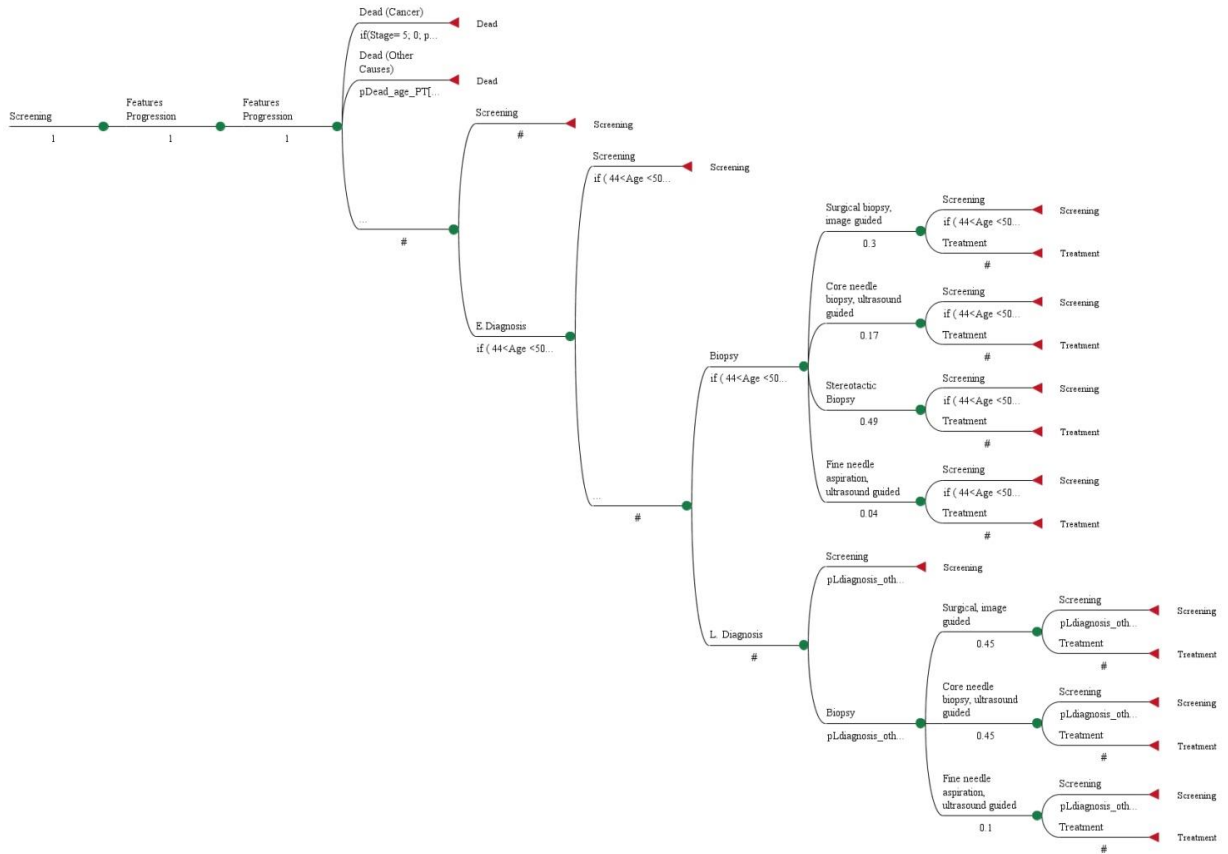


**Fig. 30.** Modeled pathway while in *Screening* (Markov state)

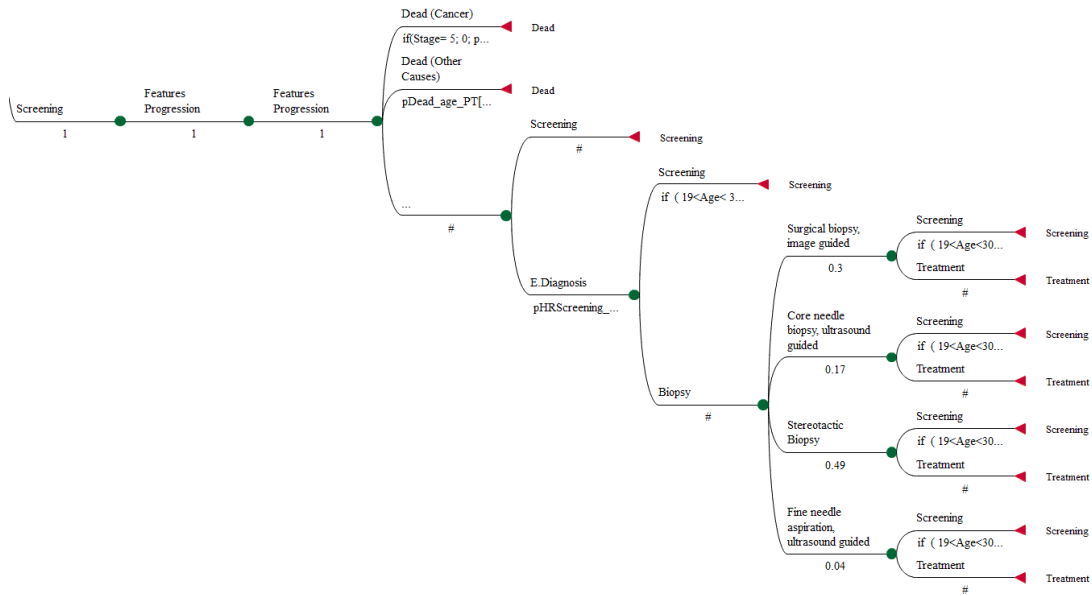


**Fig. 31.** Modeled pathway while in *Screening* (Markov state) for the groups with Screening made with MRI

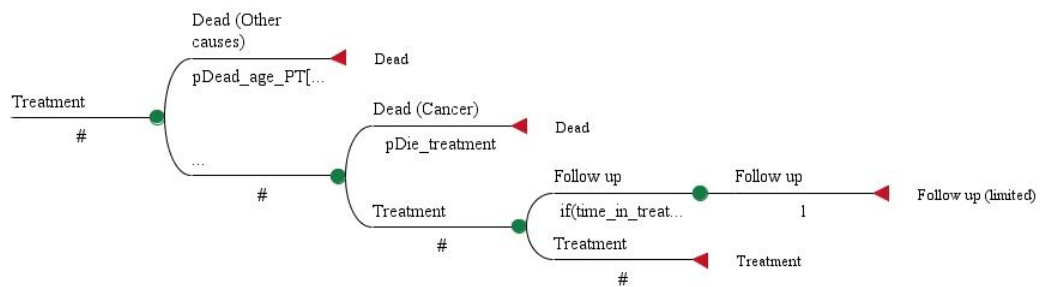


**Fig. 32.** Modeled pathway while in *treatment* (Markov state)

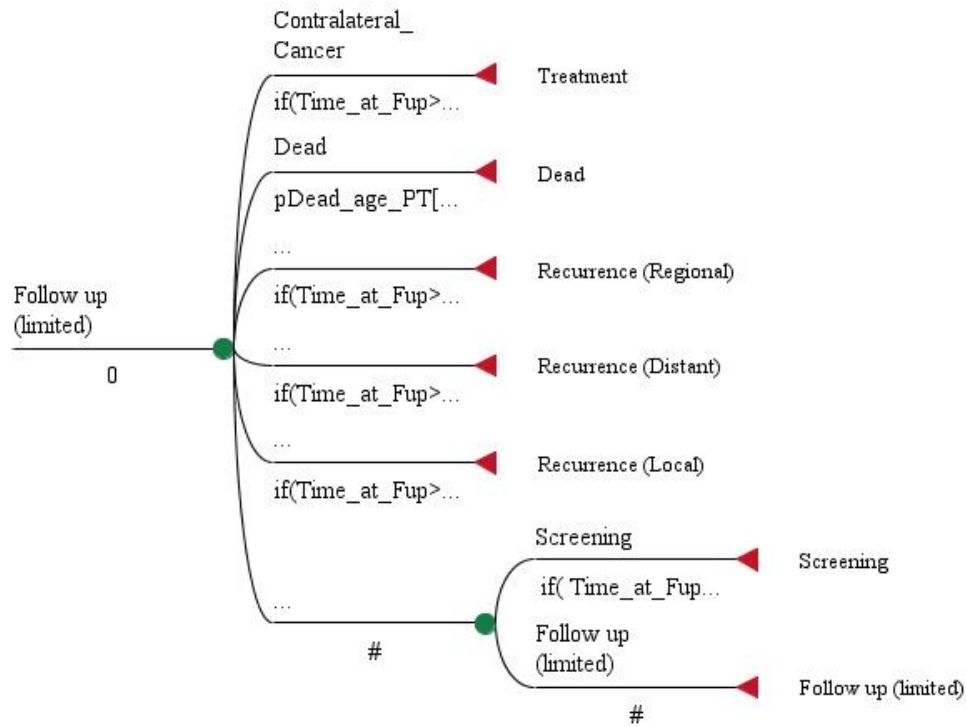


**Fig. 33.** Modeled pathway while in *follow up* (Markov state)

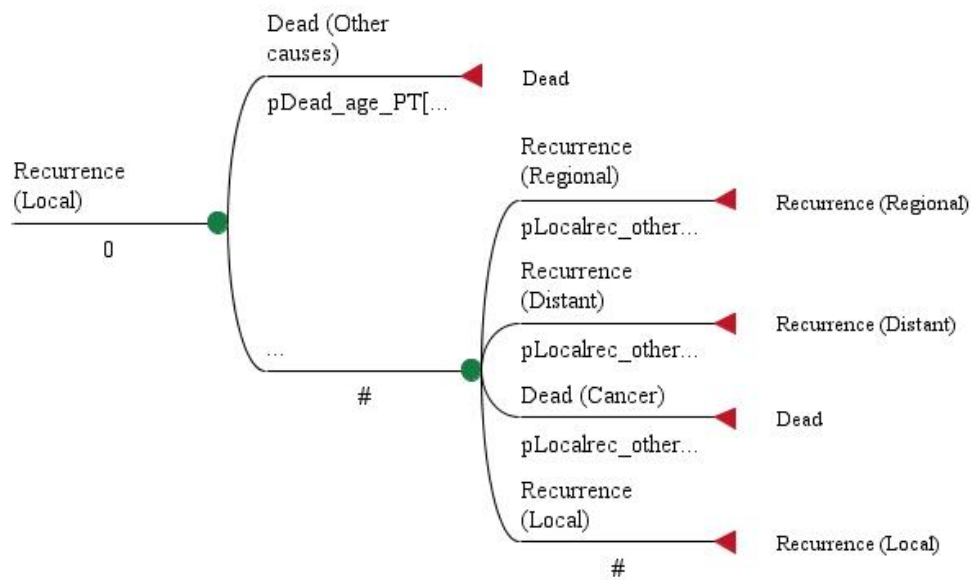


**Fig. 34.** Modeled pathway while in *local recurrence* state (Markov state)

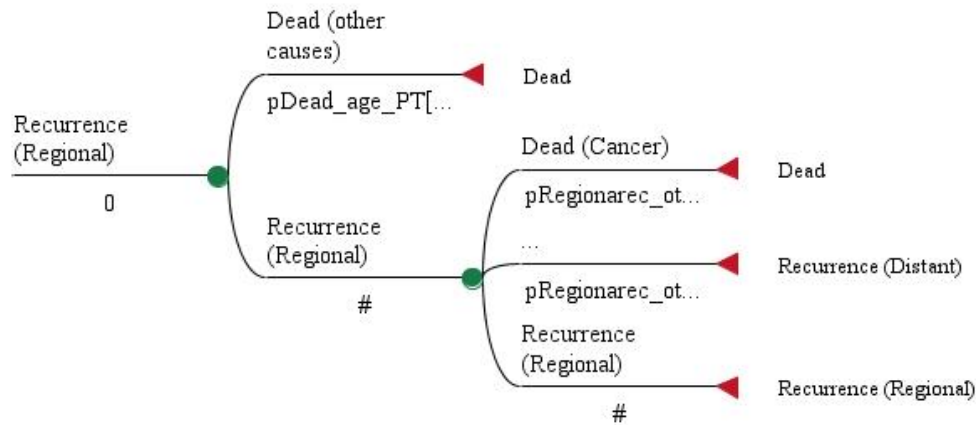


**Fig. 35.** Modeled pathway while in *regional recurrence* state (Markov state)

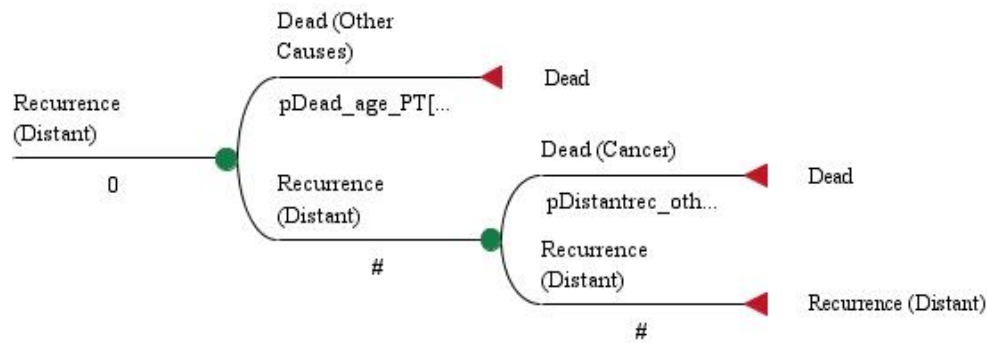


**Fig. 36.** Modeled pathway while in *distant recurrence* state (Markov state)

## Appendix IV

Age group	Mortality interval rates (%)	
	Netherlands	Portugal
20-24	0.00032	0.00015
25-29	0.00028	0.00021
30-34	0.00047	0.00036
35-39	0.00073	0.00054
40-44	0.00108	0.00091
45-49	0.00164	0.00162
50-54	0.00241	0.00291
55-59	0.00317	0.00449
60-64	0.00476	0.00643
65-69	0.00762	0.00985
70-75	0.01428	0.01543

**Table 62.** Mortality 4year-rates for the general population in Netherlands and in Portugal [118].

	5-years Survival rate (%)				
	0	1	2	3	4
20-34	0.987	0.945	0.776	0.505	0.175
35-39	0.997	0.951	0.831	0.558	0.194
40-44	0.999	0.970	0.863	0.594	0.258
45-49	1	0.976	0.878	0.626	0.254
50-54	1	0.983	0.867	0.592	0.205
55-59	1	0.990	0.875	0.575	0.195
60-64	1	0.999	0.867	0.573	0.189
65-69	1	0.999	0.878	0.576	0.203
70-75	1	0.999	0.872	0.578	0.177

**Table 63.** 5-years Survival rate by stage and by age [58].

	Exponential parameter h				
	0	1	2	3	4
20-34	0.013	0.056	0.253	0.683	1.743
35-39	0.003	0.050	0.185	0.583	1.640
40-44	0.001	0.030	0.147	0.520	1.355
45-49	0	0.024	0.130	0.468	1.370
50-54	0	0.017	0.142	0.524	1.585
55-59	0	0.010	0.133	0.553	1.635
60-64	0	0	0.142	0.556	1.666
65-69	0	0	0.130	0.552	1.595
70-75	0	0	0.136	0.548	1.732

**Table 64.** Calculated values of the exponential parameter h for the different stages and ages.

## References

1. WHO cancer. [cited 2013 15th September]; Available from: <http://www.who.int/mediacentre/factsheets/fs297/en/>.
2. Comission, E., *Cancer screening in the European Union Report on the implementation of the Council Recommendation on cancer screening*, 2007.
3. Piras, D.e.a., *Photoacoustic Imaging of the Breast Using the Twente Photoacoustic Mammoscope: Present Status and Future Perspectives*. IEEE Journal of Selected Topics in Quantum Electronics, 2010. **16**(4): p. 730-739.
4. Preston, D.L., et al., *Radiation effects on breast cancer risk: a pooled analysis of eight cohorts*. Radiat Res, 2002. **158**(2): p. 220-35.
5. Frangioni, J.V., *New technologies for human cancer imaging*. J Clin Oncol, 2008. **26**(24): p. 4012-21.
6. Heijblom, M.P., Daniele; Engh, Frank M Van Den; Klaase, Joost M; Brinkhuis, Mariël, *Photoacoustic imaging of breast tumor vascularization: a comparison with MRI and histopathology*. 2013. **8800**.
7. Montigny, E.D., *Photoacoustic Tomography :Principles and applications*. 2011(Photoacoustic imaging.).
8. Manohar, S., et al., *Photoacoustic mammography laboratory prototype: imaging of breast tissue phantoms*. J Biomed Opt, 2004. **9**(6): p. 1172-81.
9. Hoelen, C.G.A., *A new theoretical approach to photoacoustic signal generation*. The Journal of the Acoustical Society of America, 1998. **106**(2): p. 695-706.
10. Manohar, S., et al., *The Twente Photoacoustic Mammoscope: system overview and performance*. Phys Med Biol, 2005. **50**(11): p. 2543-57.
11. Piras D., X.W., Heijblom M., Ten Tije E.M., Van Hespen J., Steenbergen W., Van Leeuwen T.G., Manohar S., *Breast imaging with the Twente Photo acoustic Mammoscope*. 2011.
12. Jose, J., Manohar, Srirang, Kolkman, Roy G M, Steenbergen, W, van Leeuwen, Ton G, *Imaging of tumor vasculature using Twente photoacoustic systems*. Journal of biophotonics, 2009. **2**(12): p. 701-17.
13. Links, J.L.P.a.J.M., *Medical Imaging Signals and Systems*, P.P. Hall, Editor 2006, Pearson Prentice Hall.
14. Yao, J. and L.V. Wang, *Photoacoustic tomography: fundamentals, advances and prospects*. Contrast Media Mol Imaging, 2011. **6**(5): p. 332-45.
15. Wang, L.V. and S. Hu, *Photoacoustic tomography: in vivo imaging from organelles to organs*. Science, 2012. **335**(6075): p. 1458-62.
16. Faris, G.W., et al., *Topics in biomedical optics: Introduction*. Applied Optics, 2007. **46**(10): p. 1595-1596.
17. Ku, G., et al., *Multiple-bandwidth photoacoustic tomography*. Phys Med Biol, 2004. **49**(7): p. 1329-38.
18. Jens E. Wilhjelm, M.K.a.O.T.A., *Medical diagnostic ultrasound physical principles and imaging*, 2010, Technical University of Denmark: Kongens Lyngby.
19. Hoelen, C.G. and F.F. de Mul, *Image reconstruction for photoacoustic scanning of tissue structures*. Appl Opt, 2000. **39**(31): p. 5872-83.
20. Kruger, R.A., et al., *Breast cancer in vivo: contrast enhancement with thermoacoustic CT at 434 MHz-feasibility study*. Radiology, 2000. **216**(1): p. 279-83.
21. Kruger, R.A., ed. *Thermoacoustic computed tomography of the breast*. Photoacoustic Imaging and Spectroscopy2009, CRC Press.
22. Karabutov, A.A.O.a.A.A., *Biomedical Photonics Handbook*, in *Optoacoustic tomography*, C. Press, Editor 2003.



23. Oraevsky, A.A., V.G. Andreev, and A.A. Karabutov, *Detection of ultrawide-band ultrasound pulses in optoacoustic tomography*. IEEE Trans Ultrason Ferroelectr Freq Control, 2003. **50**(10): p. 1383-90.
24. Ermilov, S.A., et al., *Laser optoacoustic imaging system for detection of breast cancer*. J Biomed Opt, 2009. **14**(2): p. 024007.
25. Pramanik, M., et al., *Design and evaluation of a novel breast cancer detection system combining both thermoacoustic (TA) and photoacoustic (PA) tomography*. Med Phys, 2008. **35**(6): p. 2218-23.
26. Srirang Manohar, T.G.v.L., Joost M. Klaase and Frank M. van den Engh, *Photoacoustic Imaging and Spectroscopy*, in *Photoacoustic Mammography with a Flat Detection Geometry*, L. Taylor & Francis Group, Editor 2009.
27. Manohar, S., et al., *Initial results of in vivo non-invasive cancer imaging in the human breast using near-infrared photoacoustics*. Opt Express, 2007. **15**(19): p. 12277-85.
28. Michelle Heijblom, D.P., Ellen Ten Tije, Wenfeng Xia, Johan van Hespene, Joost Klaaseb, Frank van den Enghb, Ton van Leeuwena, Wiendelt Steenbergena and Srirang Manohara, *Breast imaging using the Twente Photoacoustic Mammoscope (PAM): new clinical measurements*. Clinical and Biomedical Spectroscopy and Imaging II, 2011. **8087**.
29. M. Heijblom, D.P., W. Xia, J.C.G. van Hespene, J.M. Klaase, F.M. van den Engh, T.G. van Leeuwen, W. Steenbergena, and S. Manohar, *Visualizing breast cancer using the Twente photoacoustic mammoscope: What do we learn from twelve new patient measurements?* Optical Society of America, 2012.
30. M. Heijblom, D.P., W. Xia, J.C.G. van Hespene, F.M. van den Enghb, J.M. Klaaseb, T.G. van Leeuwena,c, W. Steenbergena and S. Manohara, *Imaging breast lesions using the Twente Photoacoustic Mammoscope: Ongoing clinical experience*. Photons Plus Ultrasound: Imaging and Sensing 2012. **8223**.
31. Hilgerink, M., *Implemented Scenarios and predicted performance of the Twente Photoacoustic Mammoscope as an alternative imaging modality in Breast Cancer Diagnosis*, in *Faculty of Management and Governance - Health Technology and Services Research* 2009, University of Twente: Enschede.
32. Haakma, W., *Expert Elicitation to Populate Early Health Economic Models of Medical Diagnostic Devices in Development*, in *Faculty of Management and Governance - Department of Health Technology and Services Research*. 2011, University of Twente: Enschede.
33. Roelvink, J., *Patient preferences versus professional preferences in population screening technology : Patient centered decision making in the population screening for Breast Cancer* in *Faculty of Management and Governance - Department of Health Technology and Services Research* 2012, University of Twente: Enschede.
34. Michelle Heijblom, D.P., Wenfeng Xia, Johan van Hespene, Joost Klaase, Frank van den Engh, Ute Gamm, Mariël Brinkhuis, Ton van Leeuwen, Wiendelt Steenbergena and Srirang Manohar, *Clinical measurements with PAM I: Progress and Plans*, 2012, MIRA Imaging & Diagnostics Colloquium - U. Twente: [http://www.utwente.nl/mira/events/MIRA\\_I%26D\\_colloquia/MIRA%20IenDColloquia\\_2012.docx/](http://www.utwente.nl/mira/events/MIRA_I%26D_colloquia/MIRA%20IenDColloquia_2012.docx/).
35. Perry, N., Broeders, M., Wolf, C., De and S.e.a. Törnberg, *European guidelines for quality assurance in breast cancer screening and diagnosis*, D.-G. Health and Consumer Protection, Editor 2006, European Commission: Belgium.
36. NICE, *Classification and care of people at risk of familial breast cancer and management of breast cancer and related risks in people with a family history of breast cancer*, 2013.

37. Aebi, S., et al., *Primary breast cancer: ESMO Clinical Practice Guidelines for diagnosis, treatment and follow-up*. Ann Oncol, 2010. **21 Suppl 5**: p. v9-14.
38. M. João, H.G., S. Braga et al, *Recomendações Nacionais para o diagnóstico e tratamento do cancro da mama*, 2009, Instituto Português de Oncologia: Coimbra.
39. Groot, M.T., et al., *Costs and health effects of breast cancer interventions in epidemiologically different regions of Africa, North America, and Asia*. Breast J, 2006. **12 Suppl 1**: p. S81-90.
40. Elteren, J.J.v., *Individualized breast cancer follow-up: Cost-effectiveness for various follow-up scenarios*, in *Health Technology and Services Research* 2008, Univesity of Twente: Enschede. p. 64.
41. Herndon, J.H., R. Hwang, and K.J. Bozic, *Healthcare technology and technology assessment*. Eur Spine J, 2007. **16**(8): p. 1293-302.
42. Ijzerman, M.J. and L.M. Steuten, *Early assessment of medical technologies to inform product development and market access: a review of methods and applications*. Appl Health Econ Health Policy, 2011. **9**(5): p. 331-47.
43. Muennig, P., *Cost Effectiveness Analysis in Health: A Practical Approach*, J.W. Sons, Editor 2008, Jossey-Bass: San Francisco. p. 286.
44. Karnon, J., *Alternative decision modelling techniques for the evaluation of health care technologies: Markov processes versus discrete event simulation*. Health Econ, 2003. **12**(10): p. 837-48.
45. excellence, N.I.f.h.a.c., *Briefing paper for the Methods Working Party on the Cost Effectiveness Threshold*. 2004.
46. Trask, L.S., *Pharmacoeconomics: Principles, Methods, and Applications* T.M.-H. Companies, Editor 2011.
47. Weinstein, M.C., G. Torrance, and A. McGuire, *QALYs: the basics*. Value Health, 2009. **12 Suppl 1**: p. S5-9.
48. Russell, M.C.W.J.E.S.M.R.G.M.S.K.L.B., *Recommendations of the Panel on Cost-effectiveness in Health and Medicine*. JAMA : the journal of the American Medical Association, 1996. **276**(15): p. 1253-1258.
49. Government, A., *The concept of discounting in cost- benefit analysis*. 1996: p. 319-320.
50. Clarke, P., *How much should we be discounting the future ?*, 2010, School of Public Health University, University of Sydney.
51. Glick, H.A., *Introduction to Markov Models*, 2007: Kyung Hee University. p. 30.
52. Fryback, D.G., et al., *The Wisconsin Breast Cancer Epidemiology Simulation Model*. J Natl Cancer Inst Monogr, 2006(36): p. 37-47.
53. EUCAN. 2012 [cited 2012 April]; Available from: <http://eu-cancer.iarc.fr/EUCAN/CancerOne.aspx?Cancer=46&Gender=2>.
54. EUREG. *Incidence tables*. 2007 [cited 2013 April]; Available from: <http://eco.iarc.fr/EUREG/>.
55. Risch, H.A., et al., *Population BRCA1 and BRCA2 mutation frequencies and cancer penetrances: a kin-cohort study in Ontario, Canada*. J Natl Cancer Inst, 2006. **98**(23): p. 1694-706.
56. Sprague, B.L., et al., *Genetic variation in TP53 and risk of breast cancer in a population-based case control study*. Carcinogenesis, 2007. **28**(8): p. 1680-6.
57. Fracheboud, J.G., JH, *National report of breast cancer screening*, 2009, National Evaluation Team for Breast cancer screening.
58. Eisner, L.A.G.R.a.M.P., *Cancer of the Female Breast*. 2001(Chapter 13): p. 101-110.
59. NCSS, *Survival Parameter Conversion Tool*, 2010.
60. Auguste, P., et al., *An economic evaluation of positron emission tomography (PET) and positron emission tomography/computed tomography (PET/CT) for the diagnosis of breast cancer recurrence*. Health Technol Assess, 2011. **15**(18): p. iii-iv, 1-54.

61. Pisano, E.D., et al., *Diagnostic accuracy of digital versus film mammography: exploratory analysis of selected population subgroups in DMIST*. Radiology, 2008. **246**(2): p. 376-83.
62. Sardanelli, F. and F. Podo, *Breast MR imaging in women at high-risk of breast cancer. Is something changing in early breast cancer detection?* European Radiology, 2007. **17**(4): p. 873-887.
63. Britton, P., et al., *Measuring the accuracy of diagnostic imaging in symptomatic breast patients: team and individual performance*. Br J Radiol, 2012. **85**(1012): p. 415-22.
64. Chiarelli, A.M., et al., *The contribution of clinical breast examination to the accuracy of breast screening*. J Natl Cancer Inst, 2009. **101**(18): p. 1236-43.
65. Medeiros, L.R., et al., *Accuracy of magnetic resonance in suspicious breast lesions: a systematic quantitative review and meta-analysis*. Breast Cancer Res Treat, 2011. **126**(2): p. 273-85.
66. A.C., W.J.L.V.E.P.P.L.L.V.v.d.P.-F.M.J.C.v.d.S.G.A.P.N., *Factsheet: Mammacarcinoom in onze IKZ-regio*, 2011.
67. CEA Registry. 2013 [cited 2013 May- July]; CEA Registry]. Available from: <https://research.tufts-nemc.org/cear4/SearchingtheCEARRegistry/SearchtheCEARRegistry.aspx>.
68. Moore, S.G., et al., *Cost-effectiveness of MRI compared to mammography for breast cancer screening in a high risk population*. BMC Health Serv Res, 2009. **9**: p. 9.
69. Johnston, K., et al., *Valuing temporary and chronic health states associated with breast screening*. Soc Sci Med, 1998. **47**(2): p. 213-22.
70. Wong, I.O., et al., *Cost-effectiveness analysis of mammography screening in Hong Kong Chinese using state-transition Markov modelling*. Hong Kong Med J, 2010. **16 Suppl 3**: p. 38-41.
71. Wong, I.O., et al., *Optimizing resource allocation for breast cancer prevention and care among Hong Kong Chinese women*. Cancer, 2012. **118**(18): p. 4394-403.
72. Lee, J.H., et al., *Decision-analytic model and cost-effectiveness evaluation of postmastectomy radiation therapy in high-risk premenopausal breast cancer patients*. J Clin Oncol, 2002. **20**(11): p. 2713-25.
73. Taylor, P., et al., *Impact of computer-aided detection prompts on the sensitivity and specificity of screening mammography*. Health Technol Assess, 2005. **9**(6): p. iii, 1-58.
74. Portaria n.º 163/2013, Diário da República, 1.ª série — N.º 80 — 24 de abril de 2013, M.d. Saúde, Editor 2013.
75. Bijlage 2 bij Beleidsregel CU-2065 Tarieflijst Instellingen NZA, Editor 2012.
76. Duijm, L.E., et al., *Utilization and cost of diagnostic imaging and biopsies following positive screening mammography in the southern breast cancer screening region of the Netherlands, 2000-2005*. Eur Radiol, 2008. **18**(11): p. 2390-7.
77. Nederend, J., et al., *Impact of transition from analog screening mammography to digital screening mammography on screening outcome in The Netherlands: a population-based study*. Ann Oncol, 2012. **23**(12): p. 3098-103.
78. Plevritis, S.K., et al., *Cost-effectiveness of screening BRCA1/2 mutation carriers with breast magnetic resonance imaging*. JAMA, 2006. **295**(20): p. 2374-84.
79. Groenewoud, J.H., et al., *Cost-effectiveness of stereotactic large-core needle biopsy for nonpalpable breast lesions compared to open-breast biopsy*. Br J Cancer, 2004. **90**(2): p. 383-92.
80. António A., F.B., Sérgio B. et al *Custo do tratamento do cancro em Portugal*. Acta Med. Port. , 2009. **22**, 525-536.
81. Cardoso, F., et al., *Locally recurrent or metastatic breast cancer: ESMO Clinical Practice Guidelines for diagnosis, treatment and follow-up*. Ann Oncol, 2012. **23 Suppl 7**: p. vii11-9.

82. Hilgerink, M.P., et al., *Assessment of the added value of the Twente Photoacoustic Mammoscope in breast cancer diagnosis*. Med Devices (Auckl), 2011. **4**: p. 107-15.
83. Tree age Software, I., *TreeAge Pro 2013 User 's Manual*, 2013. p. 588.
84. Williams, A., *What could be nicer than NICE?* London Office of Health Economics, 2004.
85. EUROSTAT. *Regional GDP per capita in the EU in 2010*. 2010 [cited 2013 May]; Available from: [http://epp.eurostat.ec.europa.eu/cache/ITY\\_PUBLIC/1-21032013-AP/EN/1-21032013-AP-EN.PDF](http://epp.eurostat.ec.europa.eu/cache/ITY_PUBLIC/1-21032013-AP/EN/1-21032013-AP-EN.PDF).
86. Lowry, K.P., et al., *Annual screening strategies in BRCA1 and BRCA2 gene mutation carriers: a comparative effectiveness analysis*. Cancer, 2012. **118**(8): p. 2021-30.
87. Stout, N.K., et al., *Retrospective cost-effectiveness analysis of screening mammography*. J Natl Cancer Inst, 2006. **98**(11): p. 774-82.
88. Norman, R.P., et al., *The cost-utility of magnetic resonance imaging for breast cancer in BRCA1 mutation carriers aged 30-49*. Eur J Health Econ, 2007. **8**(2): p. 137-44.
89. Tosteson, A.N., et al., *Cost-effectiveness of digital mammography breast cancer screening*. Ann Intern Med, 2008. **148**(1): p. 1-10.
90. Pandharipande, P.V., et al., *Staging MR lymphangiography of the axilla for early breast cancer: cost-effectiveness analysis*. AJR Am J Roentgenol, 2008. **191**(5): p. 1308-19.
91. Rojnik, K., et al., *Probabilistic cost-effectiveness modeling of different breast cancer screening policies in Slovenia*. Value Health, 2008. **11**(2): p. 139-48.
92. de Gelder, R., et al., *Cost-effectiveness of opportunistic versus organised mammography screening in Switzerland*. Eur J Cancer, 2009. **45**(1): p. 127-38.
93. Ahern, C.H. and Y. Shen, *Cost-effectiveness analysis of mammography and clinical breast examination strategies: a comparison with current guidelines*. Cancer Epidemiol Biomarkers Prev, 2009. **18**(3): p. 718-25.
94. Lee, J.M., et al., *Cost-effectiveness of breast MR imaging and screen-film mammography for screening BRCA1 gene mutation carriers*. Radiology, 2010. **254**(3): p. 793-800.
95. Carles, M., et al., *Cost-effectiveness of early detection of breast cancer in Catalonia (Spain)*. BMC Cancer, 2011. **11**: p. 192.
96. Cott Chubiz, J.E., et al., *Cost-effectiveness of alternating magnetic resonance imaging and digital mammography screening in BRCA1 and BRCA2 gene mutation carriers*. Cancer, 2013. **119**(6): p. 1266-76.
97. Miles, K.A., *An approach to demonstrating cost-effectiveness of diagnostic imaging modalities in Australia illustrated by positron emission tomography*. Australas Radiol, 2001. **45**(1): p. 9-18.
98. Wang, H., et al., *Mammography screening in Norway: results from the first screening round in four counties and cost-effectiveness of a modeled nationwide screening*. Cancer Causes Control, 2001. **12**(1): p. 39-45.
99. Sevilla, C., et al., *Testing for BRCA1 mutations: a cost-effectiveness analysis*. Eur J Hum Genet, 2002. **10**(10): p. 599-606.
100. Morris, A.M., et al., *Comparing the cost-effectiveness of the triple test score to traditional methods for evaluating palpable breast masses*. Med Care, 2003. **41**(8): p. 962-71.
101. Sorensen, J. and A. Hertz, *Cost-effectiveness of a systematic training programme in breast self-examination*. Eur J Cancer Prev, 2003. **12**(4): p. 289-94.
102. Arveux, P., S. Wait, and P. Schaffer, *Building a model to determine the cost-effectiveness of breast cancer screening in France*. Eur J Cancer Care (Engl), 2003. **12**(2): p. 143-53.
103. Balmana, J., et al., *Genetic counseling program in familial breast cancer: analysis of its effectiveness, cost and cost-effectiveness ratio*. Int J Cancer, 2004. **112**(4): p. 647-52.

104. Mandelblatt, J.S., et al., *Benefits and costs of interventions to improve breast cancer outcomes in African American women*. J Clin Oncol, 2004. **22**(13): p. 2554-66.
105. Sloka, J.S., P.D. Hollett, and M. Mathews, *Cost-effectiveness of positron emission tomography in breast cancer*. Mol Imaging Biol, 2005. **7**(5): p. 351-60.
106. Lindfors, K.K., et al., *Computer-aided detection of breast cancer: a cost-effectiveness study*. Radiology, 2006. **239**(3): p. 710-7.
107. Ohnuki, K., et al., *Cost-effectiveness analysis of screening modalities for breast cancer in Japan with special reference to women aged 40-49 years*. Cancer Sci, 2006. **97**(11): p. 1242-7.
108. Care, N.C.C.f.P. *The classification and care of women at risk of familial breast cancer in primary, secondary and tertiary care*. 2006.
109. Griebisch, I., et al., *Cost-effectiveness of screening with contrast enhanced magnetic resonance imaging vs X-ray mammography of women at a high familial risk of breast cancer*. Br J Cancer, 2006. **95**(7): p. 801-10.
110. Neeser, K., et al., *Cost-effectiveness analysis of a quality-controlled mammography screening program from the Swiss statutory health-care perspective: quantitative assessment of the most influential factors*. Value Health, 2007. **10**(1): p. 42-53.
111. Okonkwo, Q.L., et al., *Breast cancer screening policies in developing countries: a cost-effectiveness analysis for India*. J Natl Cancer Inst, 2008. **100**(18): p. 1290-300.
112. Wong, G., et al., *Cost-effectiveness of breast cancer screening in women on dialysis*. Am J Kidney Dis, 2008. **52**(5): p. 916-29.
113. Lee, S.Y., et al., *Cost-effective mammography screening in Korea: high incidence of breast cancer in young women*. Cancer Sci, 2009. **100**(6): p. 1105-11.
114. Department of Health and Ageing, A.G., *BreastScreen Australia Evaluation Economic Evaluation and Modelling Study*, P.b.I.H.P.L.A.f.t.A.G.D.o.H.a. Ageing, Editor 2009.
115. Peregrino, A.A., et al., *[Analysis of Cost-effectiveness of screening for breast cancer with conventional mammography, digital and magnetic resonance imaging]*. Cien Saude Colet, 2012. **17**(1): p. 215-22.
116. Sato, M., et al., *Cost-effectiveness analysis for breast cancer screening: double reading versus single + CAD reading*. Breast Cancer, 2012.
117. WHO, *General cancer classification staging and grouping systems* 2005.
118. WHO. *Lifetables*. 2011 [cited 2013 April]; Available from: <http://apps.who.int/gho/data/view.main.61160>.